Surficial Materials Mapping using Remote Sensing and Classification Methods: A Geological Knowledge and Statistical Approach

by

Ulanna Wityk

A thesis

presented to the University of Waterloo

in fulfillment of the

thesis requirement for the degree of

Master of Applied Science

in

Earth Sciences

Waterloo, Ontario, Canada, 2014

Author's Declaration

I hereby declare that I am the sole author of this thesis. This is a true copy of the thesis, including any required final revisions, as accepted by my examiners.

I understand that my thesis may be made electronically available to the public.

Abstract

Mapping the geology of Northern regions in Canada is an essential step in providing key knowledge for resource development and economic prosperity of northern communities. However, mapping this large remote region presents a major challenge both in terms of financial resources and the time required to cover such a large area. With convenient access to remotely sensed imagery, new automatic and remote approaches are emerging that support the surficial geological mapping of vast northern regions at scales appropriate for mineral exploration and related land-use management.

An approach using LANDSAT 7 TM imagery, field-based data and a maximum likelihood classification algorithm is employed to produce remote predictive maps of the surficial materials in the Repulse Bay area, Nunavut (NTS 46M-SW, 46L-W and S and 46K-SW). Two approaches in the remote predictive mapping (RPM) process are used to determine the optimal class combination and resultant maps. The first approach employs general and field knowledge from Quaternary geologists to the map evaluation. This approach allows training areas to be grouped and merged based on Quaternary geology principles. The second approach uses statistical techniques to produce classified maps based on training areas along with measures of classification accuracy. These qualitative (geological knowledge-based) and quantitative (statistical-based) methods are used and compared to determine optimal class combinations. Four classification maps that offer the highest overall classification accuracies - through analysis of a confusion matrix and associated variability maps - were produced (two for each approach). Exposed marine sediments, carbonate-rich tills, organics and boulder terrains are the most accurately (>75%) classified of the surficial materials classes; confusion occurs between remaining till, sand and gravel, and bedrock units. Variability maps were produced using these optimal class combinations and corresponding classifications, through which it is found that the geological knowledge-based approach is more suitable for remotely mapping surficial materials in this study area.

A comparison to surficial materials maps derived from surficial geology maps was conducted with results of classification outputs using the most optimal class combinations with LANDSAT and SPOT 4/5 imagery. This visual and GIS analysis comparison allowed for evaluation of the classification products, while an overlay analysis compared a pixel-to-pixel correspondence between the maps. Although it is found that both imageries are useful for mapping marine and alluvial sediments, it has limitations in mapping organic materials, till and bedrock. It is apparent that LANDSAT imagery is more appropriate for general mapping while SPOT is better suited for mapping marine sediments.

Acknowledgements

This research was made possible by funding from Natural Resources Canada, under a Research Affiliate Program (RAP) bursary, and additional funding from the University of Waterloo. These funds, in addition to a travel grant received from the Northern Scientific Training Program (NSTP), supported fieldwork over two seasons in the Repulse Bay area, NU. Guidance from Dr. Martin Ross (University of Waterloo) and Dr. Isabelle McMartin (Natural Resources Canada and adjunct professor at the University of Waterloo) provided essential review of this thesis and with progression and direction of the research. Thank you to other thesis committee members and colleagues at the Geological Survey of Canada - Janet Campbell and Dr. Eric Grunsky (and adjunct professor at the University of Waterloo)- for playing roles in discussion of this work; and additionally Dr. Jeff Harris for providing great support in data processing and interpretation.

Dedication

This thesis is dedicated to my family and extended family for supporting me in my educational endeavors. Thank you for your endless encouragement! It is dedicated to all the wonderful friends I have met from the beginning of my time in Waterloo. Thank you for your friendship! This thesis is also dedicated to all office mates who have come and gone in ESC 203, especially Cassia and Lisa. Thank you for everything!

Table of Contents

List of Figures

List of Tables

Chapter 1: Introduction

1.1 Geological Mapping in Northern Canada

Mapping the geology of Northern regions in Canada is an essential step for providing important knowledge for both resource development and economic prosperity of northerners. The Western Churchill Geological Province is an active diamond, gold and base metal exploration area. It sets the example for Northern Canada's vast resource potential. Though surficial geology maps are available for northern regions, many are at a coarse scale and hinder the potential for effective surface exploration programs by the mineral exploration industry using glacial sediments as a sampling medium. As seen in Figure 1, many regions North of 60° latitude have not been mapped or are mapped at the 1:500,000 scale and coarser ("Some knowledge:" or "Insufficient knowledge") - a resolution ineffective for surface exploration programs. Finer scaled resolution would aid in uncovering resource potential in the north and providing a geological framework; and thus, help facilitate exploration and development programs. Such higher resolution maps would contribute to northern prosperity by giving knowledge to industries and policy makers leading to more informed decisions regarding policies, and sustainable development, thereby enhancing socioeconomic status and general welfare of northern communities.

As resource potential is to be explored and developed, governments and industry are challenged to produce geological maps in a time and cost-effective manner. To meet this demand, remote sensing resources and tools can be used as they offer cost and time efficient methods to help mapping the surficial geology (Harris, 2007; Grunsky et al., 2009).

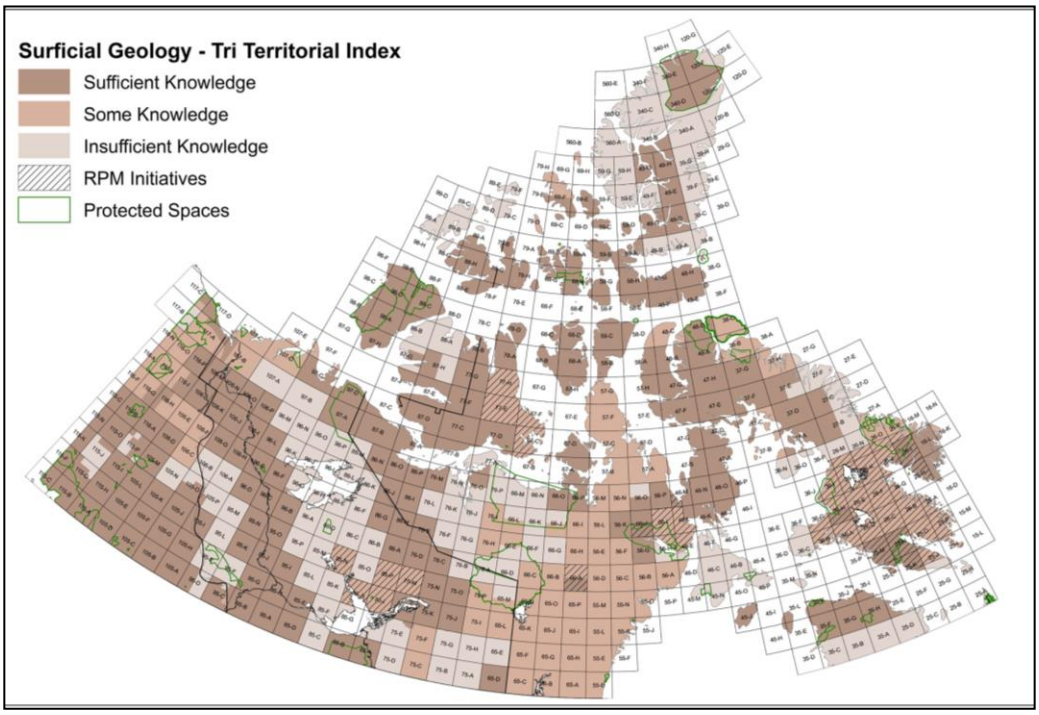

Figure 1.1: Surficial Geology Map Coverage, Canada, north of 60° Latitude (Kerr and Eagles, 2013, per. comm.).

1.2 Remote Sensing and Satellite Imagery – Geological Uses

Mapping remote locations such as Northern Canada is a time-intensive and costly process as these regions have little to no infrastructure, and short fieldwork seasons. The otherwise expensive and time-intensive field programs have been accelerated through use of remotely sensed data, which has proven to be useful in fields of geomorphology, exploration geology, engineering, geochemical hazard assessment as well as geological mapping for delineation of rock unit boundaries and sub-units (Drury, 2001).

Though limitations exist, satellite imagery expands map-able regions further than what is constrained by factors of accessibility. It offers large scale views which facilitate new discoveries by filling in regions between broadly spaced point data. General coverage of 100x100km or larger images allow small teams of geoscientists to map terrains of areas this size or larger (Clark, 1997).

Since Sugden (1978) first used remotely sensed data to map the intensity of glacial erosion by the Laurentide Ice Sheet, a variety of uses have emerged in surface mapping (Clark, 1997). Remote sensing imagery used include several sensors such as LANDSAT MSS (80m), LANDSAT TM (30m), SPOT XZ (20m), SPOT Pan (10m), SEASAT and ERS SAR (25m) as well as RADARSAT, and have proved to have a range in ease of analysis as well as limitations. Some limitations have included poor resolution, high data volume, high solar elevation, limited

coverage and terrain distortion (Clark, 1997). Table 1.1 summarizes some available remote sensors.

Table 1.1 Remote Sensor Summary

Satellite	Sensor	Starting date of operation	Resolution	Main usage	Country of origin
LANDSAT	MSS	1972	80 m	Agriculture, geology, forestry, regional planning, mapping, emergency response and disaster relief, resource management, environmental monitoring, change detection	USA
LANDSAT	TM	1982	30m		
SPOT	XS	1986	20m	Urban mapping, topographic information	France
SPOT PAN	Pan		10m		
SEASAT	SAR	1978	25m	Remote sensing of earth's oceans	USA
ERSSAR	SAR	1991	25m	Ocean-atmosphere interaction, oceanic circulation and energy transfer, ice sheet mass balance estimates, monitoring: coastal processes and pollution; land-use change and management	(Europe)
RADARSAT-1	SAR	1995	Variable (12.5m-1km)	Surface texture (height)/roughness, environmental monitoring, sea ice distribution, disaster management, hydrology, geology, agriculture, forestry,	Canada

In geomorphological and surficial geology mapping, rigorous fieldwork and air photograph interpretation generally comprise mapping efforts. Though resolution of satellite imagery (10-80m), is not as fine as that of aerial photographs (a few meters), it is readily available and usable at an array of scales and spatial resolutions. This convenience gives rise to the identification of patterns at scales that may have otherwise gone unnoticed (Clark, 1997) and allows mapping of drumlins and major eskers and other glacial landforms, investigation of their texture, as well as analysis of their distribution and spatial densities. This type of analyses contributes to reconstructing glacial histories and to understand glacial geomorphic processes (Ex. Smith and Pain, 2009).

Reconstructing glacial histories includes identifying glacial evolution, glacial maxima and glacial retreat (Clark, 1997). GIS and remote sensing facilitate greater coverage spatially, and promote inclusion of various data sources, scales and field areas (Clark, 1997). This has been exemplified in mapping of regions overlain by the northernmost part of the Laurentide Ice Sheet. Prest et al. (1968) regionally mapped the glacial landscape of Canada using air photos,

while LANDSAT has been used for large-scale paleo-glaciological mapping of the Canadian Arctic (e.g. Boulton and Clark 1990; De Angelis, 2007). It has been used extensively in geomorphological mapping of paleo-ice stream beds (i.e. Stokes, 2002) in many different regions of the Canadian Arctic (e.g. Clark and Stokes 2001; Stokes and Clark 2003; De Angelis and Kleman 2005; Stokes et al. 2006, 2009; Dyke 2008; Ross et al. 2011). Satellite imagery has also been used, sometimes with tools such as Google Earth, to identify and delineate carbonate dispersal patterns across Canadian Shield rocks in the Arctic (e.g. Stokes, 2002; De Angelis and Kleman, 2005; Dyke, 2008; Ross et al., 2011). Finally, remote sensing has been used to spectrally locate geochemical anomalies, which in turn guide mineral exploration (e.g. Taranik et al., 2009).

1.3 Previous RPM studies in the Arctic

As satellite imagery is useful in identifying and mapping landforms and geomorphological features and patterns, the idea to use the same imagery to map surficial sediments (including bedrock) has also been explored. Remotely sensed imagery has been applied in regions of the arctic as vegetation, especially tree cover, is not a major limiting factor. More specifically, this type of mapping has been accomplished using methods commonly referred to as Remote Predictive Mapping (RPM) (Harris et al., 2008).

RPM is a mapping process by which a combination or selection of any available geoscience data including field observations, sample material, air photo interpretation, geophysical and geochemical information are collected and interpreted to help scientists develop a representation of what forms the ground surface. In this process field data and other information are used to train computer classification algorithms. These algorithms use image data to calculate statistical relationships (located at field stations) and lithological/surficial units to identify and predict similar signatures in other regions. This relationship is based on the image information including spectral reflectance, magnetic-field intensity, radar backscatter, and other available properties (Schetselaar et al., 2007). This RPM classification method can be used to facilitate the speed of the geological mapping process, by streamlining and focusing the fieldwork component, thereby accelerating production of mapping and enhancing potential for northern prosperity.

A number of RPM classification studies have been conducted in regions of the Canadian Arctic, using a variety of data and applying it to the RPM method. In an RPM case study near Snowbird Lake (NWT), the RPM approach was used for purposes of field planning in addition to understanding the regional geology. Magnetic and field data as well as gamma-ray spectroscopy, a digital elevation model (DEM) and LANDSAT imagery, helped identify and map geological structures and units (Martel et al., 2005). Successes of this study included the production of field maps thereby enhancing field planning, and of producing maps of lithological domains and units as well as structural trends. In addition it recognized regions of complex terrain and poor exposure, thus identifying areas to target future field mapping. Confusion in the

predictive mapping included classification of bedrock and eskers. One conclusion of the study was that magnetic data was most useful for predictive mapping of bedrock in the study area (Martel et al., 2005).

RPM surficial unit discrimination in the Arctic has been carried out on Baffin Island (Brown et al., 2007) and Schultz Lake (Grunsky et al., 2006, 2009), Nunavut. The Baffin Island study visually examined LANDSAT imagery, and due to lack of spectral variability, warranted further computer analysis (Brown et al., 2007). It was combined with a DEM for the region, which resulted in some confusion between units. After a supervised classification using LANDSAT imagery, an accuracy of 85% was achieved (Brown et al., 2007) when compared to original training areas determined for classification. A 50% accuracy was noted when comparing the classification results with field check sites. The goal of this study was to achieve 80% accuracy with field data (different to comparison with training areas), which was not accomplished, possibly as a result of coarse scale and resolution, overlap of units, or definition of training areas from fieldwork and/or air photographs (Brown et al., 2007). The study revealed that accuracy improved by 1% when the LANDSAT data was used in concert with a DEM (Brown et al., 2007). Suggestions from this research included post-classification filtering, which improved classification accuracies (when comparing training areas to filtered maps), and the incorporation of a DEM, to improve statistical separation of the LANDSAT image (Brown et al., 2007).

The RPM study in Schultz Lake by Grunsky et al. (2006, 2009) was similar to the Baffin Island study, in that it also used LANDSAT and a DEM, but also incorporated RADARSAT data. Here, 6 surficial material types were classified using a combination of LANDSAT TM-7 data (spectral response measurements) and RADARSAT data (backscatter measures). Through the development of training areas from air photos, conducting classification, comparing statistics and field checking, it was established that certain classes were discriminated better than others. It also demonstrated that different confusion levels were present within individual LANDSAT and RADARSAT classifications. Using these data sets in combination helped delineate surficial materials better than if used individually (Grunsky et al., 2009). When comparing mapped pixels in classified maps with those pixels located in training area regions, a reasonable accuracy, greater than 80% was achieved. However, when comparing classification maps to surficial geology maps, the correspondence was less than 50% due to the effect of being generalized. This study demonstrated that LANDSAT and RADARSAT imagery are useful for discriminating certain surficial materials, namely thick till. This is because thick till has distinct differences in surficial texture and spectral response, as a result of vegetation cover, that distinguishes it easily from other materials. Using a combination of datasets increases the robustness of a classification since spectral and topographic roughness are considered in the classification, and in the end provides useful first order maps for geologists (Grunsky et al., 2009).

Building-up on the studies described above, Synthetic Aperture Radar (SAR) images have been used in mapping surficial materials in the Thelon Basin in Nunavut. The SAR sensors

collect data in daytime or night and also measures surface roughness and moisture, whose properties are important in discriminating surficial materials (LaRocque et al., 2012).

1.4 Study Area

The thesis study area is located on mainland Nunavut between latitudes 66°N and 67.5°N and longitudes 88°W and 86°W (Figure 1.2). It is situated west of the community of Repulse Bay, on the west side of Rae Isthmus. It encompasses coastal lowlands along the west coast of Committee Bay and Repulse Bay, which are part of NTS sheets 46K, 46L and 46M. Its discontinuous cover of generally streamlined glacial drift (Prest et al., 1968; Aylsworth and Shilts, 1989; De Angelis, 2007) is underlain by rocks of the western Churchill Geological Province of the Canadian Shield. These rocks include Archean through Paleoproterozoic supracrustral and intrusive rocks of the 2.7-2.6 Ga Rae Domain (Paul et al., 2002). It is also comprised of extensive regions of exposed gullied marine silts along the coast of Committee Bay in 46M-SW, and marine limit elevations increase from 140 m to 240 m northward within the area (Campbell and McMartin, 2010; McMartin et al., 2013).

This study is part of the Wager Bay Surficial Geology Mapping Activity (Fig. 1.2. Inset map) conducted by the Geological Survey of Canada as part of Natural Resources Canada Geo-mapping for Energy and Minerals (GEM) Program. This activity focuses on mapping surficial geology at the regional scale and till sampling (Campbell et al., 2013). The Wager Bay study area has complex ice flow sequences, and poorly known glacial transport characteristics (McMartin and Henderson, 2004). This study area is located within one of the most active diamond exploration regions of the Western Churchill Geological Province (Paul et al. 2002), and is located adjacent to the Repulse Bay diamond exploration camp.

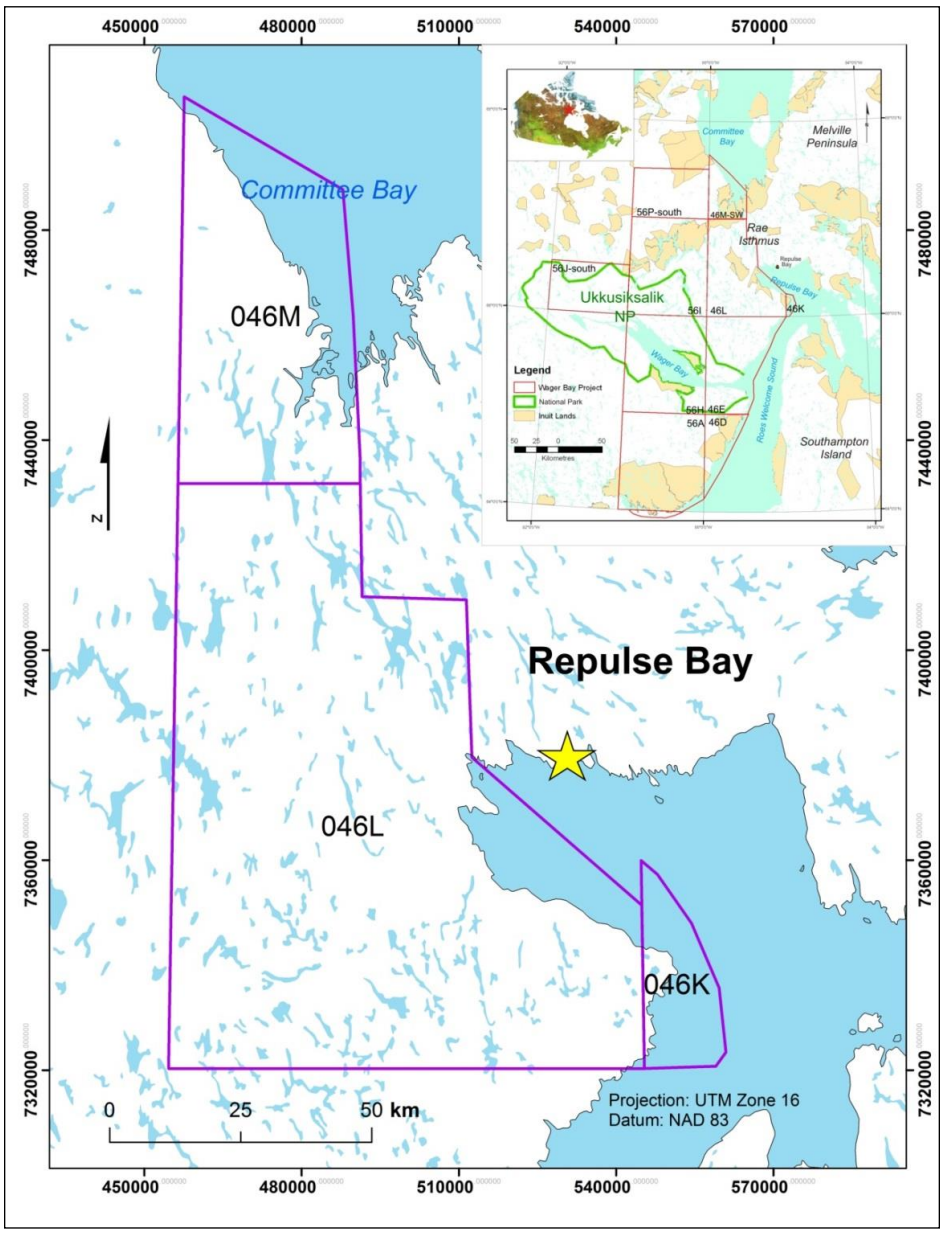

Figure 1.2: Location map of the thesis study area west of Repulse Bay, Nunavut. Inset map shows the project area around Wager Bay (from Campbell and McMartin, 2011).

1.5 Thesis Purpose/Objectives

The objectives of this thesis are to 1) investigate the impact of using a unique set of multispectral data - LANDSAT 7 TM and SPOT 4/5 imagery; 2) determine the most accurate RPM product(s); 3) compare classifications of LANDSAT and SPOT imagery using the same training areas, and 4) evaluate and compare the resultant predictive maps for accuracy against regions of known materials (regions of interest) as well as with existing surficial geology maps - results of the traditional geological mapping. As part of the latter objective (4), two interactive

processes to improving the accuracy of predictive maps are evaluated and compared: a geological, knowledge-based approach, and a statistical-based approach.

1.6 Methodology: General Overview

1.6.1 Data Acquisition, Image Preparation and Masking

LANDSAT TM-7 imagery was obtained from GeoGratis (http://geogratis.cgdi.gc.ca), a Natural Resources Canada website. Individual LANDSAT tiles were then mosaicked, through combined efforts by the Geological Survey of Canada and Blackbridge Geomatics (formally Iunctus Geomatics), to produce a seamless single image covering the study area. SPOT 4/5 imagery was obtained from and mosaicked by Blackbridge Geomatics.

As water was not to be classified in this study, it was masked out using the masking tool in the ENVI® software platform. This ensured exclusion of running water, standing water and heavily saturated areas from the classification. For both imageries this was completed using the near-infrared (NIR) channel (band 4) which easily discriminates water from land (Frazier and Page, 2000). Clouds and cloud shadows were also masked out using manual digitizing techniques and appended to the water mask for each SPOT and LANDSAT imageries. These final masks were applied to the individual LANDSAT and SPOT classification process.

1.6.2 Field Data Collection and Selection of ROIs

Surficial materials present in the study area were determined by fieldwork. Point data information was collected at specific field sites including coordinates, general terrain descriptions, geomorphological conditions, surficial material type, surface texture, boulder cover (%, presence, size, and shape), vegetation cover (%), moisture content, geomorphology, topography, drainage and lithology. Photographs were also taken at each site. These field observations ensured that classes used in the classification process were reflective of those materials existing in the predictive mapping study area.

Specific areas with distinct internal characteristics were manually delineated as polygons on air photos from a combination of air photo interpretation and field work and digitally captured in ENVI software as Regions of Interest (ROIs). They were amended upon visual exploration of spectral response of LANDSAT imagery (bands 7, 4, 2) and classes refurbished by division of classes and addition of new classes as seen fit. ROI quality assurance involved manually reshaping or eliminating ROIs to produce the most homogeneous group of pixels per class, based on their visual appearance, as produced by band combination 7, 4, and 2.

Finally, fieldwork, visual analysis/interpretation and statistical analysis helped to evaluate ROIs. ROIs that visually appeared spectrally different than other ROIs of the same class were evaluated in the field. ROI classes were also evaluated using a numerical method that calculates

the statistical separability between classes, known as the transform divergence (TD) statistic (Richards and Jia, 1999).

1.6.3 Classification Method - LANDSAT

The Maximum Likelihood Classification (MLC) algorithm – a supervised classification (Tso and Mather, 2009) – was run on 6 available LANDSAT bands using 21 surficial materials classes. The input LANDSAT imagery, associated water/cloud masks, and ROIs representing 21 classes, were entered into the algorithm to produce a classification map. Results were visually and statistically assessed, and modifications and subsequent classifications were run. This iterative process lead to the 4 most optimal classified maps of known surficial materials in the study area, which resulted in 4 groups of classes that best reflect these materials. These 4 groups of classes were determined using two approaches: 1) geological knowledge-based and 2) statistically-based.

1.6.4 Statistical and Geological Knowledge to produce a best-fit class combination

Visual assessment, or the "geological knowledge-based" (GK) approach involved determining the most appropriately mapped class combination, which was based on geological mapping results of the region, derived from knowledge of the Quaternary geology, air photo interpretation and field observations. Maps derived from this approach are generalized and formulated by definition of the process, which considers interpretations of depositional environments, geomorphology and relative age of the materials. Merging/deleting classes for subsequent trial iterations followed comparing classifications to the mapped surficial geology of the region. After which predictive maps of different class combinations were assessed. Finally, two maps were selected that were most consistent with interpreted geology.

Selecting two classification maps and class combinations was also made using a statistical approach. This considered statistics of the confusion matrix from a classification using 21 classes, and used User and Producers accuracies to provide an unbiased decision without interpretation. The purpose here was to select the most accurate maps after a number of iterations and simultaneously increase accuracy within individually mapped classes. Various modifications to class combinations were employed and applied to subsequent classifications solely based on statistics. Best classification maps were selected based on statistics including: 1) a map with highest overall accuracy and 2) a map whose confusion matrix illustrates individual class accuracies as "moderate" (35-70% accurate) or "well" (+70% accurate) mapped.

1.6.5 Classification applied on SPOT imagery

The supervised MLC algorithm (Tso and Mather, 2009) was applied to SPOT imagery, in a similar way as with LANDSAT (cf. Sect. 1.6.3). It used the best derived class combinations (2 geological knowledge-based and 2 statistical-based) (cf. Sect. 1.6.4) and was applied to classify SPOT imagery (4 bands) at 20 m resolution.

1.6.6 Comparison of SPOT and LANDSAT classifications to existing Surficial Materials Map

Qualitative and GIS comparisons were completed on a smaller region within the study area. Within a ~180 km^2 sub-region of the thesis study area, a surficial materials map was compared to SPOT and LANDSAT classifications. The surficial materials map was derived from a surficial geology map produced using traditional geological mapping techniques including fieldwork, air photo interpretation and analysis of collected field information (Campbell and McMartin, 2014). Surficial units were regrouped to best reflect and accommodate classes used in the RPM classifications. The map was converted to a raster and along with results of SPOT and LANDSAT classification maps, it was resampled to a 100 m pixel size. This was to produce a more direct comparison between the two maps. Up-scaling the classification maps mimics the generalization applied in surficial mapping which leads to large homogeneous polygons, rather than heterogeneous pixelated products. Qualitative (visual) and quantitative (using GIS) comparisons were made between the surficial materials map and remote predictive map results. The qualitative comparison visually assessed differences between the classifications within the sub study region and derived surficial materials map. The quantitative comparison measured cross-tabulation on a pixel level to measure the agreement/disagreement between individual predictive maps with the surficial materials map which indicated a numerical and spatial correspondence across the sub-region.

1.7 Thesis Structure

This thesis includes two chapters written in "paper format", as well as an Introduction Chapter and a Conclusion Chapter, which are necessary to present the research problem, purpose, and contributions as a whole. More specifically, the Introduction Chapter presents a brief rationale for the study, the most relevant previous literature on the subject, as well the objectives of the study, and overview of methodology.

The second Chapter is a government publication - an Open File Report and data release from the Geological Survey of Canada[*]. The Open File Report presents the step-by-step method to produce RPM maps for this study area and digital datasets including raster image files, classification maps and corresponding variability maps as well as other raw data. It is co-authored with Martin Ross (thesis supervisor), Isabelle McMartin (co-supervisor), as well as Janet Campbell (NRCan), Eric Grunsky (NRCan), and Jeff Harris (NRCan). My responsibilities in this project included data collection, analysis, production and analysis of output products and preparation of the report. Coauthors contributed to designing of the study presented in the Open File, and to revision and editing earlier drafts. Additional roles included Janet Campbell for

[*] Wityk, U., Harris, J.R., McMartin, I., Campbell, J.E., Ross, M., and Grunsky, E., 2013. Remote Predictive Mapping of Surficial Materials West of Repulse Bay, Nunavut (NTS 46M-SW, 46L-W and -S, 46K-SW); Geological Survey of Canada, Open File 7357. doi:10.4095/292578

helping in refurbishing training areas and breaking down surficial material classes, and Jeff Harris for working out software issues, leveling and mosaicking imagery and understanding RPM methodologies.

The third Chapter compares the classification maps produced by LANDSAT and SPOT imagery as well as a comparison of both maps to a small region of the study area mapped using traditional methods. I was responsible for the GIS methodology, visual comparison and comparison analysis. As first-author, I wrote the third Chapter as a manuscript for future consideration as peer-reviewed publication. Co-authors on this future publication will be the same as for Chapter 2 since they all contributed to the design of the study and review of earlier drafts. In addition, Janet Campbell and Isabelle McMartin compiled and modified the field-based map used in this study to better reflect units used in the classified maps.

The fourth, concluding Chapter summarizes key findings, discusses the research projects contribution to science and suggests avenues of future research that will enhance the scientific understanding of the processes and methodologies presented in this thesis.

Chapter 2: Remote Predictive Mapping of Surficial Materials west of Repulse Bay, Nunavut (NTS 46M-SW, 46L-W and –S, 46K-SW)

2.1 Introduction

Quaternary geological mapping in the Wager Bay-Repulse Bay region of mainland Nunavut was initiated in 2009 at the Geological Survey of Canada within the framework of the Geo-mapping for Energy and Minerals (GEM) Program. The purpose of this activity was to address and fill in knowledge gaps with respect to the distribution and nature of Quaternary sediments, regional drift composition, and glacial and post-glacial histories. As part of this work, a Master's thesis research project was undertaken to assist the mapping of surficial earth materials by Remote Predictive Mapping (RPM) in an area covering parts of NTS sheets 46 K, L and M located near Repulse Bay, Nunavut (Fig. 1). The purpose of this Open File publication is to release a selection of RPM classification maps and accompanying datasets for the study area specific to the thesis project.

Remote Predictive Mapping is a semi-automated approach used to increase the efficiency of mapping bedrock and surficial geology over large regions of Canada's Far North (Harris, 2008a, 2008b). It is a useful tool, especially for producing maps of regions that will not be field mapped or have limited fieldwork in the foreseeable future due to logistical constraints, high costs and the size and remoteness of the map area. The purpose of this new mapping approach is not to replace traditional geological mapping i.e. field work and interpretation of air photos, but rather to enhance the mapping process by providing insight regarding surficial materials found in these regions. These constraints on fieldwork can, in part, be addressed through the use of remotely sensed imagery which offers a broad view of large inaccessible areas, providing a wealth of geologic information that can be enhanced and processed using image analysis and GIS technologies (Harris, 2008a, 2008b). RPM is a tool to aid fieldwork, streamline the mapping process, as well as enhance extrapolation and interpretation between field observation sites.

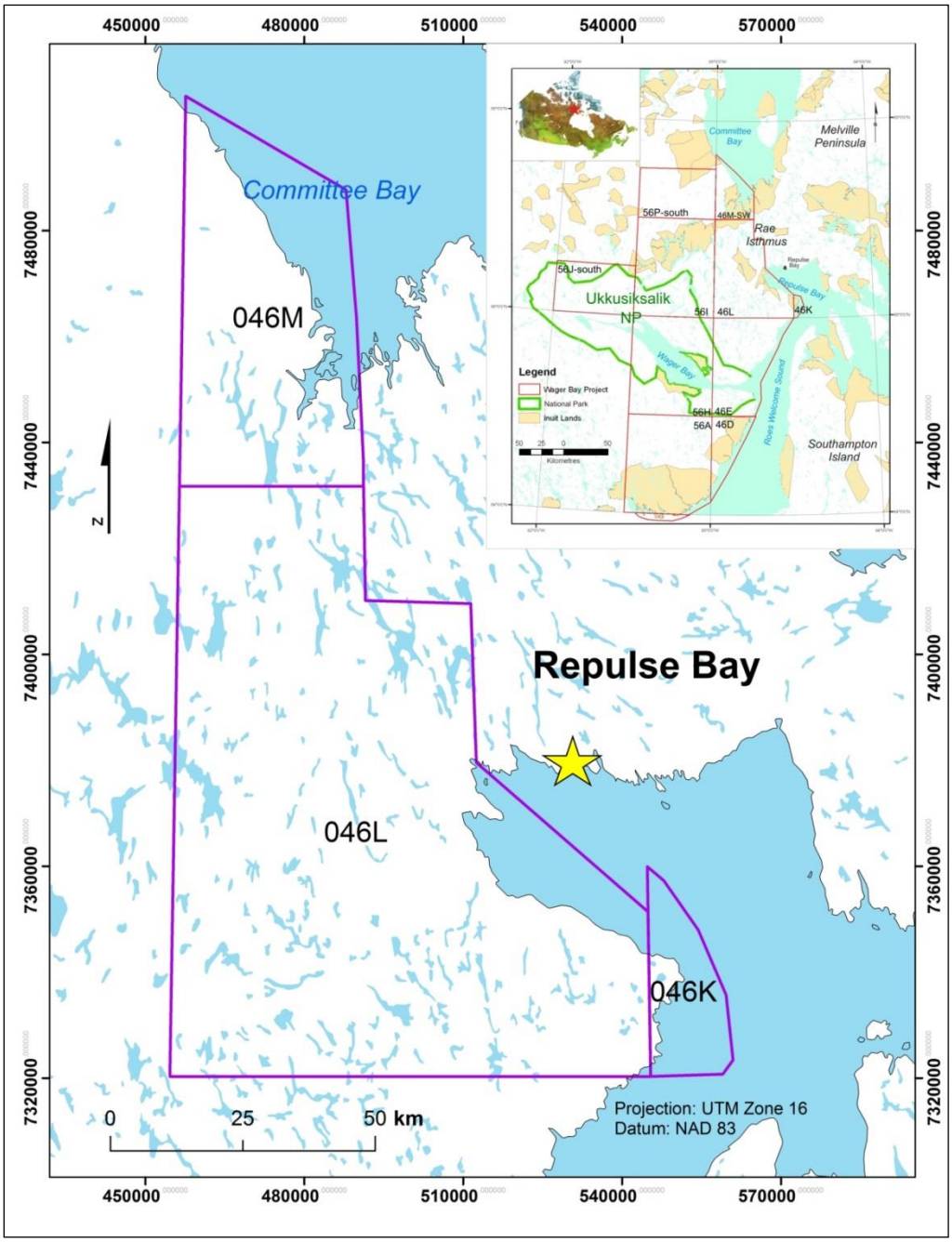

Figure 2.1: Location map of study area west of Repulse Bay, Nunavut. Inset map shows the project area around Wager Bay (from Campbell and McMartin, 2011).

This Open File report includes information regarding the regional setting of the study area, and a description of the methodology used to produce RPM maps for the Repulse Bay study area, including data acquisition and preparation, field data collection, region of interest (ROI) selection and evaluation, and classification methods. The report also discusses four of the

classification maps that offer the highest classification accuracies determined through analysis of a confusion matrix and associated variability maps. The datasets related to the RPM classification maps include: LANDSAT data, raster image files of the four classification maps and corresponding variability maps, ROIs (in the form of vector shape files in ENVI) used to produce the maps, and the base layers of the study area.

2.2 Regional Setting

The RPM study area is located on mainland Nunavut west of the northern community of Repulse Bay between latitudes 66°N and 67.5°N and longitudes 88°W and 86°W (Fig. 2.1). It is comprised of parts of NTS map sheets 46K, 46L and 46M. The region is located along the west coast of Hudson Bay, west of Committee Bay and Repulse Bay. It is underlain by Canadian Shield rocks of the western Churchill Geological Province including Archean through Paleoproterozoic intrusive and supracrustal rocks within the 2.7-2.6 Ga Rae Domain (Paul et al., 2002), and covered by fairly continuous glacial drift which is streamlined in the general direction of the regional ice flow, predominantly northward (Prest et al., 1968; Aylsworth and Shilts, 1989; McMartin et al., 2013). Marine limit elevations decrease from approximately 240 m asl to 140 m asl southward within the study area. Extensive areas of marine sand, silts and clays are exposed along the Committee Bay coastal plain in 46M-SW (e.g. Campbell and McMartin, 2010).

2.3 Methodology

The methodology used here is modified after the RPM approaches of Grunsky et al. (2006, 2009), Schetselaar et al. (2007) and Harris et al. (2008a; 2012) (Fig. 2.2). It uses data acquisition and image preparation, fieldwork and selection of training data, which are then applied to a maximum likelihood classification (MLC) algorithm to produce classification maps of surficial materials. Two approaches are used to determine the optimal class combination and resultant MLC maps: a geological knowledge-based approach and a statistical approach. The preferred optimal class combinations are then run through the robust classification method (RCM) to produce variability maps and evaluate the uncertainty of the classifications.

2.3.1 Data acquisition, image preparation and masking

LANDSAT TM-7 imagery used in this study (Table 2.1) was downloaded from GeoGratis (http://geogratis.cgdi.gc.ca), available from Natural Resources Canada, in GeoTIFF format. After collection, the individual scenes were “stitched” together by the Geological Survey of Canada and BlackBridge Geomatics (formally Iunctus Geomatics). The overlapping LANDSAT scenes were combined and leveled to produce a single visually, but unfortunately not spectrally seamless image of the study area (Fig. 2.3). LANDSAT images were projected to Universal Transverse Mercator (UTM), Zone 16, and referenced to the North American Datum (NAD83). The mosaic image was then clipped to the boundaries of the study area. Cutlines, and

borders at which individual imagery scenes were "stitched" together, are shown in white on Figure 2.4.

Water was not classified in this study. Running and standing water, along with heavily saturated areas, were masked out using the masking tool in ENVI, or more specifically spectral principles. This was accomplished by utilizing the LANDSAT near-infrared (NIR) channel (band 4), which easily identifies water (Frazier and Page, 2000). The interactive stretching tool in the ENVI interface was used to discriminate pixels with digital numbers (DN) representing water. Clouds and cloud shadows were also masked by manually digitizing cloud polygons in the ENVI software package as ROIs. Then, using simple band math, water and cloud masks were merged together to create a final mask for the LANDSAT mosaic image (Fig. 2.5). The purpose of this masking process is to exclude water bodies (inclusive of lakes and saltwater and sea ice), and clouds from the classifications, which would artificially inflate overall accuracy measures.

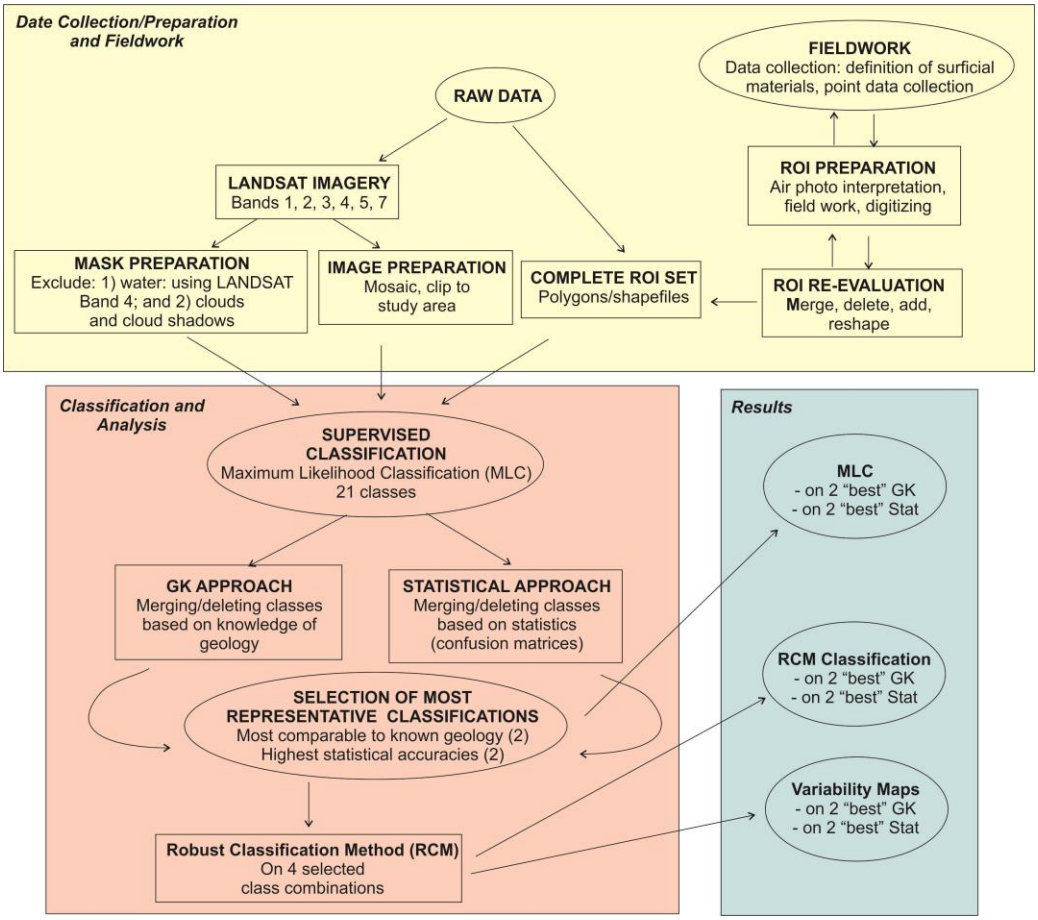

Figure 2.2: Flow chart outlining steps to produce RPM of surficial materials using supervised classification and selection (Geological Knowledge and Statistical approaches) of most representative classifications to arrive at final maps.

Table 2.1: Summary of data characteristics

Data	Source	Bands	Channels	Resolution
LANDSAT TM-7	GeoGratis (http://geogratis.cgdi.gc.ca)	1, 2, 3, 4, 5, 7	Visible, NIR, SWIR	30 meters

2.3.2- Initial field data collection and selection of ROIs

Initial fieldwork, conducted in the summer of 2010, involved determining the surficial materials present in the study area, and acquiring field observations. This included making observations regarding surficial geological units as part of the mapping activity as well as collecting point data information for specific field sites. The observations collected included site location (latitude/longitude), general terrain descriptions and geomorphological conditions. Surficial material type, surface texture, boulder cover (%/presence/size/shape), vegetation cover (%), moisture content, geomorphology, topography, drainage and lithology were systematically noted. Photographs were taken and recorded at each site. Initial field data collection ensured that the classes used in the supervised classification process reflected the diversity of surficial materials present in the study area.

The first season of fieldwork and preliminary air photo interpretation (guided by the GSC field geologists) identified eleven classes of surficial materials, having distinctive physical (mainly textural) and geomorphological characteristics.

This initial working class list included:

1. Ap – Alluvial plain sediments
2. Mg - Marine, gullied fine-grained sediments
3. Ms – Marine sands
4. O – Organic
5. SG – Sand and gravel
6. R - Bedrock
7. Tb – Till blanket
8. Tm – Modified till
9. Tv – Till veneer
10. B - Boulders
11. Tr – Ribbed till

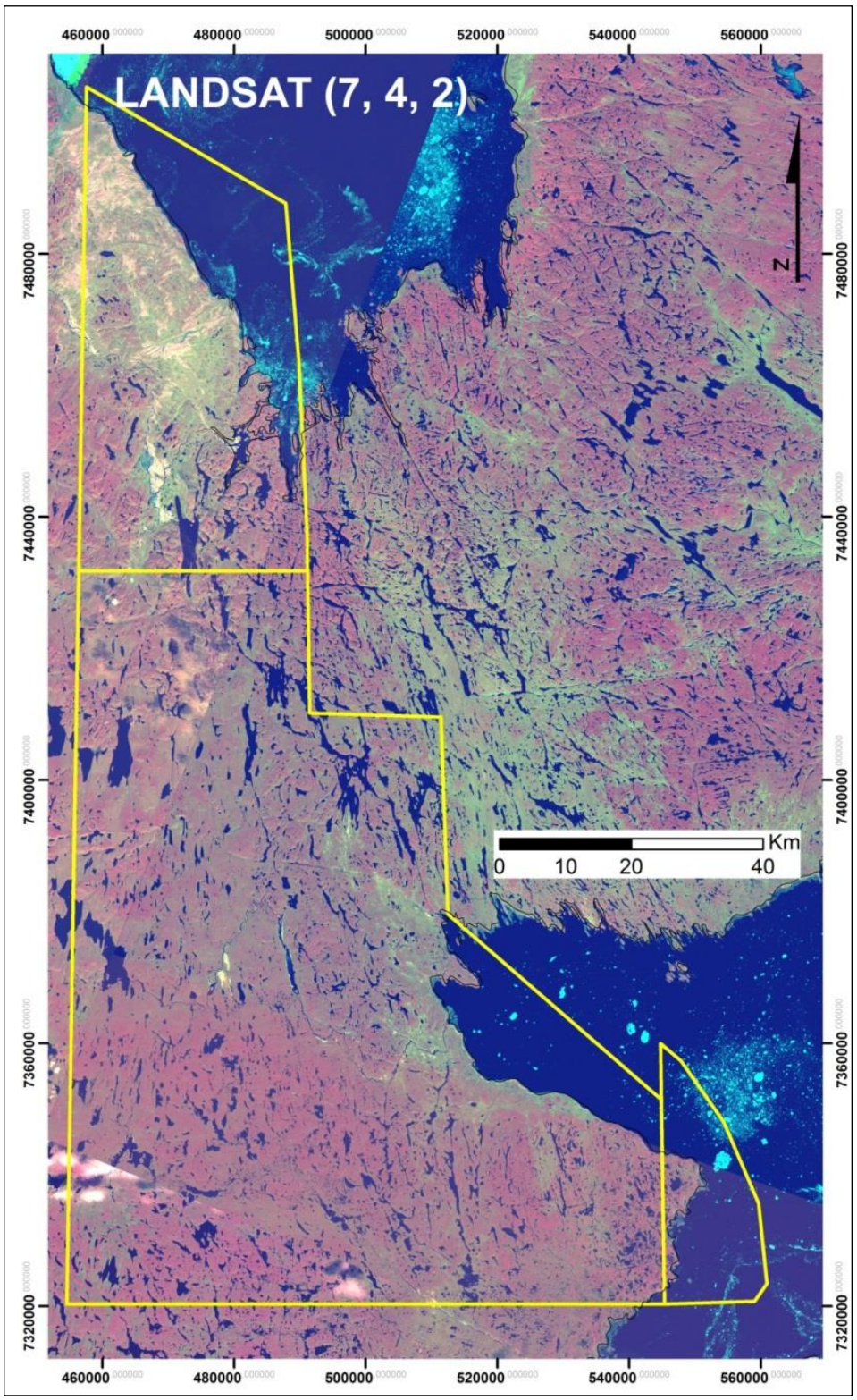

Figure 2.3: LANDSAT imagery presenting RGB bands 7, 4, 2. Study area outlined in yellow.

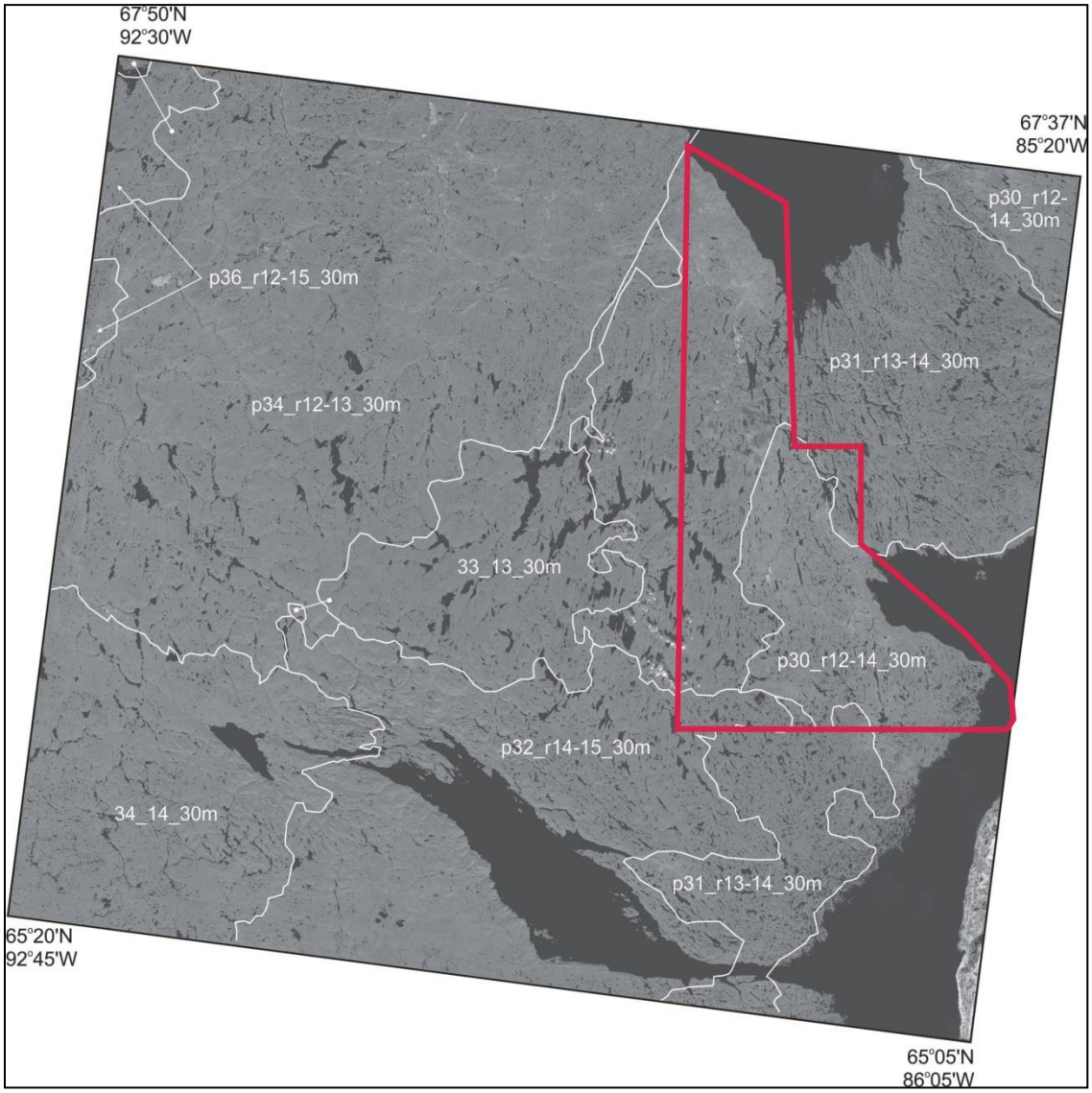

Figure 2.4: LANDSAT 7 (SWIR, band 5) imagery cut-lines over the Wager Bay North area. White lines indicate boundaries where LANDSAT scenes were merged together (Campbell et al., 2013.). The red line outlines the study area.

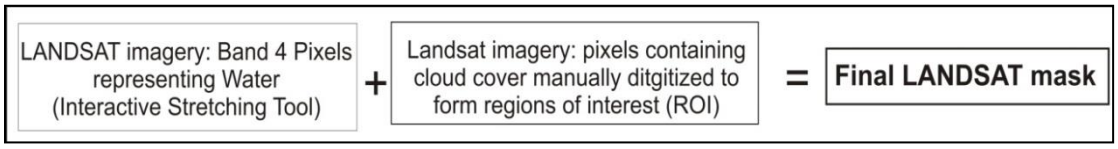

Figure 2.5: Production of final mask to mask out water and cloudy regions.

In the fall of 2010, multiple regions of interest (ROIs) were carefully selected to represent each of the 11 surficial material classes identified after the first field season. The ROIs were manually delineated as polygons on air photos, using a combination of field data, air photo interpretation and visual analysis of LANDSAT imagery. The polygons were then transferred on printed maps of LANDSAT imagery (bands 7, 4, 2) and then digitally captured in ENVI software as ROIs.

2.3.3 - Final ROI selection

Upon review of the satellite imagery in the winter 2010/spring 2011, two additional classes were added to the original 11 classes: ice-covered regions (ice/snow) as well as shallow water (Sw) thus resulting in 13 classes in total. After the second field season (July 2011) and a review of the original ROIs through visual exploration of the spectral response of LANDSAT imagery (bands 7, 4, 2), some classes were divided into sub-classes. A carbonate till unit (Ct) was also added based on the mapping of suspected carbonate till after a preliminary supervised classification in the spring of 2011 and confirmation in the field in 2011. Existing ROI polygons were assigned to sub-classes (i.e. Tb classes were divided into Tb1 and Tb2), and additional ROI polygons were defined to ensure each class had a sufficient number of ROIs to produce a robust classification. ROIs were added using air photo interpretation and visual analysis of spectral responses on LANDSAT (7, 4, 2) imagery which highlighted the spectral variation between surficial materials. It was apparent through visual analysis that the Ms, Tb, Tv, Tm, R, and SG classes could be further subdivided by differences in spectral response into subclasses (Ms1, Ms2, Tb1, Tb2, Tv1, Tv2, Tm1, Tm2, R1, R2, SG1, SG2 and SG3). Thus the final number of surficial material classes to be classified totalled twenty-one. As part of quality assurance/control, some original ROIs were manually clipped and/or reshaped while others eliminated in order to have the most homogeneous group of pixels per class based on their visual appearance (colour) using LANDSAT bands 7, 4, 2. The following table (Table 2.2) is a list of the division of classes. A further detailed description is available in Appendix A (Class descriptions). Figure 6 shows the location of the final regions of interest.

2.3.4- Evaluation of ROIs

The ROIs were evaluated through fieldwork, visual analysis/interpretation and statistics. After their initial delineation following the first round of fieldwork, the ROIs were visually assessed; and those that were spectrally (in a visual sense) different to the other ROIs of that class were investigated during the second season. As a result, a significant number of the field-verified ROIs were used for control and the basis for comparison included in the classification process. ROIs were also evaluated based on the Transform Divergence (TD) statistic which measures the statistical separability between pairs of classes. The average separability for each class is presented in Fig. 2.7. The TD statistic is a number between 0 and 2 in which values <1.0 indicate very poor separation between classes, 1.0-1.9 indicates poor to moderate separation, and 1.9-2.0 good separation (Richards and Jia, 1999). Figure 7 shows that the average class separability ranges from poor/moderate (1.0-1.9) to good (1.9-2), with the majority of classes falling under the moderate category. Those classes that are spectrally separable from others

include Ap, Sw, Mg, Ms1, Ice/Snow, O, SG3, and Ct. Till, bedrock, together with sand and gravel subclasses, are characterized by lower average TD values (moderate or poor separation), suggesting that the potential for confusion between these subclasses will occur. Confusion between classes occurs when surficial characteristics are alike. Having the same type/amount of vegetation cover, mineralogy, and similar moisture content on two different sediment classes can produce an overlapping spectral signature between classes, which may lead to class confusion. Part of this confusion is captured in the variability maps that are generated in the classification process. Once identified, these areas of uncertain classification can be excluded from the classification map if desired.

Table 2.2: List of 21 surficial material classes, with code and colour as per classified maps, and short description. The complete description of the classes are provided in Appendix A (Class descriptions).

Surficial Material Class	**Code**	**Colour Classification**	**General Description**
Exposed alluvial sediments	Ap		Alluvial sands and minor silts; exposed
Marine gullied fine sediments	Mg		Marine silts and clays; exposed sediments; gullied
Marine fine sediments	Ms1		Marine fine sands, silts and clays; some surface runoff features
Marine sands and silts	Ms2		Marine sands and silts; nearshore deposits; coarser than Ms1
Ice/snow	Ice/Snow		Frozen water
Organics	O		Thin organic deposits
Vegetated coarse sand and gravel	SG1		Glaciofluvial and marine sands and gravels
Sand and gravel	SG2		Marine fine-grained sands, silty-sands
Exposed sand and gravel	SG3		Glaciofluvial and marine sands and gravels; exposed

Table 2.2 (Continued)

Bedrock (bare)	R1		Bedrock; exposed
Bedrock	R2		Bedrock with some discontinuous material cover; lichen covered
Boulder fields	B		Broken bedrock; continuous boulder cover
Till blanket	Tb1		Thick drift cover with little boulder cover or exposed bedrock
Bouldery till blanket	Tb2		Thick drift cover; more boulders and less vegetated than Tb1
Modified till	Tm1		Modified till; eroded in places; may include sand and gravel; bouldery
Modified till	Tm2		Modified till; less bouldery than Tm1
Till veneer	Tv1		Thin drift cover; mixed with bedrock and boulders or bedrock and sand; contains more boulder/bedrock terrain than Tv2
Till veneer	Tv2		Thin drift cover; contains more moisture and vegetation than Tv2
Carbonate till	Ct		Till with carbonate clasts and calcareous matrix
Ribbed till	Tr		Till mixed with sand, gravel and boulders; eroded, disorganized, gravelly ridges, terraces and hummocks
Shallow water	Sw		Heavily sediment laden water

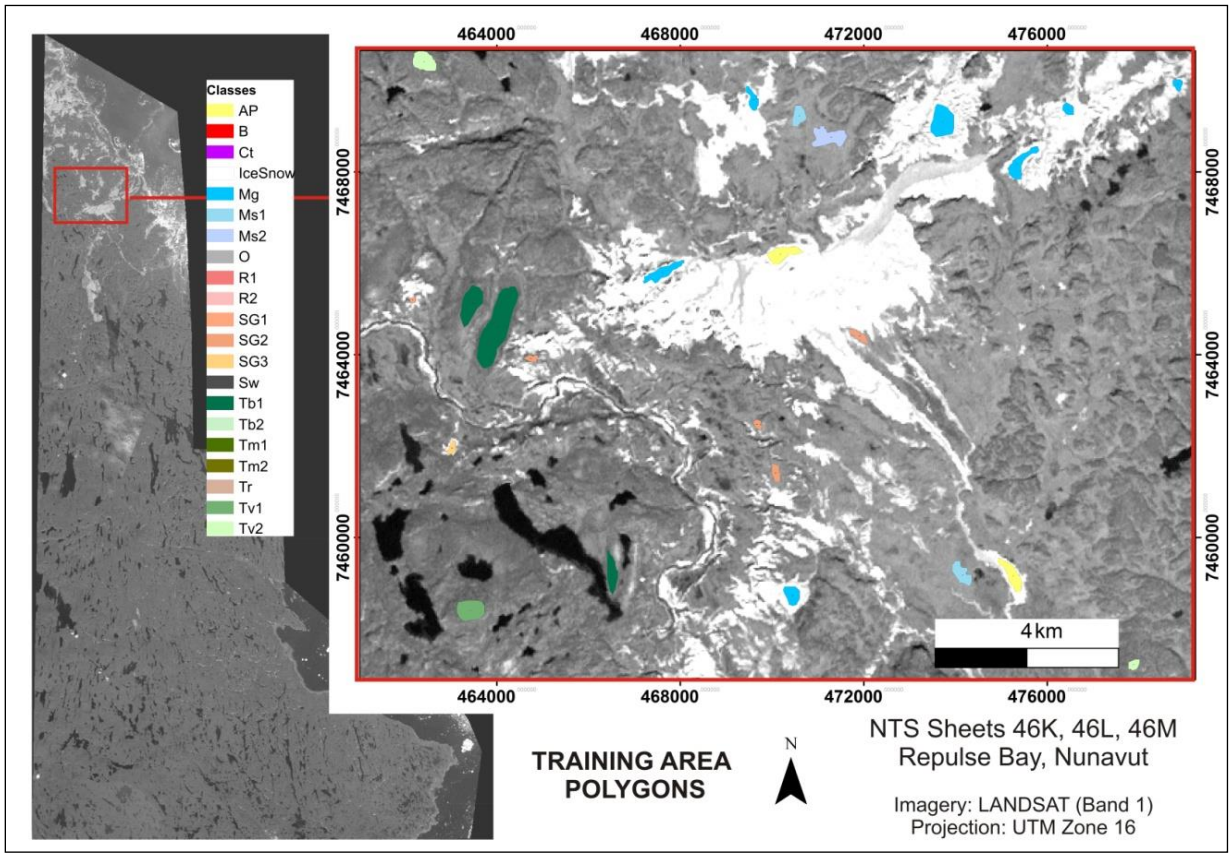

Figure 2.6: Location of ROIs used to produce classification maps. Inset map shows example of ROI polygons and their locations overlain on LANDSAT imagery (Band 1).

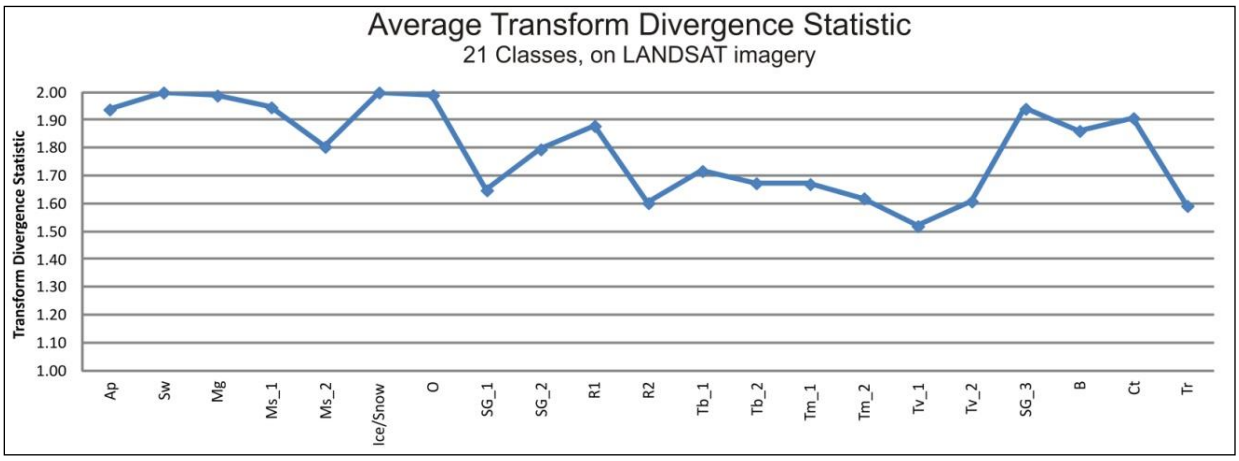

Figure 2.7: Average Separability Statistic of 21 classes for the Repulse Bay Study area. Calculated on LANDSAT imagery for the region.

2.3.5- Classification method and selection of "best" RPM classification maps

A supervised classification using single pass maximum likelihood classification (MLC) algorithms were run on all 6 available LANDSAT bands (Table 2.3), using all 21 surficial materials classes (Table 2.2).

Table 2.3: Summary of LANDSAT Bands and reflectance data used to produce MLC classification maps of surficial materials.

Band	Reflectance Data Recorded
1	Blue (B)
2	Green (G)
3	Red (R)
4	Near-Infrared (NIR)
5	Short Wave Infrared (SWIR)
7	Short Wave Infrared (SWIR)

To produce the four "best" MLC classification maps, a geological knowledge-based (GK) approach to earth material classification was evaluated against a statistically based approach involving computer-assisted numerical analyses. Each approach yielded a selection of two predictive surficial materials maps of the study area, totaling four "best" RPM maps. For purposes of this Open File, the term "best" refers to the most appropriately mapped training area combination (geological knowledge-based approach) and highest accuracies (statistical approach) of the run classification iterations.

The geological knowledge-based approach involved comparison of RPM maps with geological mapping results for this region, based on expert Quaternary knowledge, air photo interpretation and field observations. It included 1) a careful visual interpretation of the satellite imagery by the Quaternary geologists, specifically redefining ROIs spectrally and merging/deleting classes, 2) an assessment and comparison of a series of predictive maps produced from using different combinations of the 21 established classes, and the 3) selection of two of these maps most consistent with the interpreted geology (See Figure 2.8). (1) Visual interpretation of the imagery included noting comparisons of known surficial materials and their visual spectral characteristics on LANDSAT imagery (band combination 7, 4, 2). (2) An assessment of RPMs included visual comparison of classification outputs against one another, as well as considering expert Quaternary knowledge. These outputs were based on various iterations (trial and error) of class combinations suggested using geological-knowledge input. (3) The selection of the maps most consistent with geology was based on how well the RPM maps

matched the surficial geology of the region mapped by geologists. Table 2.4 presents the overall accuracies and the individual class accuracies for these two maps.

Two other "best" MLC classification maps were chosen based on an unbiased statistical approach, which investigated the statistics of the confusion matrix of a classification using all 21 classes. To produce the two most statistically accurate maps, both general (overall accuracy) and detailed (individual class accuracy – i.e. user's and producer's accuracy) data were considered. The producer's accuracy measures the number of pixels within a particular class that have been classified appropriately. The user's accuracy measures how many pixels of a class were classified properly over the total number of pixels assigned to that class (Grunsky et al., 2009). This approach produced an unbiased decision *without* expert interpretation. The goal was to select the most accurate maps through various iterations; and in the process, increase accuracy within each individually mapped surficial material class. This was accomplished by using all earth materials in the classification to produce a confusion matrix to assess which classes were mapped reasonably (70% accurate), "moderately" (35-70% accurate), and "poorly" (<35%). Classes that were mapped with an accuracy below 70% were investigated and decisions were made for further classification modifications to improve class accuracies and/or overall accuracies of the map: for example, removing or merging classes used in the original classification for a subsequent re-classification. Accuracy was obtained from the confusion matrices calculated using the ROI set employed in each classification (see Appendix B).

Table 2.4: Calculated overall and individual class accuracies of the 4 "best" MLC classification maps GK1, GK2, Stat1, Stat2. Notation "m" indicates these classes have been merged with another class; "e" indicates class was eliminated and not used in the classification.

GK1		**GK2**		**Stat1**		**Stat2**	
Overall Accuracy	**60.54**		**60.42**		**62.17**		**60.64**
Ap	77.06	Ap	77.06	Ap	76.14	Ap	76.14
Mg	88.23	Mg	88.23	Mg	88.23	Mg	88.23
Ms1	91.88	Ms1	91.88	Ms1	91.94	Ms1	92.2
Ms2+SG2	59.18	Ms2+SG2	61.63	Ms2	62.99	Ms2	"m"
O	78.54	O	81.78	O	76.92	O	77.33

Table 2.4 (*Continued*)

SG1	25.52	SG1	31.09	SG1	"e"	SG1+SG2+Ms 2	45.21
SG2	"m"	SG2	"m"	SG2	"e"	SG2	"m"
SG3	61.88	SG3	61.88	SG3	63.39	SG3	62.03
R1+R2	48.6	R1+R2	64.09	R1	70.75	R1	66.23
R2	"m"	R2	"m"	R2+Tm1	45.62	R2	31.98
B	89.19	B	92.16	B	86.22	B	81.62
Tb1+Tb2	48.01	T	49.65	Tb1	56.35	Tb1	56.99
Tb2	"m"	Tb2	"m"	Tb2	48.8	Tb2	48.03
Tm1+Tm2	61.66	Tm1	"m"	Tm1	"m"	Tm1	64.77
Tm2	"m"	Tm2	"m"	Tm2	53.51	Tm2	50.69
Tv1+Tv2	49.12	Tv1	"m"	Tv1+Tv 2	51.25	Tv1+Tv2	43.09
Tv2	"m"	Tv2	"m"	Tv2	"m"	Tv2	"m"
Ct	90.59	Ct	91.15	Ct	86.07	Ct	87
Sw	94.4	Sw	94.4	Sw	"e"	Sw	"e"
Ice	7.37	Ice	7.37	Ice	"e"	Ice	"e"

A scale for merging classes based on their separability was developed to assist in reducing the confusion between classes. The separability thresholds for this scale included: <1% for low, 1-10% for moderate and >10% for high. If confusion of an individual class was statistically high, and was higher than the accuracy of the class itself, the class was removed and subsequent classifications were run without that class. If there was a moderate or high confusion with another class, but the value was still lower than the class accuracy, these two classes were merged together to form a new class. For example, in a manual analysis of a confusion matrix calculated from a classification result, the confusion matrix revealed an accuracy of 31.79% for class R2. Since its confusion with another class (Tm1) was at 25.63%, R2 was not deleted, but merged with Tm1, producing a new class: R2_Tm1.

The various modifications to the class combinations were used in the initial classifications and applied to subsequent classifications, which included one modification to the total number of classes used (i.e. only one alteration, merging classes together, or deleting them), until adequate accuracies (>35%) were attained. The two "best" MLC classification maps selected based on statistics include: 1) a map with the highest overall accuracy (Statistical 1: STAT1), and 2) a map whose confusion matrix illustrates that individual class accuracies are all "moderately" (35-70% accurate) or "well" (+70% accurate) mapped, and none are "poorly" (<35%) mapped (Statistical 2: STAT2). Both maps are presented in Figure 2.9.

2.3.6- Variability and majority classification maps

Once the four "best" supervised classification maps were chosen, the resulting class combinations, based on different test runs involving the merging of the original 21 classes, were run through the robust classification method (RCM). The RCM algorithm produces a majority classification map, a variability map, and more summary statistics (Harris et al., 2012). The method uses a training dataset that is repeatedly and randomly split into two groups of ROIs: one for classification and the second for evaluation. These two groups comprise random collections of the ROIs for each repetition which are specified by the user. For example, in a specification of a 50% sampling percentage, each repetition will involve a different combination of 50% of the ROIs (Harris et al., 2012). Outputs of the RCM are based from inputs specified by the user, including: input files, ROIs, ROI sampling percentage, sampling type, classification method, threshold, number of repetitions, and a root name for output files (Harris et al., 2012). The user inputs specified in this study to produce variability and majority classification maps included a sampling percentage of 50, sampling type based on polygon and a repetition of 40, meaning that 40 iterations using random combinations of 50% of the data for classification and the other 50% for validation. The RCM variability (uncertainty) map provides a summary of the number of different classes that have been classified on a pixel-to-pixel basis over the 40 iterations of the RCM algorithm (Harris et al., 2012). Variability maps were produced for each the surficial material majority classification maps to show their respective spatial variability in terms of the degree of uncertainty or reliability of pixel classification in the repetitive classification processes. Masked areas were not included in the classification and accuracy assessment. The variability maps are provided in Figure 2.10 and 2.11. The RCM majority classification maps were produced but are not discussed in this thesis as they were an additional product of the RCM method from which variability maps were produced. For purposes of this research, the RCM method was used to produce variability maps and focus was placed solely on using MLC due to time constraints and various iterations of class combinations that were run.

2.4 Results and Discussion

2.4.1 Maximum Likelihood Classification Maps

The four "best" Maximum Likelihood Classification (MLC) maps show similarities and differences with respect to the classification of surficial materials (Figs. 2.8 and 2.9). General consistencies across the four maps include similar mapping of the classes Ap, and Mg/Ms-related

sediments. These materials were mainly classified in the northernmost coastal region of the study area. Various combinations of till classes are consistently mapped in the mid to southern part of the study area. Rock and boulder units are generally mapped in similar areas across the four maps; however their classification densities in these areas differ. For example, in the central and western south of the study area, these units are more pronounced in the GK2 and Stat1 maps than in the GK1 and Stat2 maps although they appear in the same areas. This is the same scenario for the region in the North of the study area that occurs south of the dominated marine sediments (blue colours, as per the legend). Carbonate till is also mapped with some consistency across all four maps in the southeastern area, but with more variability within the central-eastern area. As discussed below, though repeated regional patterns are recognized, significant differences also prevail when comparing the four classified maps with one another. Table 2.5 below presents the class combinations used in the 4 "best" MLC maps that will be described in the following sections. Note that the ribbed till (Tr) class was entirely eliminated from all classifications as it disrupted classifications, as per visual analysis, and was clearly overrepresented for this region.

2.4.1.1 Map GK1: Geological Knowledge 1

Map GK1 (Fig. 2.8a), using 15 surficial classes (Table 2.5), classified the northern portion of the study area with dominant surficial materials comprising marine sediments and sand and gravel (Ms1, Ms2+SG2, Mg). Some of these sediments (Ms2+SG2) were also mapped along rivers and at low elevation in the south-central part of the study area along the coast, below the known limit of marine inundation. An extensive till cover (Tb1+Tb2 and Tm1+Tm2) was mapped (classified) in the central and southern region of the map, and carbonate tills were mapped in the southeast and central eastern regions.

The Ms2+SG2, Ms1 and Ct classes were mapped with reasonable accuracy based on the current surficial geology mapping activities undertaken at the GSC (Campbell and McMartin, 2010, 2011, 2014; Campbell et al., 2011; McMartin et al., 2012, 2013). Bedrock (R1 and R2) and boulder (B) regions were more sparsely distributed than evident during field mapping.

Table 2.5: Class combinations used to map the "best" MLC maps in this study; "m" indicates the class was merged with another class; "e" indicates removal of the entire class.

	GK1	**GK2**	**Stat1**	**Stat2**
Ap	Ap	Ap	Ap	Ap
Mg	Mg	Mg	Mg	Mg
Ms1	Ms1	Ms1	Ms1	Ms1
Ms2	Ms2+SG2	Ms2+SG2	Ms2	"m"
Ice/Snow	Ice/Snow	Ice/Snow	Ice/Snow	Ice/Snow
O	O	O	O	O
SG1	SG1	SG1	"e"	SG1+SG2+Ms2
SG2	"m"	"m"	"e"	"m"
SG3	SG3	SG3	SG3	SG3
R1	R1+R2	R1+R2	R1	R1
R2	"m"	"m"	R2+Tm1	R2
B	B	B	B	B
Tb1	Tb1+Tb2	T	Tb1	Tb1
Tb2	"m"	"m"	Tb2	Tb2
Tm1	Tm1+Tm2	"m"	"m"	Tm1
Tm2	"m"	"m"	Tm2	Tm2
Tv1	Tv1+Tv2	"m"	Tv1+Tv2	Tv1+Tv2
Tv2	"m"	"m"	"m"	"m"
Ct	Ct	Ct	Ct	Ct
Tr	"e"	"e"	"e"	"e"
Sw	Sw	Sw	”e”	”e”

2.4.1.2 Map GK2: Geological Knowledge 2

Similar to map GK1, map GK2 (Fig. 2.8b) classified the northern region with a dominance of marine sediments and sand and gravel (Ms1, Ms2+SG2, Mg). Marine sediments were also mapped similarly to map GK1 along the central coastal areas. A higher proportion of boulder fields and bedrock was mapped in the entire region, but are present in the same general areas as in map GK1. Though till was mainly classified in the central and southern parts of the map, its overall distribution is much less than that of Map GK1 because of the increased areas mapped as bedrock and boulders. Carbonate tills were mapped consistently between map GK1 and GK2, located in the southeast and central east portions of the region.

Similar to map GK1, Ms2+SG2 as well as Ms1 appear to be mapped reasonably well based on geological knowledge of the region, while the mapping of the boulder (B) class in map GK2 is more representative in the central/southern portion of the map in comparison to GK1. Bedrock is more pervasive in map GK2 than in map GK1, especially in the southeast portion of the study area along Repulse Bay and just west of southern Committee Bay. Although the three till units used in the previous classification were combined to form a single class in map GK2, the abundance of till classified here has significantly decreased.

2.4.1.3 Map STAT1: Statistical 1

This classification resulted in widespread abundance of marine sediments in the north - Ms and Mg and some Ap (Fig. 2.9). Till classes are dominant across most of the central and southern parts of the map; however, the southern areas contain a fair amount of bedrock as well as modified till. Marine sediments also occur near the central-east coast, with carbonate till in the southeast.

Based on geological field knowledge, marine sediments appear to be classified appropriately. The second marine sediment subset (Ms2) does not show much difference when combined with SG2. As per field observations, this map showed better predictions for the classification of boulder fields, which were mapped in eastern corridors of 46L, and the central portion of the study area. Carbonate till was not classified as abundantly in NTS 46M (northern study area), which is a more accurate representation when compared to field knowledge.

Although the statistical method (i.e. TD value) suggested that R2 and Tm1 are highly confused with one another and thus, could be combined, both units are not the same surficial material: R2 is bedrock while Tm1 is a bouldery till. It is possible that spectral characteristics of classes such as Tm1 and R2 (or R1) will vary with changes in bedrock lithology, but more likely with changes in boulder cover (percentage cover and boulder lithology) and with moisture content. These variations affects spectral signature within like-classes. The STAT1 map did not classify as much exposed bedrock (R1) as seen in the field, and assigned more areas as lichen-covered bedrock (R2). Although R1 is more pervasive in the central region and corresponds more closely to the surficial field mapping observations (Campbell and McMartin 2010, 2011, 2014), it is under-mapped in the north.

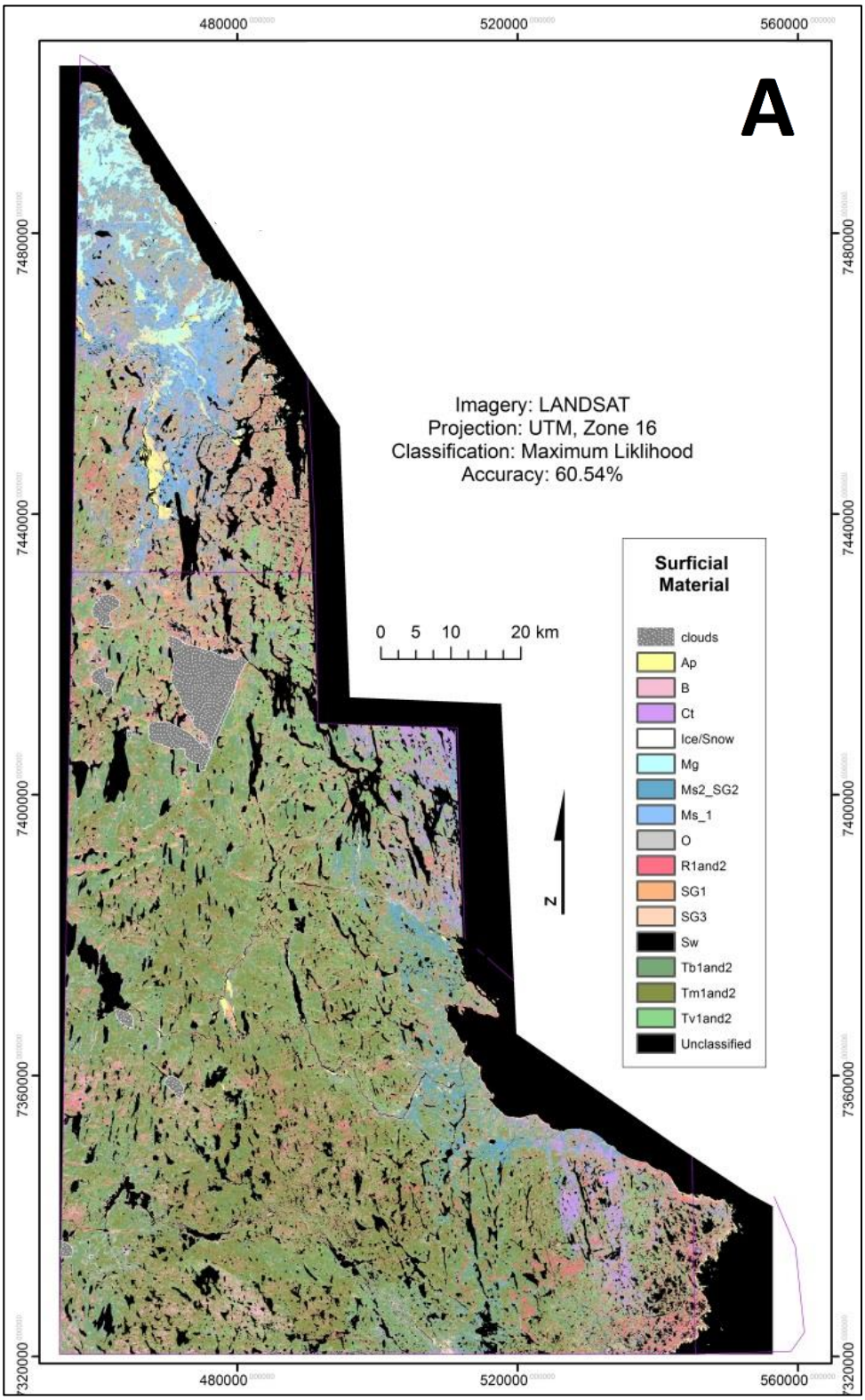

Figure 2.8: Best predictive surficial materials map based on Geological Knowledge. A) GK1 using 15 surficial classes and; B) GK2 using 12 classes; see text for details. Classifications produced by Maximum Likelihood Classification algorithm on LANDSAT imagery.

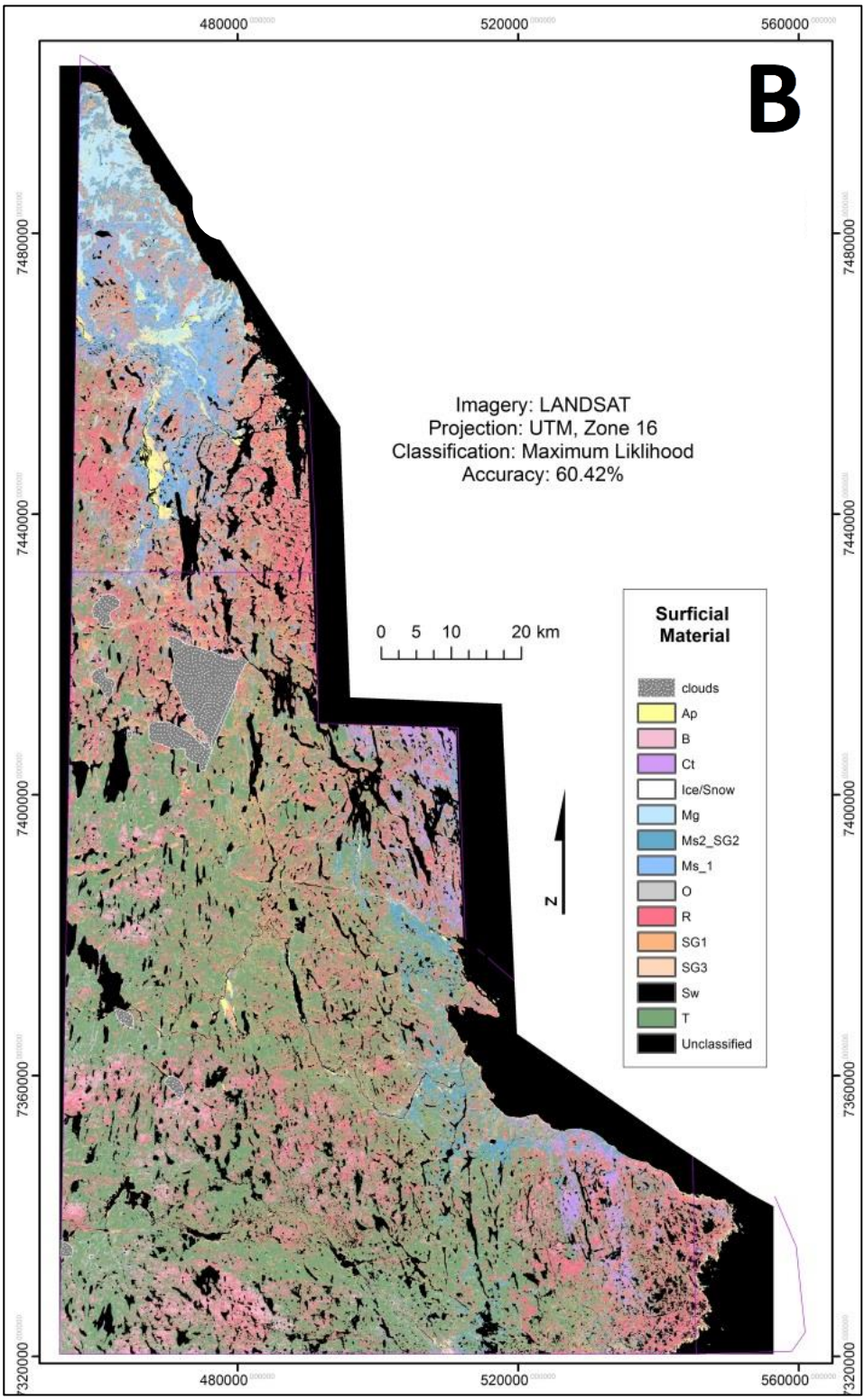

Figure 2.8: (Continued)

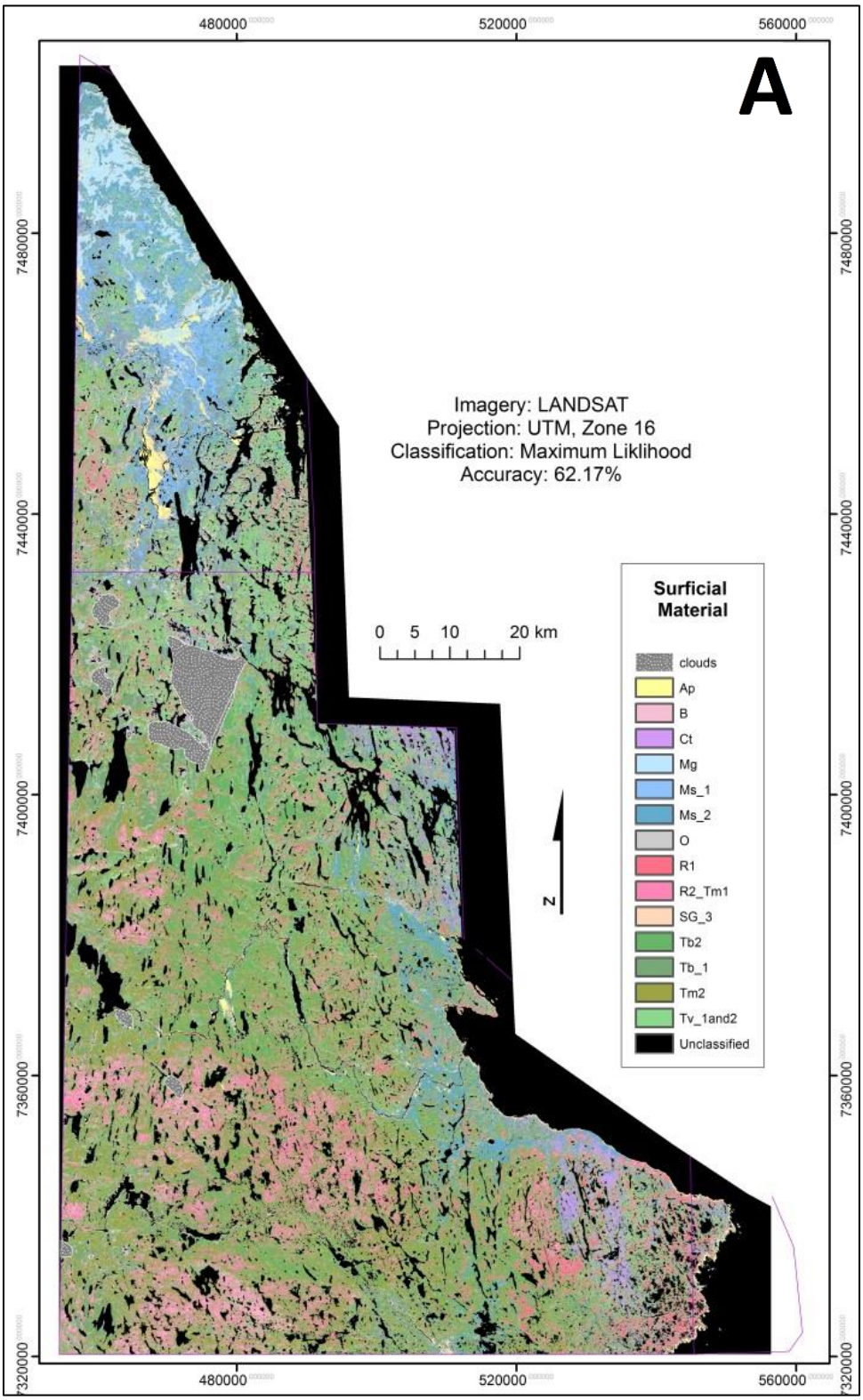

Figure 2.9: Best predictive surficial materials map based on Statistics. A) STATS1 and; B) STATS2; see text for details. Classifications produced by Maximum Likelihood Classification algorithm on LANDSAT imagery

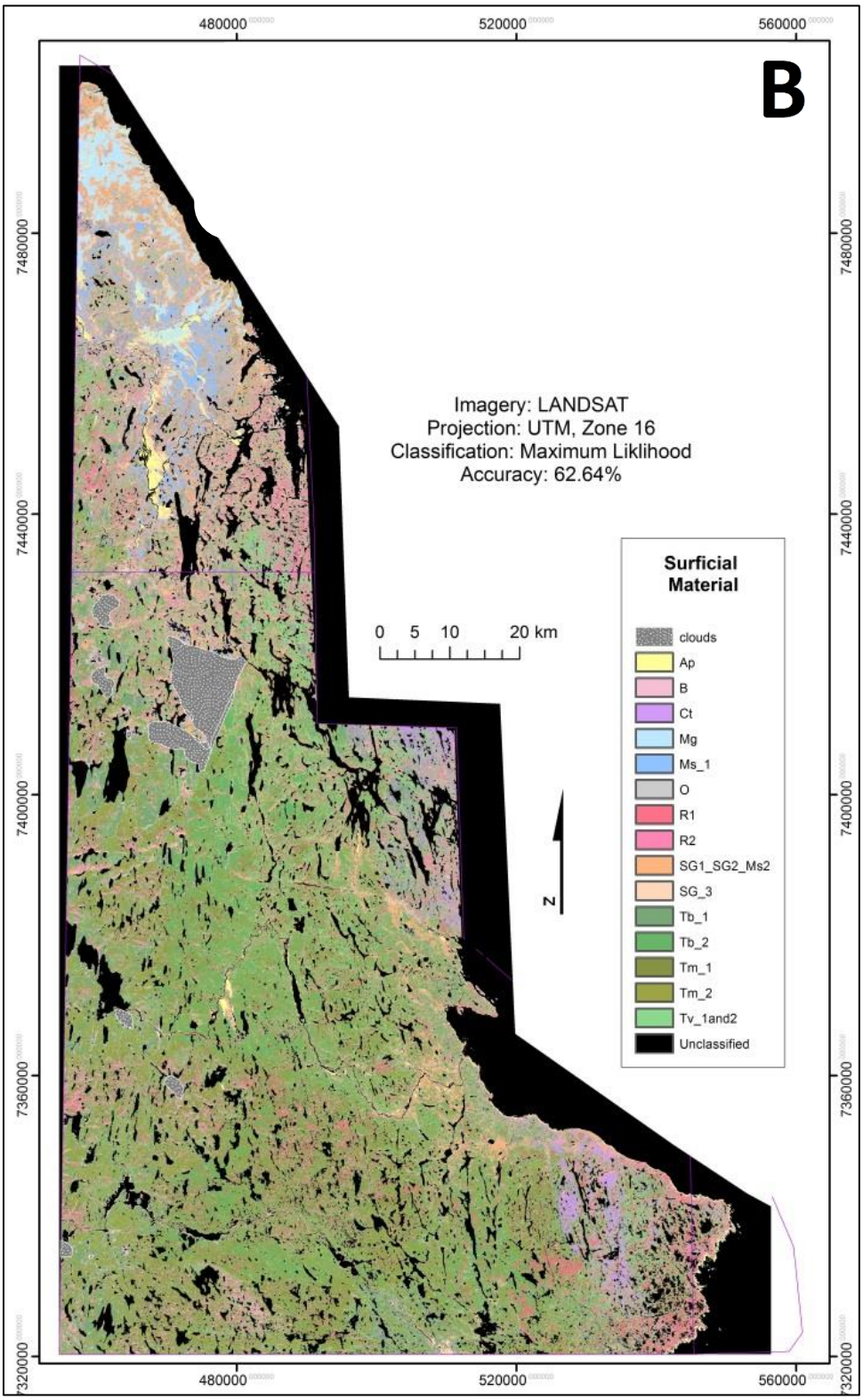

Figure 2.9: (Continued)

2.4.1.4 Map STAT2: Statistical 2

Unlike the other three maps, this map classified a sizable portion of the north as the merged class SG1+SG2+Ms2 (Fig. 2.9). This classification indicates that sands and gravels are also dominant in the north, and along the central coastal areas; while the other maps suggested marine sediments were the dominant classes. This map shows more bedrock and boulder fields in the north when compared to STAT1 and comparable distribution to GK1; while it classified significantly less of these units in the north than GK2. Though less boulders and bedrock are mapped here, they do occur in generally the same regions on all maps; however their abundance is much less pronounced. The carbonate till is classified consistently in the southeastern portion of the map.

This classified map shows the least similarity to the present knowledge of the surficial geology of the region. Carbonate till is classified in the north where in fact it does not occur; very little of the boulder class has been classified; there is no improvement with the mapping of R1 than in the previous map; and the statistically suggested class combination of SG1+SG2+Ms2 is not a sound combination of surficial materials as it does not differentiate marine fine sands from glaciofluvial sand and gravel. The Ms1 class is mapped appropriately, and not much of SG3 class has been classified. The STAT1 class combination produces a map with more till in the main central and southern portions of the study area, when compared to the other 3 maps.

2.4.1.2 Variability Maps

The four variability maps produced through the RCM algorithm have a maximum of 4 classes that form contiguous areas of variability. A much smaller number of pixels have variability of 5 to 9 classes (Figs. 2.10 and 2.11). Although general trends and areas of relative variability are similar across all four maps, the degree of variability differs. Spatially, less variability occurs in the northern region of all four maps. This suggests the area has a higher classification accuracy or higher systematic error. The greatest variability in all four maps occurs in the central part of the study area, and extends into the south for the STAT1 and STAT2 maps (Fig 2.11).

Maps GK1 and GK2 show less variability overall when compared to STAT1 and STAT2 maps (Figs. 2.10 and 2.11). These latter maps show more uncertainty in the southern third of the study area as well as in the western part. For example the STAT2 map shows the central area to have more variability than the STAT1, GK1 and GK2. The map showing the least variability in classification is GK2, followed by GK1, STAT1 and STAT2. The low variability of map GK2 suggests this RPM map is the most robust or reproducible of the four classified maps. Interestingly, while the scene boundary is highlighted in maps GK1, GK2, and STAT2, it is much less pronounced in map STAT1. This may be due to the particular class combination used for this classification or from scene characteristics associated with these classes.

In general, higher variability is present in till and bedrock-dominated areas (as per classification maps), while less variability is evident in areas mapped as marine sediments and/or sands and gravels, as well as carbonate tills. Regions dominantly classified as till and bedrock are mapped as being more variable and less certain in maps STAT1 and STAT2. It is important to note that the variability maps clearly indicate the effects of an unbalanced mosaic as linear discrepancies on these maps parallel that of the LANDSAT cutlines to create the mosaic (ref. Fig. 4). This will be further discussed in the following section.

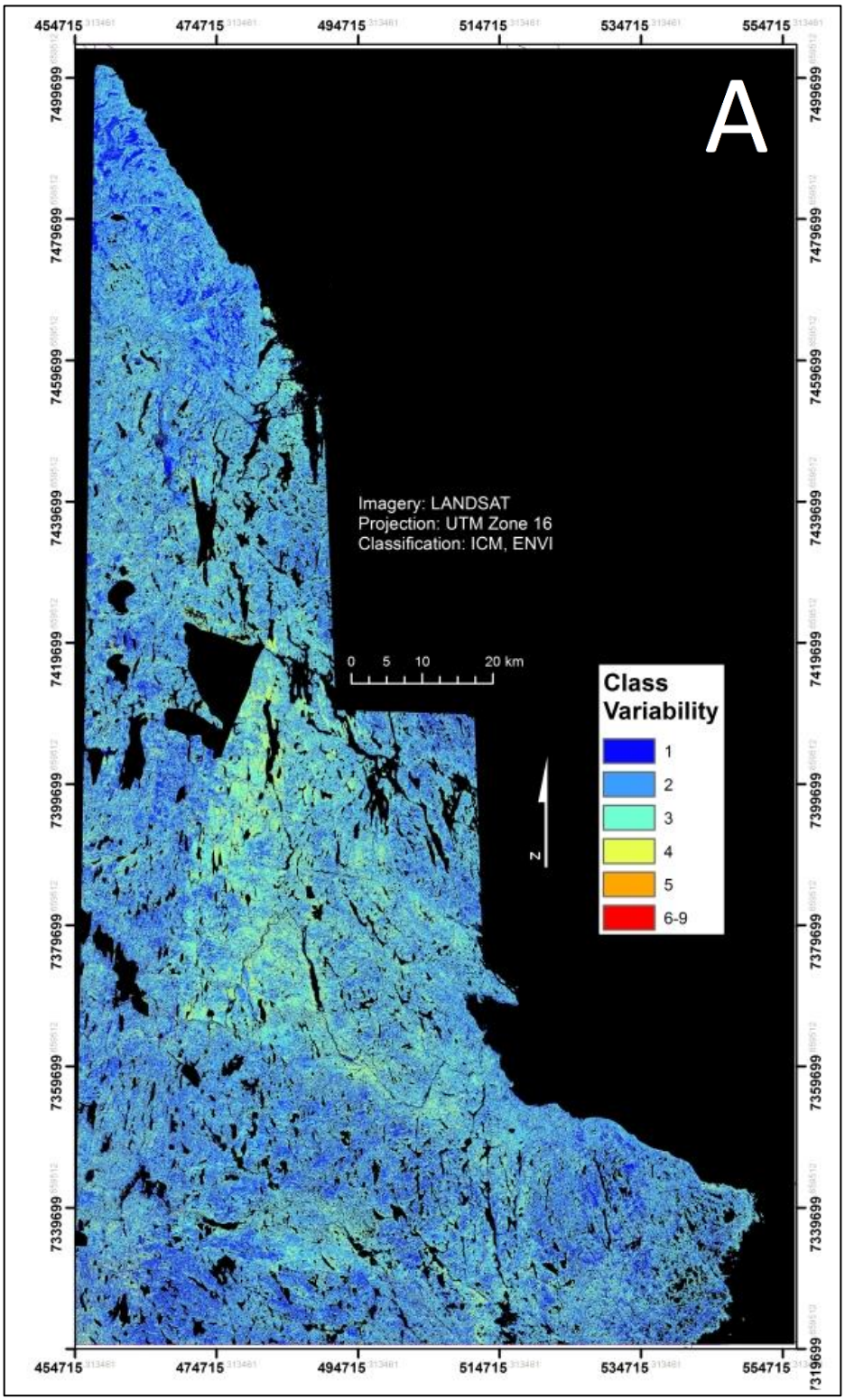

Figure 2.10: Variability maps for 2 predictive maps based on LANDSAT imagery and 'best' class combinations as derived from Geological Knowledge. A) GK1, using 15 classes and; B) GK2, using 13 classes; see text for details. Presents more class variability and confusion (warmer red tones) and regions of less variability and more certainty (cooler, bluer hues).

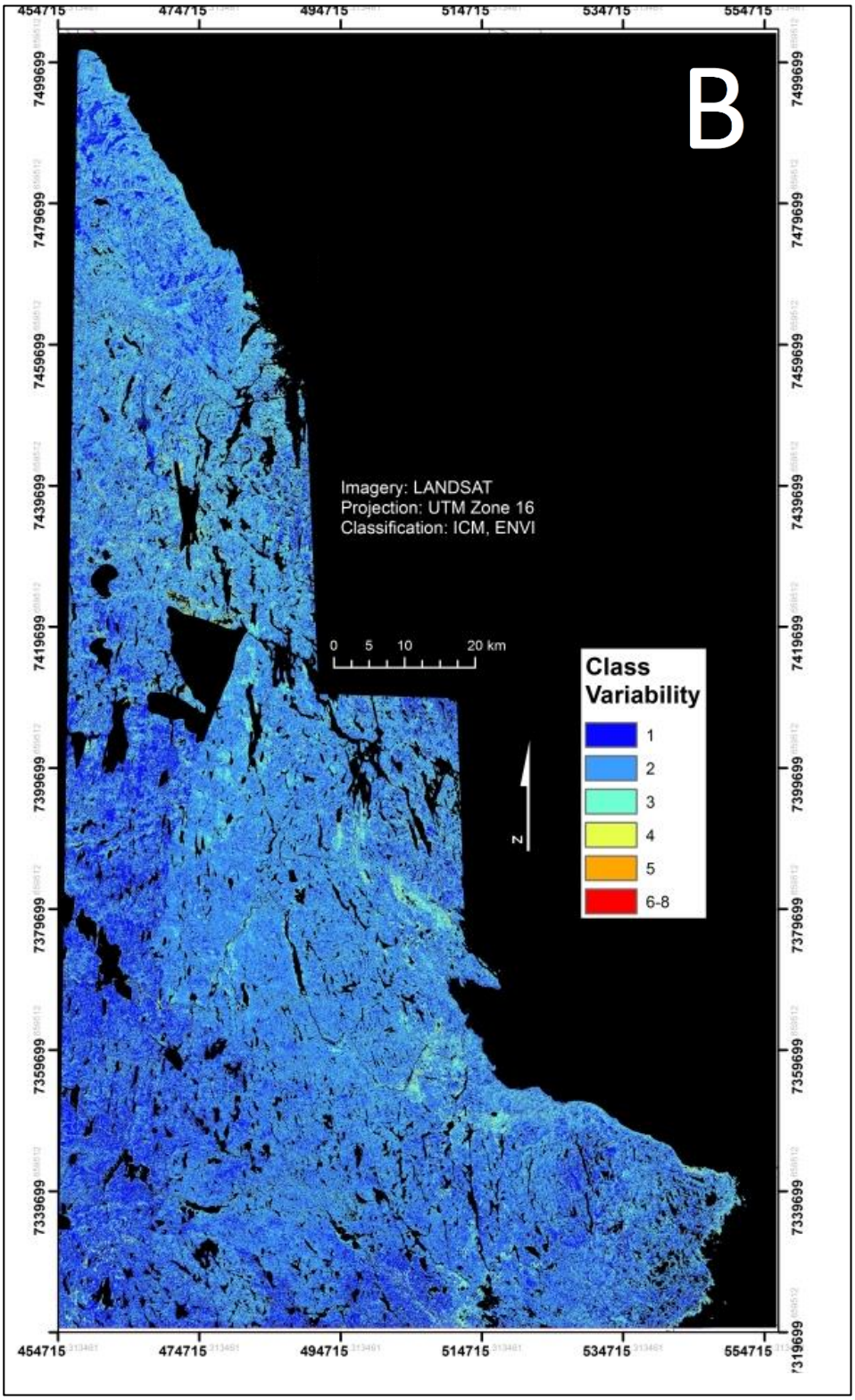

Figure 2.10: (Continued)

2.5 Summary and recommendations

An initial 21 surficial materials classes were used in a supervised classification (single pass maximum likelihood classification - MLC) to classify LANDSAT imagery of the study area west of Repulse Bay, Nunavut. From this, classes were removed and/or combined based on two approaches: 1) geological knowledge, which compared MLC predictive maps to Quaternary knowledge of the area, and 2) statistical, which strictly analyzed statistics of confusion matrices. Two maps, representing the most optimal results from each approach were selected and variability maps were produced on those class combinations using the Robust Classification Method (RCM) to determine which class combination and resultant classification was less variable, and in turn more accurate.

Based on the variability maps produced for each of the 4 "best" MLC classification maps, it appears that a geological knowledge-based approach to produce remote predictive maps is more suitable for mapping surficial materials in the Repulse Bay area. The variability maps based on a statistical approach (STAT1 and STAT2) show a generally greater degree of variability for the mapped region, in comparison to the variability maps based on a geological knowledge-based approach (GK1 and GK2). As demonstrated in the geological knowledge-based approach, the RPM process must include a direct input by Quaternary geologists. This proved to be most useful in merging, splitting, or removing classes from classifications, using geological criteria, and in turn, coming up with classifications more representative of the actual geology. The statistical method to create these maps suggested merges of classes that were not similar by geological standards, i.e. merging R2 and Tm1 – a bedrock unit with surrounding till combined with modified till containing sand and gravel.

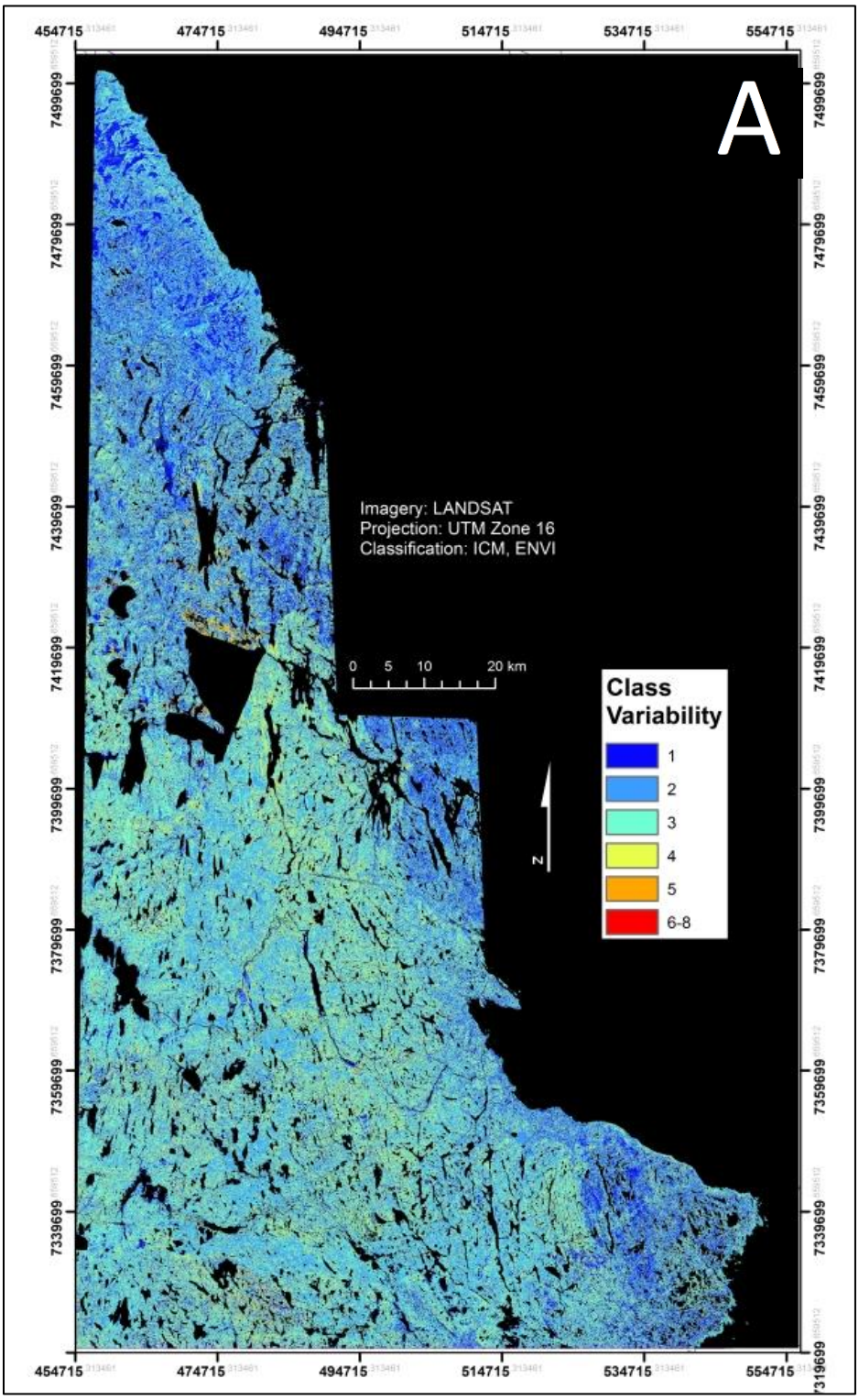

Figure 2.11: Variability maps for 2 predictive maps based on LANDSAT imagery and 'best' class combinations as derived from statistical approach. A) STATS 1 and; B) STATS 2; see text for details. Presents more class variability and confusion (warmer red tones) and regions of less variability and more certainty (cooler, bluer hues)

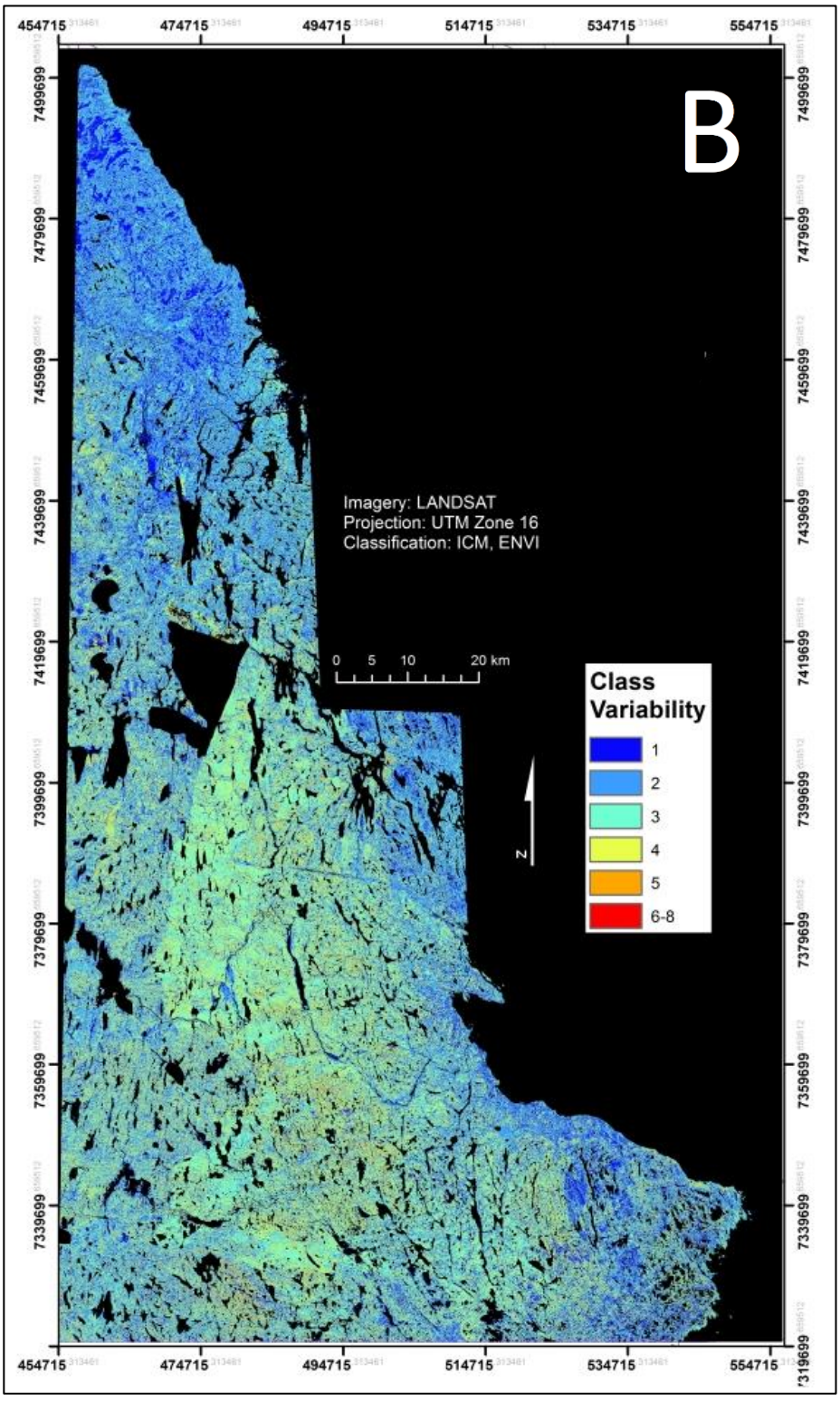

Figure 2.11: (Continued)

It is important to note however that a direct comparison between predictive maps derived from remotely sensed data and geological maps produced through fieldwork and air photo

interpretation will not always be conclusive because the processes behind producing the RPM and geological maps are quite different. LANDSAT data capture information at much higher spatial detail and high spectral variability, on a pixel-to-pixel basis. Some of this variability is noise and some is signal that represents the underlying bedrock (when exposed) as well as cover (surficial materials and vegetation).

A recommendation for further work is to use a well-balanced LANDSAT mosaic. The effects of an unbalanced mosaic were not as apparent in the classification maps versus corresponding variability maps produced on the same LANDSAT imagery. The scene boundaries are the result of seasonality and/or atmospheric differences between neighbouring images, which were not acquired during consistent conditions, therefore causing ill-correspondence for similar materials on either side of the boundaries. It is unlikely that differences in surficial materials are directly correlated to where scene boundaries occur. This issue is being addressed by the Canadian Centre for Remote Sensing (CCRS) and the Geological Survey of Canada (GSC).

Another recommendation is to use other parameters such as terrain (digital elevation models), texture, or other remotely sensed data, since LANDSAT provides one element of the surficial environment (e.g, RADARSAT). These data would provide additional parameters to classify the surficial materials and not only rely on spectral information from LANDSAT imagery.

Finally, although the Robust Classification Method (RCM) was used to produce the variability maps based on the combination of classes defined for the 4 "best" MLC maps, majority classification maps derived from the RCM were not discussed in this report. RCM is a technique that helps to present a more robust estimate of overall classification accuracy and to level out statistical variance in the training areas (Harris et al., 2012). The RCM should form an integral part of the supervised classification, and be used at the beginning of the classification process.

In conclusion, RPM will not substitute field mapping by the Geological Survey of Canada. Rather, this new approach is intended to be a supportive tool to direct, optimize, and perhaps enhance conventional geological knowledge. The supervised classification maps presented in this Open File are based on a physical parameter of the surface (spectral reflectance), while geological maps synthesize many parameters including photo-geologic variables (i.e. tone, texture, shape, pattern, context and association), field observations (e.g., of earth materials and geomorphic processes) and expert knowledge. The use of remotely sensed data for surficial materials mapping thus compliments the geological mapping process. The maps presented in this Open File and the methodology used to produce them have aided the GSC's mapping efforts of the greater Wager Bay region of Nunavut, which is one of the outputs for the Geo-mapping for Energy and Minerals (GEM) program.

Chapter 3: Mapping Surficial Materials from LANDSAT TM-7 and SPOT 4/5 imagery using Classification methods: A case study from Repulse Bay, NU

3.1 Introduction

Remote sensing using satellite imagery is applicable to a wide variety of Earth observations problems and has been used extensively in the geosciences, especially in the fields of glacial geomorphology (Clark et al., 2000; DeAngelis, 2007; Lytwyn, 2010; Walsh et al., 1998), bedrock mapping and mineral exploration (e.g. Drury, 2001; Martel et al., 2005; Harris, 2008), as well as to study surficial physical properties of other planets such as Mars (Jakosky, 1986; Mellon et al., 2000). Remote sensing can be used as a tool to enhance, but not fully replace, the field mapping process. It accelerates traditional mapping efforts by streamlining fieldwork and providing further insight into surficial materials of the mapped regions. It can also provide first-order geologic information in areas that cannot be mapped in the field due to lack of infrastructural access or logistical support (Drury, 2001; Harris, 2008; Sabins, 2007; Vincent, 1997).

Currently, surficial geology maps are sparse in Canada north of 60 degrees latitude, and of those regions that have been mapped, only approximately 50% have been mapped at scales of 1:500,000 or larger (Kerr and Eagles, 2012). The 1:500 000 scale is not optimal for mineral exploration programs and land-use management decisions, as it provides only broad information on glacial history and the Quaternary environment, and not enough detailed and local information on the nature and distribution of surficial sediments. Surficial geology maps provide insights into ice-flow and sedimentation history, which is necessary to trace mineral indicators and geochemical pathfinders found in glacial sediments back to the mineralized bedrock sources (i.e. Paulen and McMartin, 2009). Thus, surficial maps produce data that support mineral exploration programs, sustainable resource development and land-use management and are vital to drift prospecting, terrain management and mineral resource interpretation. Information on the surficial environment can be augmented and improved by the use of remotely sensed imagery.

The Repulse Bay area includes a variety of Quaternary glacial and post-glacial landforms and sediments (McMartin et al., 2013), and has high potential for mineral resources including diamonds, precious and base metals (i.e. Campbell and McMartin, 2011). However, surficial geology maps in this region are not suitable for effective mineral exploration programs using drift prospecting, and field-based observations are lacking (McMartin et al., 2013). The Geological Survey of Canada has identified the Repulse Bay region as a priority mapping area and, as a result, a framework mapping project was initiated in 2010 to fill in the knowledge gaps and produce surficial geological maps (e.g., Campbell and McMartin, 2010, 2011; Campbell et al., 2011; Wityk et al., 2011; McMartin et al., 2012; Wityk et al., 2012; Campbell et al., 2013; McMartin et al., 2013;Wityk et al., 2013; Campbell and McMartin, 2014;).

Remotely sensed imagery and associated image processing techniques are useful for geological mapping. However, limitations related to spatial and spectral resolution, landscape complexity, type of data, and atmospheric conditions at time of data acquisition (Lu and Weng, 2007) present operational challenges for the mapping of landforms and surficial materials from optical remotely sensed data. If these complexities, which affect spectral responses of surficial materials, could be better addressed, the applicability of remote predictive surficial materials mapping would further increase the rate at which the surficial geology of remote regions of Northern Canada could be mapped.

This paper presents a case study on the application of Remote Predictive Mapping (RPM) to the mapping of surficial materials in the Repulse Bay area. More specifically, the study aims at evaluating SPOT 4/5 imagery for mapping surficial materials in the study area and comparing SPOT-derived predictive maps with previously classified maps based on LANDSAT imagery as well as with a surficial geology map (Campbell and McMartin, 2014) for a smaller region of the study area. The comparison of classification maps to the surficial geology map is based on both qualitative (visual) and quantitative (GIS-based) methods.

3.2 Background

Since Sugden (1978) first used remote sensing to map the intensity of erosion by the Laurentide Ice Sheet, this technology has been further used for a variety of other geologic purposes by subsequent researchers from the 1980s to the present day (Clark, 1997, and references therein). Since this time, multispectral imagery has been key to the study of glacial geology, mainly in regions that do not have adequate infrastructure (i.e. (Vincent, 1997; Drury, 2001; Sabins; 2007; Harris, 2008; Shelat et al., 2012)).

LANDSAT data have been used to classify and map mega-scale glacial lineations (Stokes et al., 2006) and other linear features such as drumlins and eskers based on their shape, location and distribution (i.e. Clark et al., 2009;; Smith and Pain, 2009; Spagnolo et al., 2010). Other remotely sensed data, such as SPOT XZ (20m), SPOT Pan (10m), SEASAT and ERS SAR (25m), and RADARSAT, as well as Shuttle Radar Topography Mission (SRTM) data have also been used to map landforms (e.g., Clark, 1997; Lowell and Fischer, 2005; Mie et al., 2005;Liverman et al., 2006; Batterson and Taylor, 2007; Hickin and Levson, 2008; Ross et al. 2009). The application of satellite imagery to glacial geomorphology facilitated reconstruction of glacial histories (Clark, 1997; Smith and Pain, 2009) and aided the understanding and interpretation of regional ice flow dynamics (e.g. Tippet, 1985, De Angelis and Kleman, 2005; De Angelis, 2007). The latter in turn advanced the understanding of previous ice-sheet behaviour (e.g. Boulton and Clark, 1990) and provided insights into surficial sediment mapping and also resource exploration and development programs in the Canadian North.

Mapping bedrock lithology with the use of remotely sensed data has been undertaken in the Canadian North since 2005 and has had some success. In the past decade, bedrock lithology

mapping in Canada has been conducted in the Snowbird Lake area (NWT) (Martel et al., 2005), Borden Peninsula in Northern Baffin Island (Rencz et al., 2000), Baffin Island (Harris et al., 2005; Harris, ed. 2008), Boothia mainland (Schetselaar and Ryan, 2009), and Victoria Island (Behnia et al., 2012), Nunavut. They have included some fieldwork in the study regions, or have included legacy field information for production of RPM maps. These are important case studies which new RPM studies can build upon.

LANDSAT imagery has been used to recognize features such as carbonate glacial dispersal fans (Schau et al., 1993), but it has rarely been used to map other types of glacial sediment properties in the Canadian Arctic. Traditionally, mapping surficial geological methods have included the use of aerial photo interpretation, field traverses and surface sediment sampling. These methods are time consuming and expensive due to remoteness and limited infrastructure (Shelat et al., 2012). Recently, a method using satellite imagery in conjunction with image processing techniques (classification), rather than solely visual interpretation and/or fieldwork, has been developed to create maps of surficial materials (e.g. Brown et al., 2007, 2008; Grunsky et al., 2006, 2009; LaRocque et al., 2012).

A study on northern Baffin Island near Conn Lake (Brown et al., 2007, 2008) has been undertaken to map surficial materials using a RPM approach. RPM involves compiling and interpreting geoscience data (such as remotely sensed and geophysical information), which is used to produce predictive maps regarding information on structure, lithology, geophysical and surficial information for purposes of supporting field mapping. The Baffin Island study yielded results of 85% accuracies for LANDSAT classification using all training areas (also referred to as "regions of interest": ROIs). The term "accuracy" in RPM studies often refers to classified pixels within ROIs, and specifically to the percentage of pixels that were classified correctly within an ROI. In the Baffin case study, the accuracy indicates that 85% of the pixels within the ROIs were correctly classified. With the incorporation of a DEM, accuracies improved by only 1% (Brown et al., 2007). When comparing full classification maps with field observation and ground truthing of surficial materials, an accuracy of ~50% was achieved, much lower than when comparing with training areas only (Brown et al., 2007).

Several studies under the Geo-mapping for Energy and Minerals (GEM) program at the Geological Survey of Canada have been conducted over the last few years. They include Schultz Lake (Grunsky et al., 2006, 2009), Wager Bay (Campbell et al., 2013) on mainland Nunavut, Hall Peninsula and Foxe Basin on Baffin Island, Nunavut (Harris et al., 2012) and Hearne Lake in the Northwest Territories (Stevens et al., 2013). At Schultz Lake, LANDSAT TM-7 and RADARSAT-1 imagery classified surficial materials types with accuracies of >80% within ROIs, with the highest accuracy attained when using both types of data and all of the ROIs. Nonetheless, some units were not easily differentiated and mapped due to considerable overlap in their spectral and textural signatures (Grunsky et al., 2009). To qualify these accuracies of over 80%, both studies included "water" as a class which greatly increased overall accuracies

due to the size (number of pixels) of the water class and the spectral separability when compared to remaining classes in the Schultz Lake study (Grunsky et al., 2009).

The study by Harris et al., (2012) on Baffin Island predictively mapped surficial materials using spectral reflectance characterisitics of LANDSAT imagery and topographic variability using a digital elevation model (DEM) and its derivatives. Mapping 9 classes produced an overall accuracy of the majority classification of 77.7%; with a producer accuracy average of 64%. It presented confusion in mapping organic materials and wet fine sediments, which were combined to form a single class during post-processing. This map has not been verified by field checking. It represents a prediction of materials based on knowledge of a field geologist.

Similarly, a predictive surficial materials map was produced using radiometrically normalized LANDSAT 7 data at Hearne Lake (NWT) (Stevens et al., 2013), air photo interpretation, as well as legacy data, and field expert knowledge. When comparing the classification to training data, the 7 mapped classes were 81.7% accurate. Errors were due to similarities in moisture content and surface vegetation between classes. For example regions where bedrock is vegetated and till has high occurrence of isolated bedrock outcrops have similar spectral signature. Misclassifications primarily occurred between till veneer and till blanket classes. This work provides information which can be used to assess surficial materials and terrain risks to infrastructure as well as for guidance of mineral exploration and future mapping (Stevens et al., 2013).

In Wager Bay, LANDSAT was also used and 12 surficial material classes were produced using the Robust Classification Method (RCM) (Campbell et al., 2013). The classifications were then later analysed statistically and then geologically evaluated. Average accuracies of the iterations were 41.2%, with a maximum accuracy of 46%, lower than the aforementioned RCM studies.

3.2.1 Classification

In the early 20th century (1912-1922), the idea of maximum likelihood was developed by R.A. Fisher as described in Aldrich's (1997), which eventually resulted in the well-known and used Maximum Likelihood classification algorithm. The maximum likelihood methodology as described by Aldrich (1997) was used to classify remotely sensed imagery. This classification method has been applied to remote sensing since the 1970s for the production of thematic maps (Strahler, 1980). The classification of multispectral imagery results in an image (map) where each pixel is assigned a class membership (e.g. land cover classes, Briggs, 1987). Maximum Likelihood is the most frequently used classification techniques (e.g., Benedictsson et al., 1990; Foody et al., 1992; Gonzales and Woods, 1992; Paola, 1994; Paola and Schowengerdt, 1995; Stuckens; Foody, 1996; Franklin et al., 2002; Harris et al., 2012; et al., 2000; Behnia et al., 2012;).

Image classification approaches comprise two general methods (pixel-to-pixel vs. object based classification). Pixel-to-pixel classifiers are divided into supervised and unsupervised approaches, the difference being the degree of user input to the classification process. Additionally, different algorithms can be used depending on the data distribution (parametric or non-parametric). Further details on image classification techniques are presented in Lu and Weng (2007), as well as in Tso and Mather (2009), and Landgrebe (2003).

A supervised classification is a semi-automatic approach used to classify imagery on a pixel-to-pixel basis. It is semi-automatic as it incorporates knowledge provided by experts on the terrain to be classified (Harris, 2008). This *a priori* knowledge is input by the geologists as training data in the form of polygons that represent a known surficial material. These training areas (polygons) are referred to as "regions of interest" (ROIs) and capture and represent the spectral signature of each surficial material to be classified (Harris, 2008; Harris, 2012). Pixel based classifiers automatically allocate each pixel in the image to one of a specified number of classes (Briggs, 1987), based on which spectral signature (class) it best matches (Figure 3.1)

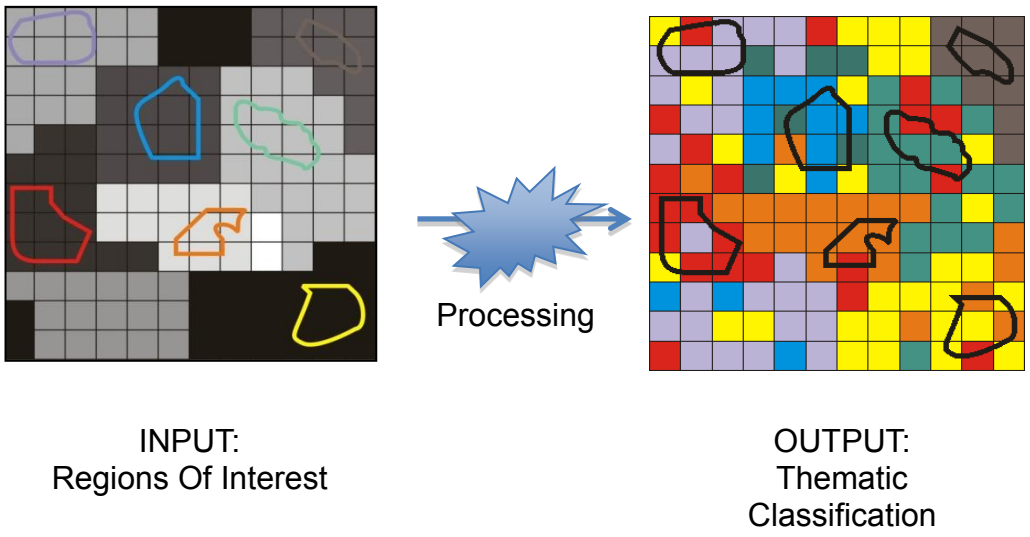

Figure 3.1: Conceptual model of classification process. The spectral response from digitized regions of interest (ROIs) on satellite imagery (input) are used to classify image pixels into surficial material classes (output) where pixels are labeled according to statistics of regions of interest.

Since the early 90s, improvements to the classification process have been made (Aplin et al., 1999a; Foody, 1996; Franklin et al., 2002; Gallego, 2004; Gong and Howarth, 1992; Kontoes et al., 1993; Pal and Mather, 2003; San Miguel-Ayanz and Biging, 1997; Stuckens et al., 2000). Some improvements have included developing more advanced algorithms, using different types

of remotely sensed imagery, and adding textural information which incorporates spatial patterns as well as geoscience data into the classification process (i.e. topography, soil, road, census data) (Lu and Weng, 2007). Though progress has been made, a number of challenges remain that can impact the effectiveness of classification techniques. Challenges include issues concerning balanced mosaics, representative regions of interest and input data for classification, variability in surficial materials to be classified, data availability and quality, to name a few. The classification approach requires selecting training data, processing imagery; selecting and applying appropriate classification algorithms, post-classification processing and assessing accuracy (Lu and Weng, 2007).

3.3 Study Area

The study area is situated on mainland Nunavut, Canada, along the north-northwestern coast of Hudson Bay, and west of Committee and Repulse bays (*Figure 3.2*). It is between latitudes 66°N and 67.5°N and longitudes 88°W and 86°W and is made up of parts of NTS map sheets 46K, 46L and 46M (Wityk et al., 2013).

The physiography of this region has a low relief and gently rolling hills within which are groups of bedrock hills, lakes, shallow valleys and depressions; this is typical of the Canadian Shield in Keewatin (McMartin et al., 2013). Distinct landform assemblages feature drumlins, meltwater corridors, and, at lower elevations, gullied marine sediments which are exposed along the Committee Bay coast (Campbell and McMartin, 2014; McMartin et al., 2013;).

The bedrock of the region includes Archean through Paleoproterozoic supracrustral rocks of the 2.7-2.6 Ga Rae Domain of the Western Churchill Geological Province (Paul et al., 2002). Overlying the bedrock are glaciofluvial deposits and a dominant sandy diamicton (McMartin et al., 2013). The glacial diamicton, or till, is a poorly sorted, massive, silty sand diamicton with shield and carbonate-rich end-members (McMartin et al, 2013) whose elongated landforms are oriented in the northward direction, generally following the direction of the regional ice flow (Aylsworth and Shilts, 1989; McMartin et al., 2013; Prest et al., 1968). Marine sediments, which are dominant along the coastal plain west of Committee Bay consist of sands, silts and clays (e.g. Campbell and McMartin, 2010, 2014). Continuous permafrost and a discontinuous tundra vegetation cover are also characteristic of the region (McMartin et al., 2013).

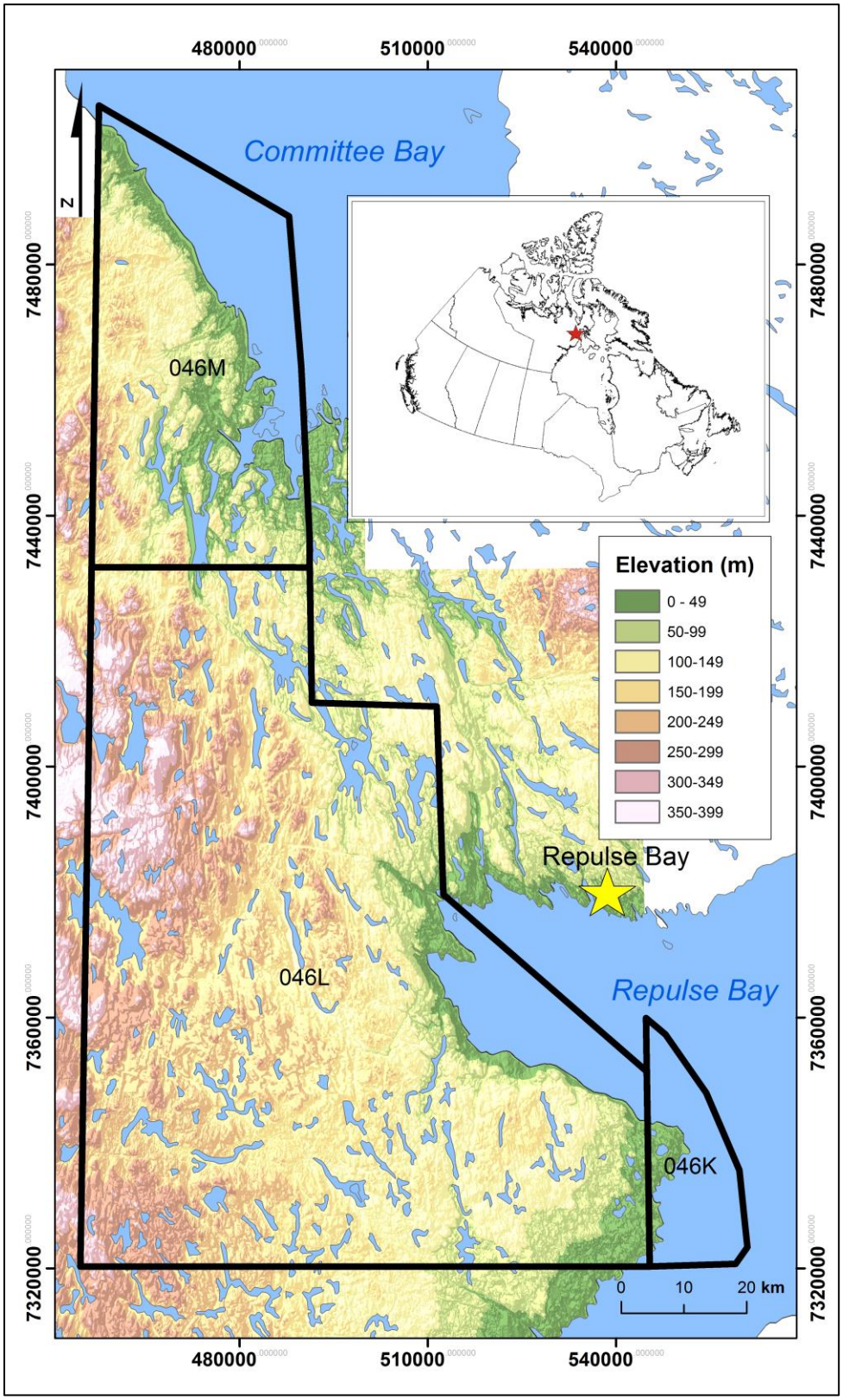

Figure 3.2: Location Map of RPM study area - within black boundaries. Near Repulse Bay, NU, Canada.

3.4 Methodology

The method used in this study is derived from a seven-step RPM approach developed to remotely map the geology of Canada's North (Grunsky, 2006; Grunsky et al., 2009; Harris et al., 2008, 2012; Scheltselaar et al., 2007). Modifications to the methodology include an additional field component prior to processing, analysis and interpretation of satellite imagery, and an improved procedure for creating, updating, and ground-truthing ROI's (Wityk et al., 2013). Wityk et al. (2013) identified regions of interest from fieldwork, air photo interpretation and image analysis. These regions were digitally transcribed to LANDSAT data within the ENVI™ image analysis system and then used to classify surficial materials. Performing a number of iterations using a variety of class combinations, analysis of the resultant classifications and subsequent re-classifications provided the optimal class combinations for mapping the surficial materials of this region (For more information see Chapter 2). These resultant class combinations and ROI data (Chapter 2) were applied to classify SPOT 4/5 imagery. The two class combinations resulting from this work differ from one another as one (class combination 1) sub-divides till into three subclasses (till veneer, till blanket and modified till) while the other (class combination 2) does not differentiate these units (*Table 3.2*).

In addition to the RPM of surficial materials for the entire study area, a small subset of the study area was used to compare LANDSAT (Wityk et al., 2013) and SPOT classification maps with one another and also to compare the classification maps to an existing surficial geology map (Campbell and McMartin, 2014). The surficial materials map used for comparing the classifications was derived from a surficial geology map produced from air photo interpretation and analysis of collected field data (Campbell and McMartin, 2014). The legend for this surficial geology map was modified to reflect the RPM classes, which were largely derived from spectral signatures captured by the remotely sensed imagery. This required merging some surficial geology units together, which represent different depositional environments (as mapped in the surficial geology map). It is acknowledged that the RPM surficial classes reflect only differences in spectral response and do not incorporate geological process information; however, this was done to accommodate a direct comparison between the modified surficial geology map and predictive surficial materials maps.

3.4.1 Data Acquisition, Image preparation and Masking

SPOT 4/5 imagery were obtained from BlackBridge Geomatics (formerly Iunctus Geomatics), who also combined and levelled the data resulting in a visually seamless mosaic image of the study area. The image was then projected to Universal Transverse Mercator (UTM), Zone 16, and referenced to North American Datum (NAD 83), and finally clipped to the study area. A LANDSAT mosaic combining all images was also created by BlackBridge Geomatics, projected to the corresponding projection and clipped (Chapter 2; Wityk et al., 2013).

Table 3.1: Summary of characteristics for remote sensing data used in this study - bands, channels, and resolution.

Data	Source	Bands	Channels	Resolution
LANDSAT TM-7	GeoGratis, NRCAN	1, 2, 3, 4, 5, 7	Visible, NIR, SWIR	30 meters
SPOT 4	IUNCTUS	1, 2, 3, 4	G, R, NIR, SWIR	20m
SPOT 5	IUNCTUS	1, 2, 3, 4	G, R, NIR, SWIR	10m (B1-B3) 20m (B4)

A water mask was created from the SPOT NIR data (band4) using the interactive stretching tool in ENVI™. Clouds and cloud shadow regions were also masked out by manually digitizing these features on a SPOT ternary image (NIR, red, green) and, through simple band math, these masks (water, clouds, cloud shadows) were combined together (*Figure 3.3*). This procedure is important to prevent water bodies and clouds from being classified as a surficial material during subsequent steps.

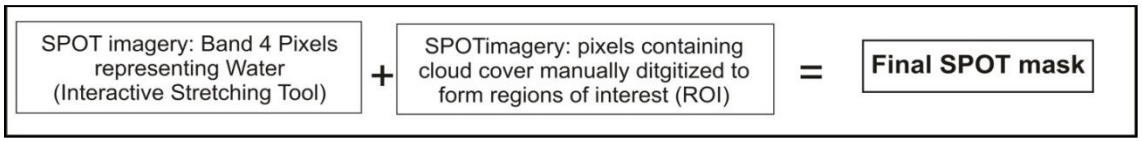

Figure 3.3: Production of final SPOT mask to mask out water and cloudy regions, modified from Wityk et al. (2013).

3.4.2 Classification of surficial materials

A supervised maximum likelihood classification algorithm (Tso and Mather, 2009) was applied to the SPOT imagery using ENVI version 4.8 software. It utilized the aforementioned two different class combinations (from results of Wityk et al., 2013), and the associated ROIs, which were applied to classify all 4 bands of the SPOT imagery (20m resolution) (*Table 3.2* – for complete description of all class units see Chapter 2). According to Wityk et al. (2013), ROI separability tested on LANDSAT imagery using the Transform Divergence (TD) statistic indicates that the classes with better separation include Ap, Sw, Mg, Ms1, Ice/Snow, O, SG3 and Ct. Lower TD values indicating moderate or poor separation were seen for tills, bedrock and sand and gravel subclasses - which suggested potential confusion between these subclasses in subsequent classifications (Wityk et al., 2013 - Chapter 2). In comparing average TD values for each class between LANDSAT and SPOT imagery, it was found that a better separation between classes occurred on the LANDSAT data.

These class combinations used for SPOT classification were those that produced the most optimal classification results for the study area using LANDSAT (Wityk et al, 2013). To arrive at these optimal combinations, classes were removed and/or combined based on 1) geological

knowledge – comparing classification outputs to the known geology determined by field observations and air photo interpretation of the region; and 2) statistics – analysis of confusion matrices based on classification results (Wityk et al., 2013).

The ice and shallow water classes were not included in the SPOT classification. The ice ROIs were derived from LANDSAT imagery and were not found in the SPOT imagery due to temporal and seasonal differences between the two image types. Shallow water ROIs were located within the masked (water mask) region of the SPOT data and not included in the classification.

Table 3.2: Class Combination for SPOT Classifications comprising the following materials: Alluvial plain (Ap), Marine gully sediments (Mg), Marine silty sands (Ms), Sand and Gravel (SG), Organics (O), Bedrock (R), Boulder fields (B), Till blanket (Tb), modified Till (Tm), Till veneer (Tv), Carbonate till (Ct), Shallow water (Sw).

Class Combination 1	Class Combination 2
Ap	Ap
Mg	Mg
Ms1	Ms1
Ms2+SG2	Ms2+SG2
O	O
SG1	SG1
SG3	SG3
R1+R2	R
B	B
Tb1+2	Tb1
Tm1+2	
Tv+2	
Ct	Ct
Sw	-
Ice	-

Maps were labelled as such:

- L1 – LANDSAT imagery, class combination #1 (“GK1”, from Wityk et al., 2013)
- L2 – LANDSAT imagery, class combination #2 (“GK2”, from Wityk et al., 2013)
- S1 – SPOT imagery, class combination #1
- S2 – SPOT imagery, class combination #2

Confusion matrices for L1 and L2 (“GK”1 and “GK2” from Wityk et al., 2013) and for S1 and S2 were calculated from the four classifications to provide classification accuracies based on ROI’s used for the entire mapped study area (Wityk et al., 2013). To provide a measure of the performance of the classification process, the matrix produces a table which tallies the

number of pixels classified correctly within ROIs of each class on the classification output. Further, qualitative and GIS comparisons were executed on a smaller region within the study area.

3.4.3 Qualitative and quantitative comparisons to the Surficial Geology map

Surficial geology maps and predictive (classification) materials maps are produced using different methods and thus offer different information. A predictive map is based strictly on the spectral response of surficial materials seen on a pixel-to-pixel basis and thus produces a heterogeneous map of the surface whereas a surficial geology map incorporates information and interpretation on depositional environment, geomorphology, glacial processes, provenance and relative age, producing a more homogeneous and often comprehensive map of the surface and its geology and geomorphology. Thus, as mentioned above, in order to make comparison between the surficial geology and predictive surface materials maps, a number of geological units were modified and regrouped to best reflect and accommodate classes used in the RPM method. The groupings were made based on the physical properties of the sediment material, independent of deposit type or origin/process. This is why the same geological unit may also be ascribed to different RPM classes. For example, though deltaic sediments (Md, as per surficial geology unit) are deposited in marine environments, they are made up of sands and gravels and therefore were regrouped into the sand and gravel (SG1_SG3) RPM class. This comparison of surficial geology and predicted surficial materials was conducted on a sub-region of the study area (Fig. 3.4). Assignment of surficial geology units to RPM classes are shown in

Table *3.3*. Though RPM classes indicated SG1 and SG3 (SG1 as vegetated and SG3 as exposed), surficial geology mapping does not make this distinction, therefore SG1 and SG3 RPM units were combined into one unit. No boulders or carbonate till (RPM classes) were mapped in this sub-region (Campbell and McMartin, 2014) and were therefore excluded for this comparison. RPM units of modified till (Tm) and carbonate till (Ct) were combined with and labelled as Tb. These modifications to the RPM classes and surficial units created uniformity for the GIS comparison

Table 3.3: Surficial Geology Units (as determined by Campbell and McMartin, 2014) and their groupings/regroupings to reflect RPM classes.

RPM Class	Surficial Geology Unit Code	Surficial Geology Unit	Type of Deposit
Ap	Av	Alluvial veneer	alluvial
	Af	Fan sediments	alluvial
	Ap	Floodplain sediments (alluvium)	alluvial
	At	terraced Sediments	alluvial
Mg	Mgu	marine undifferentiated (gullied)	Marine
	GM-gu	glaciomarine undifferentiated (gullied)	glaciomarine
MS1	GMb	glaciomarine blanket	glaciomarine
	Mb	marine blanket	Marine
	M	marine undifferentiated	Marine
	GM	sediments undifferentiated	glaciomarine
	Mv	marine veneer	Marine
Ms2	Mn	nearshore sediments	Marine
	Mv	marine veneer	Marine
	GMb	glaciomarine blanket	glaciomarine
	Mt	terraced sediments	Marine
O	O	organic deposits	organic
R	R	undifferentiated bedrock	bedrock
SG1_SG3	GFp	outwash sediments	glaciofluvial
	GFt	terraced outwash sediments	glaciofluvial
	GFc	ice contact sediments	glaciofluvial
	GMd	deltaic sediments	glaciomarine
	Md	deltaic sediments	Marine
	GMn	Submarine moraine sediments	glaciomarine
	Mr	littoral sediments	Marine
Tb	Tb	till blanket	glacial
	Th	hummocky till	glacial
	Tm	moraine complex	gacial
Tv	Tv	till veneer	glacial

Qualitative (visual based on spatial similarities) and quantitative (using GIS) comparisons were made between the predictive maps and the field-based modified surficial geology map within a ~180 km^2 (as measured within the ArcGIS software package) subset of the entire study area. First, a simple visual comparison was undertaken to assess differences and similarities between SPOT and LANDSAT classifications and the modified surficial geological map. Second, a cross-tabulation which summarizes the agreement and disagreement between two maps was undertaken on the predictive and surficial geology maps. To facilitate the comparisons, the 20 m (SPOT classification) and 30 m (LANDSAT classifications) pixel

resolution of the classification maps were up-scaled (resampled) to a 100 m pixel size using the ArcGIS majority-based resampling tool. This was deemed necessary because the surficial map produced from fieldwork and air photo interpretation consists of large homogenous polygons rather than heterogeneous pixels. The geologist can recognize some of the natural heterogeneity of surficial materials through air photo visualization, but the final maps generally don't retain much of this detail evident on the remotely sensed imagery. The up-scaling process is applied to mimic the "filtering" (generalization) process geologists apply during mapping thus facilitating a comparison between the two different maps.

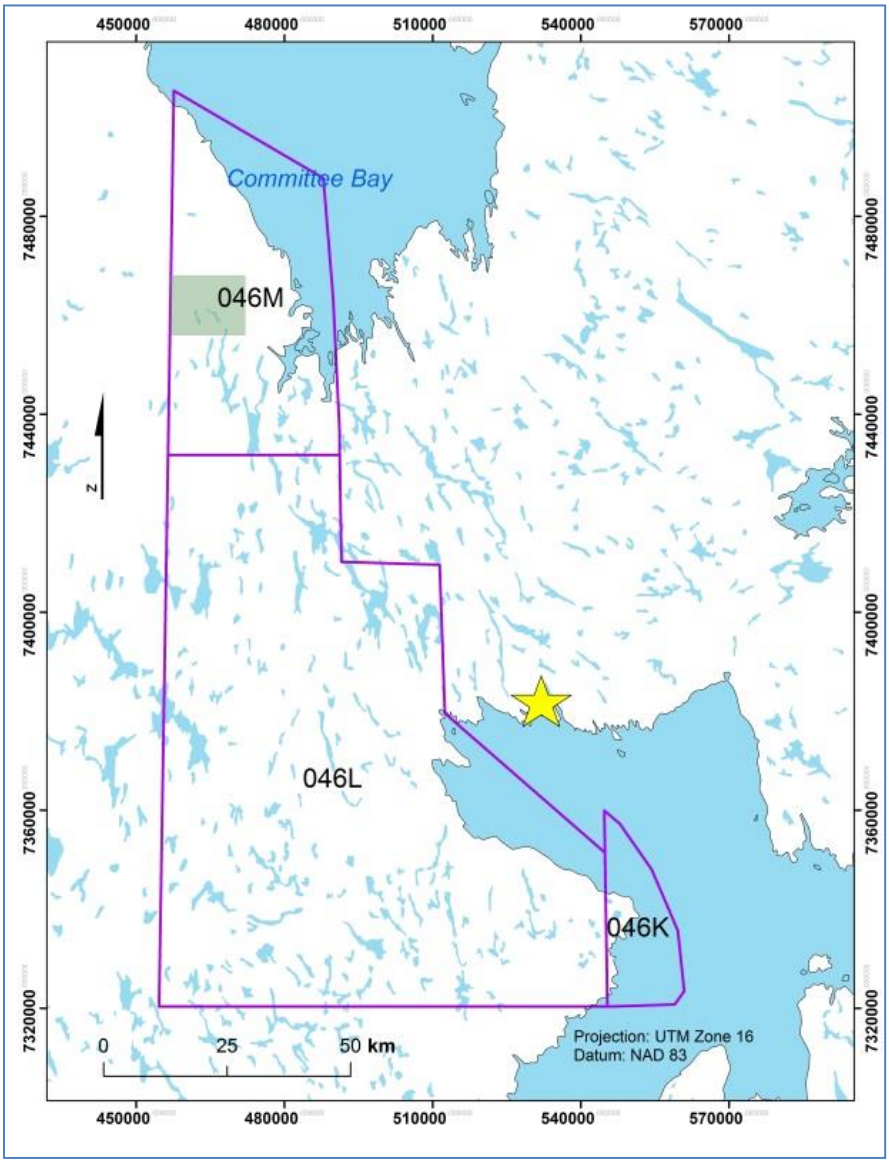

Figure 3.4: Location of the sub-region where classification results are compared against a surficial geology map (within green-shaded box).

3.5 Results

3.5.1 Statistical Results

Confusion matrices using ROIs for ground truth were computed automatically using the classification results for L1, L2, S1 and S2. This process plots ROIs along the x axis against classification results with respect to ROI pixels (that were used to create the map) along the Y-axis (Lillesand and Kieffer, 2000). ROI pixels are compared to the resultant classification pixels to determine the proportion of pixels (percentage) classified correctly for each input class. It is important to note that the confusion matrices were computed by checking the regions of the classification map which are located where ROI polygons were determined, with the ROIs which produced the classification maps. Using the ROIs as both classification input data as well as for computing confusion matrices provides an overestimation of the accuracy.

Because the ROIs were carefully chosen to be representative of the main terrain types and sediment characteristics of the study area, the confusion matrix exercise is considered to give insights into the accuracy of the entire map area. It is not a measure of the accuracy of the classification with respect to sediments on the ground; it is a measure of how accurately pixels within the regions of interests are identified. This measure is then extrapolated for the entire study area. Detailed accuracies (user's and producer's accuracies) of individual classes were also considered. Producer's accuracy" is a measure of how well the pixels within a training dataset were classified whereas the "user's accuracy" refers to how well the map is classified (probability that a classified pixel represents the proper class) (Smits et al., 1999). Table 3.4 summarizes the results displaying individual class accuracies (producer's accuracy) and overall class accuracies for the 4 classifications are indicated in

Table *3.7.* Confusion matrices have to be interpreted cautiously as they have been run on the entire study area, using only a small portion of the map for validation (ROIs).

Table 3.4: Summary of producer's accuracies of 4 classification maps according to confusion matrices computed using ROIs. High accuracy: 75-100% (green), Moderate accuracy: 51-74% (blue), Low accuracy: <50% (red).

	L1	**S1**	**L2**	**S2**	
Class Combination # 1 ↓					Class Combination # 2 ↓
Ap	77.06	77.22	77.06	77.22	Ap
Sw	94.04	/	94.9	/	Sw
Ms1	91.88	91.49	91.88	91.49	Ms1
Ms2Sg2	59.18	44.89	61.63	47.18	Ms2Sg2
O	78.54	81.5	81.78	83.18	O
Sg1	25.52	26.3	31.09	41.26	Sg1
Sg3	61.88	67.45	61.88	67.45	Sg3
B	89.19	87.07	92.16	89.82	B
Ct	90.59	89.27	91.15	89.87	Ct
Mg	88.23	89.96	88.23	90.01	Mg
Ice/snow	7.23	/	7.37	/	Ice/Snow
R1&2	48.6	38.91	64.09	52.18	R
Tb1&2	48.01	47.3	49.65	38.64	T
Tm1&2	61.66	43.94			
Tv1&2	49.12	26.88			

Table *3.5: Overall accuracy of classifications per surficial material class based on Maximum Likelihood classification confusion matrices.*

High	Moderate	Low
Ap	SG3	SG1
Sw *L	Ms2+SG2	Ms2+SG2 - *S
Ms1	SG2 - *L	Tm
O	B - *C1	Tb
B		Tv
Ct		T * C2
Mg		B - *C2
** L - LANDSAT only; * S - SPOT only; * C1 - class combination 1 only; *C2 - class combination 2 only*		

The User's Accuracies for the 4 classifications are summarized in the tables below (Table 3.6). Complete confusion matrices are found in the Appendix C.

Table 3.6: User accuracies for 4 classifications: LANDSAT 1, SPOT 1, LANDSAT 2 and SPOT 2

Class	LANDSAT 1 User	SPOT 1 User	LANDSAT 2 User	SPOT 2 User	Class
Ap	64.6	79.15	64.6	79.15	Ap
Sw	99.1		99.1		Sw
Ms_1	80.5	73.54	80.5	73.54	Ms_1
Ms_2_SG2	49.93	34.43	47.16	29.22	Ms_2_SG2
O	36.74	19.5	30.98	15.99	O
SG_1	29.8	35.32	24.23	28.91	SG_1
SG_3	67.16	64.96	67.05	64.96	SG_3
B	25.01	20	17.56	16.93	B
Ct	56.27	57.6	55.15	56.55	Ct
Mg	92.27	89.37	92.27	88.91	Mg
Ice/Snow	100		100		Ice/Snow
R1and2	50.8	40.6	27.99	21.02	R1
Tb_1and2	81.73	86.67	91.3	92.96	T
Tm_1and2	56.22	47.57			
Tv_1and2	52.5	29.09			

Confusion matrices across all 4 classifications produced similar results, revealing that certain surficial sediments were consistently mapped with higher accuracy than others. Similarities in producer's accuracies across confusion matrices of a number of classification iterations and class combinations indicate that Ap, Ms1, O, B, Ct, and Mg classes are accurately mapped in both class combinations and both LANDSAT and SPOT imageries (Table 3.4). This

was expected as the transform divergence (TD) statistic for these classes indicated that they are easily separated and distinguishable from other classes based on their spectral signature (TD statistic values available in Appendix F and G). Confusion and lower accuracies are evident for various till types, bedrock, and sand and gravel classes. All till types were mapped with moderate (51-74%) or low (<50%) producer's accuracy with the exception of carbonate till (> 88% accuracy for all 4 classifications).

Looking at the user's accuracy (Table 3.6) it is evident that the mapped classes with the higher accuracies (user's accuracies of 75% or higher) include: Mg, Tb1and2 (combination 1)/T (combination 2), Ms1 and Sw and Ice/Snow (for LANDSAT classifications) and Ap (for SPOT classifications). Moderate user's accuracies (51-74%) are evident in Ap (LANDSAT Classification), SG3, Ct, and Ms1 (SPOT classification). Finally the poorest user's accuracies (<50%) are in classes including MS2_SG2, O, SG1, B, R1and2 and Tm1_2 (SPOT) and Tv1_and2 (SPOT).

Generally, LANDSAT overall accuracies are higher than SPOT for both class combinations (

Table 3.7) and according to the confusion matrices, more classes are mapped accurately with LANDSAT than SPOT (Table 3.4, Table 3.5). LANDSAT more accurately classified Ms1, Ms2, Sg2, B, Mg, and all Till units (inclusive of Carbonate Till). Conversely, O, SG and Mg were more accurately mapped by SPOT.

Table 3.7: Overall accuracies for 4 classification maps:

Classification	Overall Accuracy
LANDSAT 1	60.54
SPOT 1	54.25
LANDSAT 2	60.42
SPOT 2	53.18

The confusion matrices were run using all the ROIs used for classification. Visual interpretation and GIS comparisons of the predictive maps to the modified surficial geology map have been completed to enhance this comparison in qualitative and quantitative analyses.

3.5.2 Comparison of predictive surficial materials maps to surficial geology map

The detailed surficial geology map (cf. Fig. 3.4 for location of the sub-region) is shown on Figure 3.5A. As indicated in the methodology, this map was rasterized and upscaled and is thereafter referred to as Surficial Materials Map 1 or SM1 (Fig. 3.5B).

As can be seen on Figure 3.5B, SM1 shows a dominance of alluvial and marine sediments in the eastern portion of the sub-region (blue and yellow). The alluvial sediments (Ap, yellow) comprise exposed sands and minor silts, while the marine sediments (Blues) are made up of exposed and gullied marine silts and clays (Mg), grass-covered fine sands, silts and clays (Ms1), and grass and lichen-covered sands and silts (Ms2_SG2) (Wityk et al., 2013). Sand and gravel (SG1) are predominant in the southwest and central west area (orange), tills are concentrated in the center (greens), and patches of bedrock (red) are scattered in the northern and southern portion of the map. Sand and gravel are covered by grasses and dried lichen and form marine deltaic deposits or glaciofluvial ice-contact deposits (Wityk et al., 2013). Tills consist of three groups 1) Tv (light green) - thin drift cover mixed with bedrock and boulders or bedrock and sand covered by sparse grasses and mosses; 2) Tb (medium green) - thick drift cover with little boulder cover or exposed bedrock covered by grassy-moss vegetation; 3) Tm (olive green) - modified till which has been eroded in places, and includes some sand and gravel, also covered by grass and moss.

LANDSAT classification maps for the sub-region were clipped from the maps provided in Wityk et al. (2013) (Figure 3.6A, 6B)). SPOT classifications maps were also produced using the same class combinations (Wityk et al., 2013) to produce S1 and S2 (Figure 6C, 6D). Subsets of these results are compared to the surficial materials map SM1 derived from the surficial geology map.

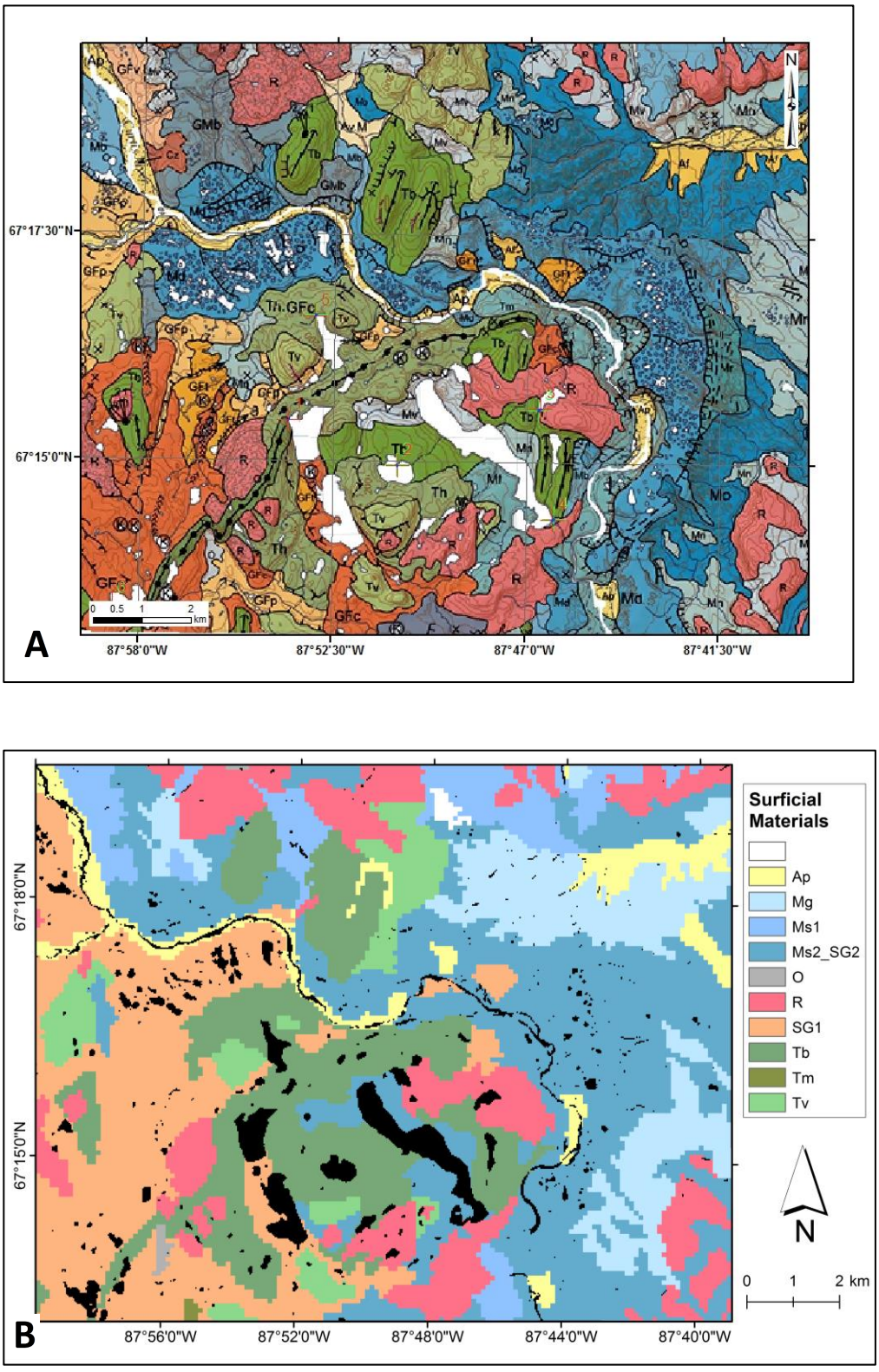

Figure 3.5: Mapped Surficial Geology. A) Sub-region of surficial geology map (Campbell and McMartin, 2014) extracted for comparison with classification maps. B) Surficial Materials Map (SM1) derived from surficial geology map (Campbell and McMartin, 2014).

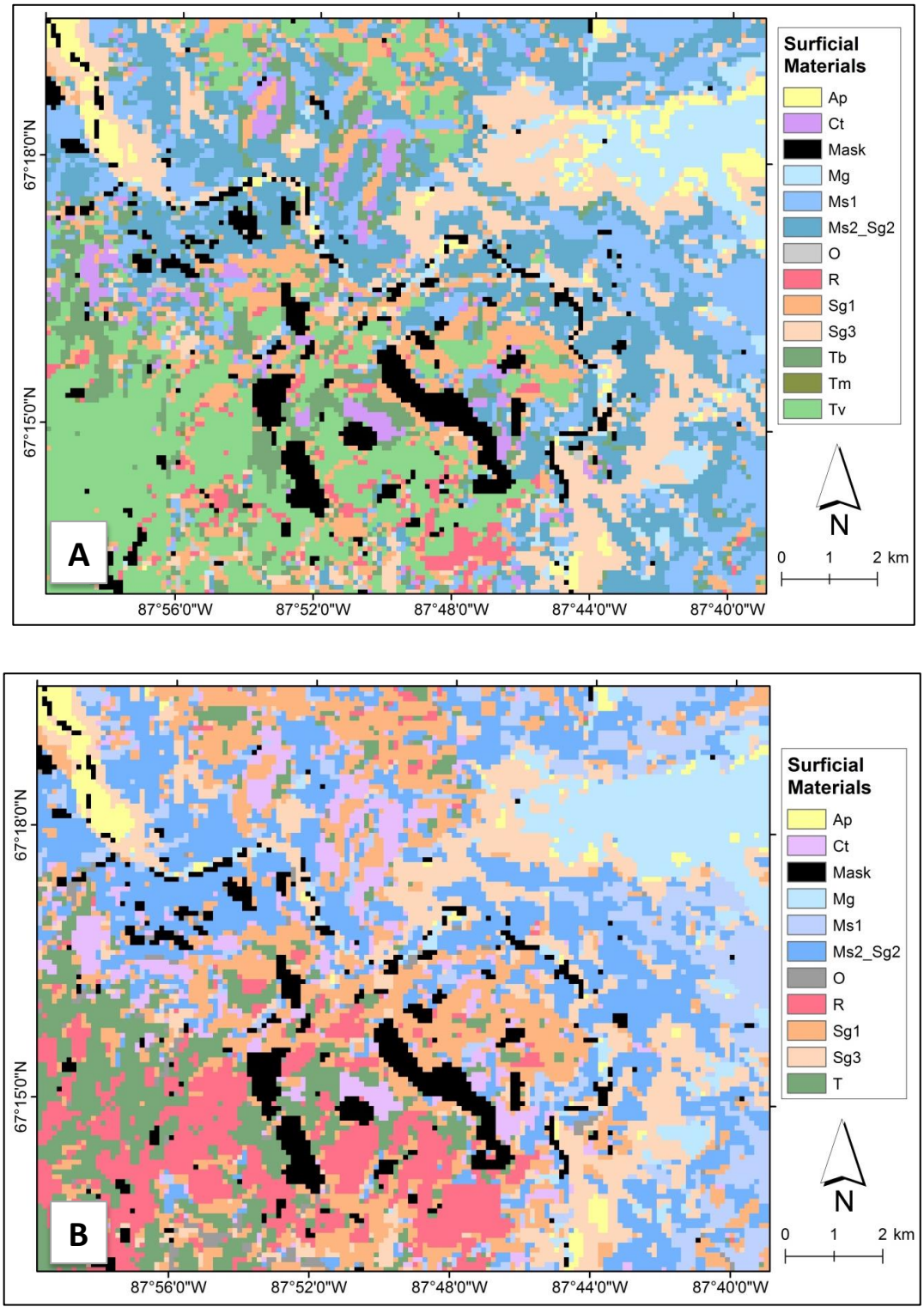

Figure 3.6: Classification Results using LANDSAT and SPOT data and 2 class combinations. A) L1 :LANDSAT imagery + class combination #1, B) L2: LANDSAT imagery + class combination #2, C) S1: SPOT imagery + class combination #1, D) SPOT imagery + class combination #2.

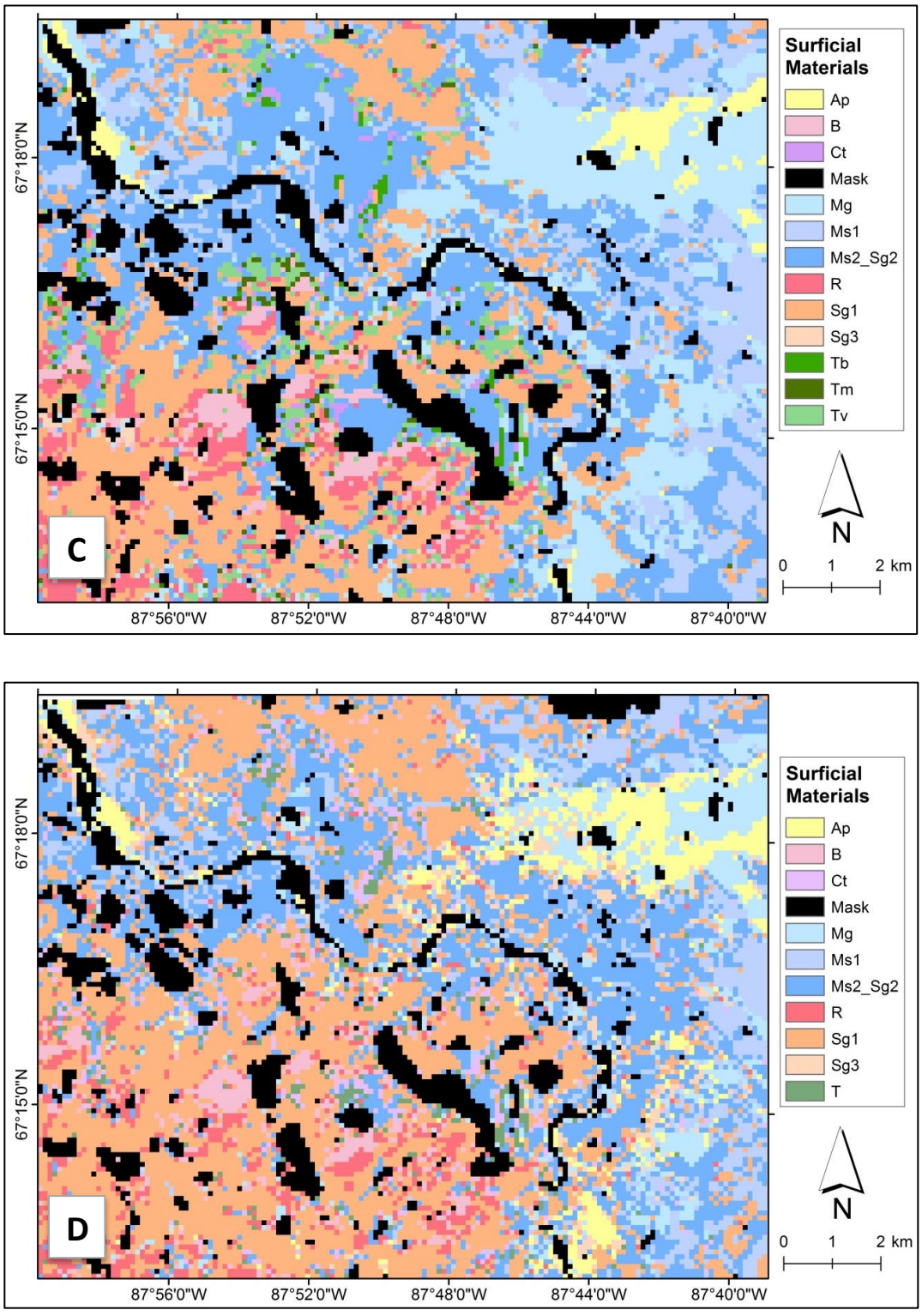

Figure 3.6: Classification Results using LANDSAT and SPOT data and 2 class combinations. A) L1 :LANDSAT imagery + class combination #1, B) L2: LANDSAT imagery + class combination #2, C) S1: SPOT imagery + class combination #1, D) SPOT imagery + class combination #2.

3.5.3 Visual Comparison Analysis

The four predictive maps (Fig. 3.6) generally predict large zones of marine and alluvial (fine sand, silts and clays) sediments in the east, which is consistent with the surficial materials map SM1 derived from the surficial geology map. The L1 classification predicts till in the central region, which is also consistent with the SM1 map. However, the SPOT and LANDSAT classifications are different from SM1 especially in the southwest and west portions of the sub-region. While SM1 displays a dominance of sand and gravel (orange) with some regions of till (green) in the west and southwestern portion of the map, L1 predicts large areas of thin till veneer (green) and L2 predicts large areas of both till and bedrock in these areas. The S1 and S2 predictive maps show larger areas of sand and gravel in the southwestern and central regions. SPOT maps show minimal occurrences of bedrock (red) and very little till (green) when compared to SM1. S2 shows little to no till (green) in the central and southwestern portion of the study area. L2, which uses the same class combination as S2, predicts occurrences of till (green) in the southwestern portion of the map, however, it overpredicts till in the west, inconsistent with SM1. It is also important to note that L1 and L2 maps predict a fair amount of carbonate tills (purple), which are not mapped on SM1. The prediction of carbonate till was field-checked and found that the till here was not calcareous. This is an example of the confusion between these materials as indicated by the confusion matrices, where it was shown that carbonate till (Ct) is confused with till (T) and with the till blanket subclass (Tb1_2). It is important to note, that the predicted Ct unit fell within areas of mapped till (both Tv and Tb) on the SM1 map. This is acceptable as the Ct class is indeed a "till"-category unit.

Multiple reasons could explain why SPOT and LANDSAT classifications are different from one another and also from the SM1. First, this could be due to spectral and spatial resolution differences in the imagery used. SPOT is of lower spectral resolution than LANDSAT, and does not collect reflectance data in the 2.2µm SWIR band (LANDSAT band 7) or the 0.4 µm blue band (LANDSAT band 1). However, more spatial variability may be seen in the SPOT imagery due to the higher spatial resolution (20 m compared to 30 m for LANDSAT). Lower spatial resolution imagery such as LANDSAT can filter out more of the spatial details captured by higher resolution sensors such as SPOT (Behnia et al., 2012). Furthermore, boundaries between different surficial materials are often gradational (i.e., thin till and bedrock outcrop). This fuzzy transition would not be captured with the maximum likelihood classifier used in this study as it is a hard classifier in which boundaries are sharp. Another reason for these differences could be a result of the creation of ROIs, which was partly based on LANDSAT data. As SPOT was not included in this process, classifications on LANDSAT data may have been favoured

3.5.4 GIS Comparison - Pixel to Pixel analysis

The pixel to pixel comparison results of L1, L2, S1 and S2 predictive classification maps are presented in Table 3.8. The agreement (% match) between the classification maps and the modified surficial geology map (SM1) is highest for the LANDSAT and SPOT classifications derived from training combination #1 (23% and 21%, respectively). The agreement is lowest for training combination #2(6%). *Figure* 3.7 shows the agreement between the predictive maps L1 and S1 and SM1.

Table 3.8: Pixel-to-pixel comparison statistics for 4 classification maps to modified surficial geology map SM1.

Imagery	Classification Combination	Match	Total Pixels	% match
LANDSAT	1	4138	18000	**22.99**
SPOT	1	3852	18000	**21.40**
LANDSAT	2	1127	18000	**6.26**
SPOT	2	1176	18000	**6.53**

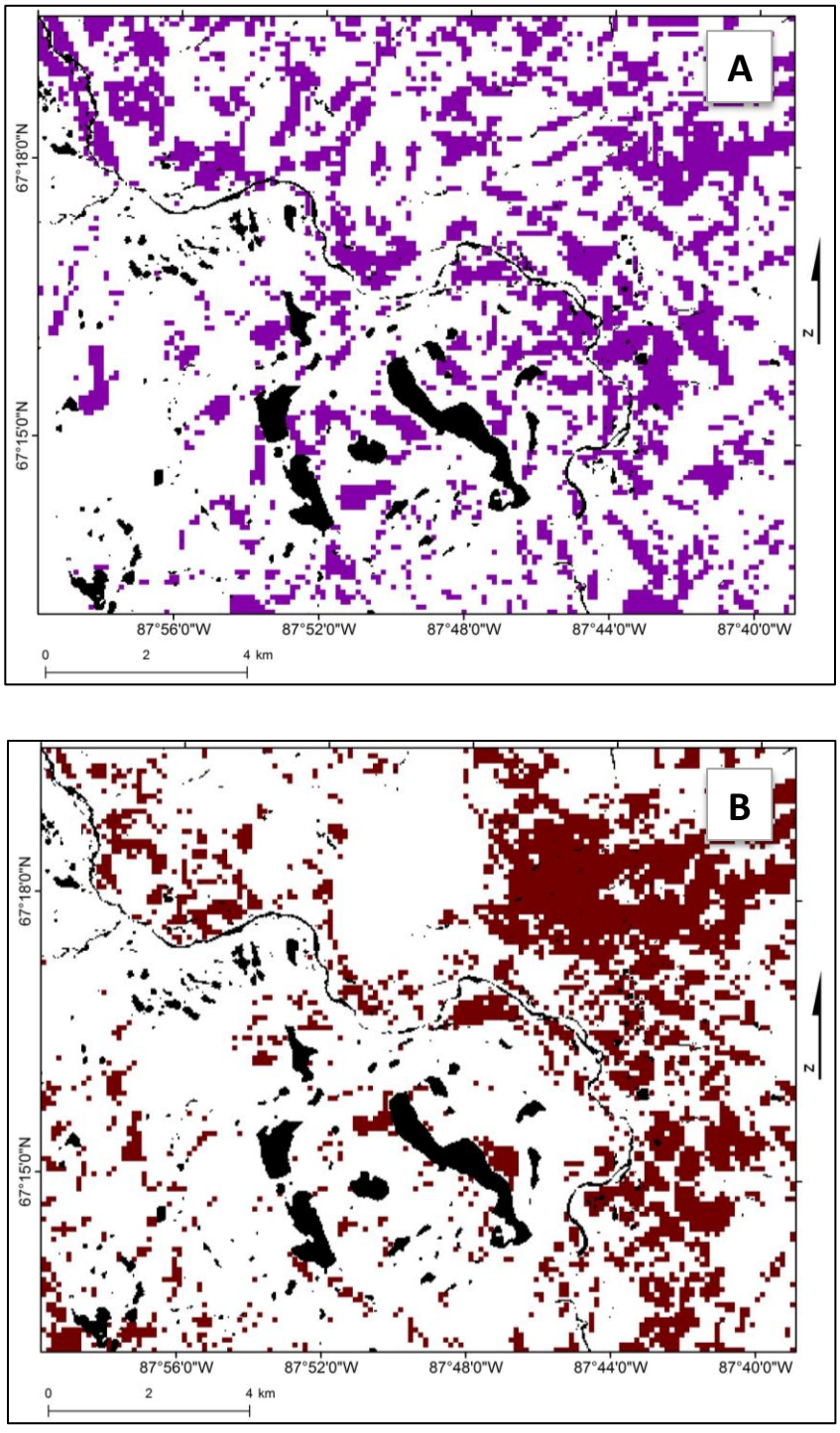

Figure 3.7: Correspondence maps indicate regions where a pixel-to-pixel correspondence was evident between classification maps (L1 and S1) and surficial materials. White space indicates a "non-match" with surficial geology and coloured regions presents a "match". A) Correspondence between surficial materials and LANDSAT 1 (L1) classification results. B) Correspondence between surficial materials and SPOT 1 (S2) classification results.

The L1 agreement map (Fig. 3.7A) shows a stronger correspondence with SM1 (Fig. 3.7B) across the region, while S1 displays better similarity in the northeast and east portions of the region. These areas correspond to a dominance of marine sediment classes (Ms1 class and some Ms2_sg2). Thus, S1 bares more resemblance, in particular where marine sediments are present, to SM1, which may be related to the higher spatial resolution of the SPOT sensor. Both classification maps display mostly white spaces (non-match) concentrated along the central and west areas, and southwest areas particularly for L1. According to SM1, the southwestern portion of the map consists mainly of sand and gravel with small areas of till and bedrock (Fig. 3.5). In contrast, the L1 and L2 maps predict mostly till and bedrock in this region, whereas S1 and S2 maps predict more sand and gravel (SG1_SG3), and generally less till than SM1. Nonetheless, a poor spatial match remains with sand and gravel in that area between S1, S2, and SM1.

In addition to the LANDSAT 1 classification, which has an overall 23% match with the modified surficial geology map, individual class correspondences were also computed for this classification (Table 3.9). Tm was not included in this correspondence exercise; while SG1 and SG3 were grouped together as they are the same material, just unexposed (SG1) and exposed (SG2). This was done to simplify the comparison. From this computation it can be seen that there is relatively stronger agreement for the marine and alluvial sediments (Ap, Mg, Ms1, Ms2_Sg2) between the predictive and modified surficial geology map (between 30 and 35%, match). Less agreement is found for the organics, bedrock and thick tills (between 18 and 19%), with sand and gravel (SG1 and SG3) having the least agreement, at only 7%. This is consistent with the visual comparison.

Table 3.9: Individual class correspondence for LANDSAT 1 classification, most accurate in terms of comparison to surficial materials map SM1.

Class/Material	# Pixels in LS1 Classification	Corresponding # Pixels	# Pixels in Surficial Materials Map	Match % (corresponding/ surficial material)
MS2_SG2	3710	1692	4792	**35.31**
Tv	3068	266	786	**33.84**
Ms1	2363	340	1011	**33.63**
Tb_Ct	1821	781	2559	**30.52**
Ap	466	227	761	**29.83**
Mg	922	522	1777	**29.38**
R	1705	404	2111	**19.14**

Table 3.9 (Continued)

O	105	6	32	**18.75**
SG1_SG3	2742	213	3047	**6.99**

This pixel-to-pixel comparison reflects partially the data presented in the confusion matrix computed using the ROIs within the entire study area (Table 3.4). For example, the alluvial (Ap) and Marine sediments (Mg, Ms1) had the highest accuracies of over 77% for L1. In contrast, the marine sub-class Ms2_Sg2 only yielded a moderate to low classification accuracy of ~59% while the GIS analysis indicates the highest match of all the classes (35%). Classes with higher correspondence between SM1 and the L1 classification included 2 of 3 till units (Tv and Tb_Ct) (33% and 31% correspondence – Table 3.8). These results compare with those of the confusion matrix, which indicated that till units were mapped with poor accuracy (Tv - 49% and Tb_Ct equivalent Tb - 48%) – both cases demonstrate relatively poor accuracy. Bedrock (R), and Organic (O) units had lower correspondence, yielding approximately 19% match with SM1. The confusion matrix indicates organics were mapped more accurately (78%) while Tb and R were poorly accurate (~48%). The lowest corresponding class was that of Sand and Gravel (SG1_SG3) which yielded less than 7% match with the SM1 map, similar to what is seen with the confusion matrix as these units were mapped with poor (SG1 – 35.32%) and moderate accuracy (SG3 – 64.96%).

3.6 Discussion

This study shows that overall, LANDSAT imagery more easily predicts (classifies) surficial materials than SPOT imagery. Certain surface materials classes are classified with a relatively high degree of confidence with both types of imageries, while the classification process does not as easily distinguish others.

In the study area, marine (Mg, Ms1 and Ms2_SG2) and alluvial (Ap) sediments (fine sands, silts and clays) are similarly mapped using both the LANDSAT and SPOT datasets and generally compare favorably with a sub-set of a modified surficial geology map. These materials show a unique spectral response and bear a general spatial resemblance to that of the modified surficial geology map. Although some misclassifications do occur within these units, it is important to note that these misclassifications are moderate. For example, some misclassification of Ms2 is classified as Ms1, which is of the same sediment material family - being of mainly marine fine sediments but grass covered. A softer comparison, taking into consideration exceptions such as this would increase the correspondence percentages. This may be accomplished through grouping classes together (post-classification), and conducting a comparison using broader sediment categories. Other surficial materials especially till, vegetated sand and gravel, and bedrock are not accurately classified. Confusion occurred between these

materials on the four classification maps, and produced a poor association when compared to the modified surficial geology map.

Despite the up-scaling step, the predictive classification maps remain much more heterogeneous than the surficial geological map. Some of the heterogeneity may be real, but some is due to other factors than surficial material types such as vegetation, soil water content, and other complicating factors. The comparison exercise is therefore more useful to identify areas where both the RPM process and the geologist's "filtered" map are in agreement rather than to assess RPM maps accuracy. The comparison will help determine which type of materials are mapped the same way by the two approaches and which ones are more challenging to either the RPM approach, the geologist doing air photo interpretation, or both. This could provide useful insights into optimizing the use of RPM for geological mapping such as identifying problematic areas where field work is necessary to reduce uncertainty. It is important to recognize that this comparison is not a measure of one map being *better* than the other; both maps offer valuable information and therefore contain slightly different information.

The RPM process shows limitations distinguishing tills from sands and gravels, bedrock, at least using optical reflectance data. Perhaps the boulders on the till surface and the similar mineral composition of all these materials (e.g. the till may contain a large proportion of locally-derived bedrock) yield a similar spectral signature. The distribution and density of boulders (% boulder cover) on the till surface could thus have an important impact on the degree of confusion between till, boulder fields, and bedrock, perhaps even more so if the boulders are derived from local bedrock. It would be interesting to compare areas where boulders and material in the till are locally-derived against areas where material has a more distal provenance, yet similar textural matrix. Perhaps the use of radar data, as demonstrated by Grunsky et al. (2009), could help distinguish between some of these surficial materials which are confused optically by adding parameters of surface roughness and moisture to help separate various surficial materials. Interestingly, mapping these materials may also be more challenging to the geologist. The use of RPM could thus be used to identify priority areas, i.e. areas with high confusion and disagreement with surficial materials map, for more targeted field work.

Other factors such as variations in water content, vegetation, boulder cover, or slope and aspect, could complicate mapping of till. For example, a study that mapped surficial materials representing predefined moisture contents highlighted the relationship between various surficial units and water contents (Lesemann et al., 2013). A drumlinized till surface, for example, could contain well-drained till at the top of drumlins, while drumlin swales may be water-saturated. While the same till type covers both regions the spectral response would differ due to differences of moisture content. The spectral signature of a drumlinized till surface discontinuously covered with boulder fields may indeed overlap with that of other materials such as boulder fields, and areas characterized by a mix of thin discontinuous till and bedrock outcrops and bedrock with boulders. This raises the notion that there is high pixel-to-pixel variability (noise) in areas characterized by these types of terrains. For example, it is quite clear from field observations that

a 30x30m surface area may encompass terrain with boulders, till with low boulder coverage, and bedrock, which would be mapped and generalized as till veneer (Tv). In contrast, areas of fine grained marine (or sandy alluvial) sediments are generally more homogenous and laterally extensive leading to much less pixel-to-pixel variations inside these regions and, therefore, a more unique (non-overlapping) spectral signature. The latter areas also tend to form flatter surfaces and may also have more homogenous water content. It is important to note that this RPM methodology considers one characteristic to distinguish surficial materials - spectral reflectance in 6 LANDSAT bands - when a number of other features have influenced the mapping of these materials. Again incorporation of images derived from a DEM and/or radar data could help distinguish surface materials that are confused optically.

The remotely sensed data produces maps that are representative of a single physical surficial parameter - spectral reflectance (Behnia et al., 2012). Differences between the classification maps may be a result of differences in spectral resolution (LANDSAT having visible blue band as well as short-wave-infrared band, not found in SPOT imagery). This is also due to class combinations used (combination 1 or 2). This exercise of class combinations would alter the number of pixels assigned to each group and number of ROI's allocated for each class which would also have an impact on the output.

3.6.1 Comparison with the surficial geology map

The agreement between the modified surficial geology map and the classified maps is low, but this is expected. This expectation stems from the fact that the map production process of these outputs is different. The relatively low agreement does not suggest either of the maps to be incorrect. For instance, there is more detail seen in the classification maps (Fig. 6) as they are based on 20 and 30 m spatial resolutions of remotely sensed data, while the traditionally mapped outputs (Fig. 3.5) incurred more generalization resulting from fieldwork and air photo interpretation. These maps are therefore not directly comparable. Nonetheless, the comparison exercise provides interesting insights. For the traditionally produced map, a number of features were considered and integrated including photogeologic characteristics (tone, texture, shape, pattern, context, association) and field observation (Behnia et al., 2012). Using the RPM process in concert with that of traditional geologic mapping is complimentary as they offer different perspectives. It is suitable to incorporate both processes to produce surficial maps (Behnia et al., 2012).

3.6.2 Comparison to Previous Studies

Two other studies related to RPM of surficial materials in the Arctic were completed by others: 1) Wager Bay North Area (Campbell et al., 2013), and 2) Schultz Lake Area (Grunsky et al., 2009). Though methodologies and numbers of classes used vary from one study to the next, general trends are noticed in that materials that are better mapped and more poorly mapped are the same across the three studies. This is according to the classification accuracy based on a comparison with the original training areas used. Similar to this Repulse Bay area study, the Wager Bay North study found that alluvial plains (Ap), marine sediments (Mg and M), organics

(O), boulders (B), and carbonate-rich till (Ct) were among the classes which were mapped with higher accuracies (Campbell et al., 2013). This is also consistent with findings at Schultz Lake, indicating that boulders and organic deposits have high accuracies as well (90% and 75%, respectively) (Grunsky et al., 2009). Though the Wager Bay study indicates that there were limitations in distinguishing and mapping bedrock, resulting in poor accuracies, predictive mapping of bedrock at Schultz Lake was accomplished with more accurate results (78%).

Similarities are also apparent across the three studies with respect to the poorest mapped materials. In all cases, sands and gravels were mapped with poor accuracies, and till units also produced low accuracies. However, at Schultz Lake, thick tills were distinguished well and yielded a high accuracy (82%), while thin till did not (49%).

This comparison emphasizes that, in regions of the arctic, optical imagery in RPM efforts perform better at mapping alluvial plains, marine sediments, organic materials, boulders and carbonate-rich tills, while showing limitations in mapping bedrock, till, and sands and gravels.

3.6.3 Pixel Size/Resolution

Given that the resolution of the imagery is much finer than that of the modified surficial geology map, which partitions the map area into large homogenous polygons, the RPM maps likely capture more heterogeneity than the modified surficial geology map and indeed likely the original surficial geologic map. Some of this heterogeneity may be noise, due to variations in water content for example, but part of it may be true sediment heterogeneity. For instance, in regions mapped as alluvial (yellow) and marine (blue) sediments, potentially more details are provided by the satellite imagery - which shows pixels of blue (marine sediments) within the yellow (alluvial sediments) and vice versa. This may indicate sediment texture variations within a unit or, alternatively, small discontinuous patches of a unit within the larger, dominant, unit in an area. These details may not have been captured by the geologist during mapping or have been lumped due to the scale and level of details of the surficial map. This indicates that visual examination of the imagery is required and points to the need for ground-truth to validate the RPM map. This is further supported by the fact that relatively high confusion exists to some extent with all units. Further research may be conducted to address reasons for this confusion and provide additional insight on how to mitigate it.

3.6.4 Problems and Limitations

Limitations to this study include: (1) only one type of data (spectral reflectance) was used to produce the classification maps, (2) the ROIs were created using LANDSAT imagery (and not the SPOT data), and, (3) the ambiguity in the comparison of the RPM classifications with the modified surficial geology map, which are not directly comparable.

The ROIs produced for classification were created and digitized using a combination of fieldwork, air photo interpretation and LANDSAT imagery. This influenced the delineation of the ROIs as they were evaluated and selected based on their visual appearance on the LANDSAT data and around certain characteristics that are not otherwise transferrable to SPOT imagery due

to differences in bands, pixel size and slight difference in season of acquisition. Therefore, this skewed classification results in favor of the LANDSAT imagery.

The dissimilarities in classes of the RPM and of the geology map led to some ambiguity in comparing the two types of maps. The RPM process is based on image characteristics while the surficial geology map is based on fieldwork, interpretation of various characteristics on air photos, and expert knowledge and experience. Furthermore, the modification of the geology unit classes into RPM classes is approximate at best. Since the maps and associated legends were created from two different methodologies, the outputs are not directly comparable. In addition, it is not possible to compare the outputs against a "true" map of the reality. In other words, both maps (RPM and geology) have their own uncertainties. The RPM classes were derived from initial fieldwork and air photo interpretation; however, they were mainly delineated and selected using LANDSAT signatures of the surficial materials. The surficial geology classes included information regarding process and depositional environments otherwise not considered in the RPM process. As discussed above, a second problem to this comparison is that resolution is dissimilar in the two maps being compared. While the SPOT and LANDSAT classification maps are at a 20 or 30 m resolution, the derived modified surficial geology map is that of a 1:100,000 scale resulting in generalization of the natural heterogeneity in surface materials that exists on the ground.

Despite the important limitations, the comparison exercise was a necessary step towards understanding the fundamental differences between RPM maps and geological maps. This exercise indeed confirms that even an up-scaled RPM map is not directly comparable to a geological map and yields low spatial (pixel-to-pixel) agreement results. This suggests that important uncertainties persist with RPM and it may not be appropriate to use spectral reflectance alone to map certain surficial materials. A closer look at the results in their spatial context also reveals that some of the disagreement may be due to real heterogeneity captured by RPM within certain units; heterogeneity that may be simplified or missed by traditional geological mapping. These aspects of RPM versus surficial geology maps needs to be further investigated; they are particularly important if RPM maps are to be used to help plan and optimize geological field mapping.

3.6.5 Solutions and Future Work:

For future work, additional data such as RADARSAT imagery and derivative products from a DEM could be incorporated to provide information on textural and topographic properties of surface materials (i.e. Grunsky et al, 2009). In producing ROIs in subsequent work, a suggested approach is to create ROIs using mediums independent of those to be used for classification. For instance, produce ROIs without influence of imagery, visual spectral signatures and pixel sizes (i.e. without digitizing over the imagery). It is suggested to create ROIs using an independent medium and transfer them to appropriate format for further ENVI classification. This would reduce bias towards the classification. It would also be beneficial to

create ROIs with a more even distribution across the study area where possible; to ensure that the widest-possible spectral range is captured and applied in the classification algorithm to identify like-pixels, or materials.

Object-based classification may also be implemented as an alternative to pixel-based classification. This approach segments imagery into groups of pixels (objects) and considers information such as topological entities, shape and length (Baatz et al., 2004). This would reduce spectral variation within classes and provide information on contextual properties (Guo et al., 2007).

Further improvements, over and above what we have done in the study, could be made to facilitate the comparison between predictive maps and traditional geology maps to account for some of the expected ambiguity. As accomplished in this paper, modifying the surficial geology map to accommodate a comparison to the RPM classes resulted in losing the details regarding depositional environments and processes. To mitigate this, it would be effective to consider depositional environments in the creation of ROIs by incorporating other data types to capture both spectral and spatial characteristics of surficial materials. This would create a fairer ground for comparison between the two maps thereby creating maps with different techniques yet maintaining legend consistency. Producing classes that consider physical properties (i.e. vegetation type/cover, moisture content) would also be beneficial, as it would help discriminate spectral signature ranges. It would be reflective of what the signatures are influenced by and the information that they capture. For example, using units such as dry till, wet till, till with vegetation cover, boulder till could be more easily compared in this type of exercise. In addition, to account for the discrepancy of scale, the predictive map could also be generalized using a spatial filter to reduce some of the heterogeneity captured before comparison to the traditional surficial geology map.

Finally, is beneficial to create a final map of surficial materials/geology using both the traditional mapping approach and the RPM methodologies. The simultaneous use of both approaches would provide a map with key information; interpretation and statistics to produce a more robust and representative map of surficial sediments by ensuring both processes and spectral information are incorporated. For example RPM has the capacity to include more detail down to a smaller pixel-level scale (i.e. 30 m) as well as including spectral information. Recent surface geology maps completed or under progress for the project (Campbell and McMartin, 2014; McMartin and Campbell, in press) have already benefited from the informal (visual) use of surficial materials classification maps produced by RPM (Wityk et al., 2013; Campbell et al., 2013). Further work could develop a more robust methodology that uses RPM classification and traditional field mapping approaches alongside one another.

By applying these recommendations, further insight will be gained on how to make the RPM process more effective and reliable and enhance the mapping procedure of surface materials and sediments in the Arctic.

3.7 Conclusion

This study shows the potential benefit of using RPM as part of a surficial geological mapping exercise in the Canadian North and, possibly, other northern environments. The classification maps derived from multi-spectral responses helped identify areas where uncertainty is low (e.g. marine sediments), and areas of potential "real" heterogeneity that is difficult to capture while doing air photo interpretation (e.g. alluvial and marine sediments). Classification maps may also be used to help identify problematic areas (e.g. discontinuous till mixed with other materials) where more field work may be required. LANDSAT and SPOT imagery yielded different results with LANDSAT showing an overall "best fit" with a modified surficial geology map and SPOT showing better results for specific materials. Overall accuracies for the two LANDSAT classifications were slightly over 60%, while SPOT classifications yielded overall accuracies of 53% and 54%. Both imageries indeed prove to be better at mapping certain surficial sediments than others, when visually compared to the traditional but modified surficial geology map to RPM classes. Overall, in the arctic tundra environment near Repulse Bay, SPOT and LANDSAT imagery were useful for mapping marine and alluvial sediments, while showing limitations in mapping organic, till and bedrock.

The RPM approach offers cost and time efficient techniques and has significant potential for mapping the surficial materials of areas beyond the tree line. Vegetation can complicate the use of geological RPM, however very little tree cover occurs in the arctic tundra providing a prime environment for the application of RPM. The high cost of logistics coupled with a short field season (mainly July and August), prolongs the production time of surficial maps produced from fieldwork. RPM allows the geologist to map regions that are inaccessible for field work, direct and focus field mapping, and aid in the interpretation of geological features all of which contribute to reducing the time and effort required to produce a traditional surficial geological map. Remotely sensed data provides more information regarding moisture, vegetation, etc. that can be extracted and used to infer sediment properties, yet, to date has been underused in the mapping of surficial materials.

Chapter #4: Conclusion

4.1 Developing the RPM classification method for the Arctic Tundra Landscape

The RPM classification method is still a relatively new approach for the production of surficial materials maps in the Arctic tundra. As RPM methods continue to evolve and be tested, this research provided further development and testing of the existing RPM classification method (Scheltselaar et al., 2007) and additionally the RCM classification method (Harris et al., 2012). One of the most important conclusions of this work is that targeted fieldwork prior to the creation of training areas remains a key component of the RPM mapping process. It is critical to thoroughly describe the material and the local landscape of potential training area using field observations. Another outcome is that when two or more approaches, are used and compared (e.g. field observations + remote sensing), it is possible to determine a class combination that best represents the true geology of the region. This study also suggests that LANDSAT imagery may produce better overall maps than SPOT, whereas SPOT may perform better for certain sediment types. In all cases, the geological expertise remains necessary to reduce and minimize geological inconsistencies from automatic classifications due to the complexity of the spectral signatures that are influenced also by factors other than geology.

This thesis presents a unique comparison of output classification maps to a traditionally mapped surficial materials map, using a pixel-to-pixel comparison. This comparison has led to additional insights into the RPM approach and its differences to the traditional mapping approach, shedding light on which materials are more easily mapped than others, and which types of data are the more optimal choices and for what purpose. It also emphasizes the importance of scale and the fact that there is no "true" map, which leads to think more critically about RPM, but also about traditional map products and information. Essentially, traditional surficial geological maps incorporate geomorphology, textural, age and depositional environment interpretations, while RPM materials maps use the spectral signature to determine the nature of the surficial materials. The latter may capture more natural heterogeneities than geological maps, but some of these heterogeneities are related to other factors (e.g. water content, lichen cover) than surficial materials characteristics. The next challenge would be to better understand these heterogeneities and develop techniques to filter (or upscale) the RPM map to create more homogenous zones that better capture the spatial continuity of sediment type distribution. Such RPM maps would approach the scale and style of a traditional geological map and may be more intuitive to use.

4.2 Thesis Contributions

This thesis advanced and developed ways to enhance the RPM process for mapping surficial materials in the Arctic Tundra. The following are the most significant contributions made in this research.

4.2.1 Incorporation of the Geological Knowledge into the Iterative RPM process

Part of the iterative RPM process in this project included looking at classification outputs and determining if classes of surficial materials were mapped appropriately. This was done using the geological expertise of the surficial geologists within the study area and also using calculated accuracies related to confusion matrices run on output classifications. Decisions regarding which classes (surficial materials) were to be removed or merged with others were taken to produce new class combinations for subsequent classifications in hopes of producing more realistic outputs. After conducting this iterative process, it was determined that more optimal class combinations and associated RPM outputs were produced when incorporating input from geologists. The geological knowledge-based approach was more suitable for producing more realistic classifications of surficial materials in the Repulse Bay study area. This approach suggests that using geological criteria and oversight of Quaternary geologists in the RPM method results in the production of more comprehensive predictive maps of surficial materials in this type of terrain.

4.2.2 Open File – Data Release

As a result of this thesis, a government publication was released by Natural Resources Canada – "Remote Predictive Mapping of Surficial Materials West of Repulse Bay, Nunavut (NTS 46M-SW, 46L-W and –S, 46K-SW)"- Wityk et al., 2013. This Open File publication (GSC OF 7357) includes a data release of the created predictive maps of the study area, and a methodology description of how they were created. The data released in this publication are raster image files of the classified predictive maps using LANDSAT data as well as associated variability maps and training area polygon data which were used in the classification process. It discusses the 4 best-representative classification maps, which were the results of an iterative process to arrive at them and the variability of classifications across the maps. Finally the publication provides a discussion regarding two approaches, statistical and geological knowledge-based, which were used in an attempt to generate more optimal classification outputs. Finally, it highlights the importance of incorporating geological knowledge into the RPM approach.

4.2.3 Predictive Maps (First Order)

As a result of this thesis, a set of first order surficial materials maps of the study area were created for NTS Map Sheets 46M-SW, 46L-W and –S, 46K-SW, which cover an area that had not been previously mapped for surficial geology at the beginning of the project. This work contributed to the knowledge of the RPM process in the Arctic Tundra and furthered the understanding of Remote Predictive Mapping techniques. These techniques can be applied to future projects with similar themes and applications, and produce classifications at 30 m and 20 m resolutions.

4.2.4 On Regions of Interests (ROIs) and Related Classes

On the theme of ROIs and Classes, findings from this thesis led to the suggestion to split heterogeneous material (classes) prior to classifying and also that it is more optimal to run preliminary classifications, in early iterations, with a greater number of classes than fewer. This facilitates the ability and option to lump classes later on in the RPM process (assuming that user input and inclusion of geological knowledge is also being incorporated to do so and perform subsequent manual iterations). For example, it was found that the best results were produced when similar classes (those that were either statistically or visually confused with one another) were combined together. For example, merging of marine silty sands subclass-2 (Ms2) with sand and gravel subclass-2 (SG2 – mainly made up of marine silty sands) eliminated much confusion and a better map output. Though Ms2 is unsaturated and SG2 is moist, both are marine silty sands that are covered by grassy vegetation.

It was also determined that the number of classes used in a classification has an impact on the outcome and can therefore play an important role in map accuracy. Introducing a higher number of classes introduces a smaller margin for error. For instance, classification maps with a single till unit had a reduced accuracy than those with 3 till units. Classifications are based on classes and determining which classes to use is critical for the output classification maps and their accuracy.

4.2.5 LANDSAT is better than SPOT data for overall map accuracy

In comparing two types of imagery to classify surficial materials in this project, it was found that LANDSAT presented higher overall accuracies than SPOT imagery when evaluating confusion matrices. These results, based on classification outputs produced with LANDSAT and SPOT and the training data used to create these classifications (ROI's), showed that LANDSAT imagery produced maps with ~60% ROI accuracy, while SPOT presented ~54% ROI accuracy. The LANDSAT data also provided results that are more reflective of the expected surficial materials of the region. The latter expectations considered field knowledge and field mapping expertise of geologists involved in the project. The reason for differences between LANDSAT and SPOT classifications is attributed to difference in spectral resolution, or number of bands the imagery contains. LANDSAT imagery contains bands in the shortwave infrared (SWIR) bands, which contains light not visible to the human eye. Therefore, this provides more information within the imagery and results in differences in spectral responses from the same materials.

4.2.6 Comparison to Available Surficial Materials Map

This RPM study was conducted alongside a surficial geology mapping project. The surficial mapping project included expertise in surficial geology mapping, interpretation of past glacial histories and environments as well as extensive fieldwork and planning. This facilitated a direct comparison to be made and encouraged collaboration with geologists.

Further, the study facilitated a more quantitative comparison between geological mapping and RPM outputs by form of a digital, pixel-to-pixel comparison in a small area. In this

comparison, it was found that LANDSAT classifications produced a higher overall correspondence to the surficial materials map than classifications using SPOT imagery. This again suggested that LANDSAT produces more accurate classification results. When considering spatial distribution of correspondence across the smaller area used for comparison, it was noted that the distribution of corresponding pixels using LANDSAT imagery appeared to be more evenly distributed spatially across the study region when compared to SPOT imagery. It is important to note, however, that in the SPOT correspondence map, pixels were more concentrated in certain areas, or generally within certain materials of geologically mapped classes. This concentration of correspondence, typically occurring in regions of like-materials, suggested that SPOT is more sensitive to mapping particular classes due to its different spectral response than LANDSAT - marine sediments and alluvial plains in particular – and may therefore be useful imagery to map these types of materials.

4.2.7 RPM: Limitations and Issues

Mapping surficial materials using the RPM method has inherent limitations and issues, some of which can be mitigated and some which cannot be avoided. Limitations lie in the data used (imagery) and also within the materials they are set out to classify. Imagery may be the cause of misclassification as it can be radiometrically unbalanced. This happens when two or more scenes of imagery are captured at different seasons or times are stitched together to form a single image. Differences in season also influences moisture content and vegetation cover, therefore affecting the spectral representation of the surficial materials. Imagery used may also capture clouds, which does not represent surficial sediments therefore causes misclassified pixels and/or regions. Surficial materials that are similar to one another in terms of composition or vegetation cover may influence classifications of their pixels and confusion between their classifications. Materials in this area tend to have gradual transitions and not hard boundaries, which is difficult to capture with spectral information.

4.3 Implications of Work

4.3.1 Aggregate Resources and Mineral Exploration Applications

As discussed, using the RPM approach alongside the traditional mapping method is an asset in streamlining mapping of surficial materials in the arctic tundra. It is useful in identifying locations to focus fieldwork and resources required for fieldwork such as time and funding to make field expenditures more effective. The Canadian Arctic is host to base metals, diamonds, uranium, gold and nickel-copper-platinum group elements. If more efficient bedrock and surficial materials mapping of the arctic tundra is completed, exploration of such resources in the north will be improved. Further exploration and discovery of available mineral resources will therefore positively influence northern communities and the national Canadian economy.

This RPM approach and associated research can be useful to industry as it encourages the collaboration of the remote sensing and geology communities to work together thereby enhancing the scientific progress. This collaboration can facilitate the achievement of

accelerated mapping results and increase potential in the development of additional and more efficient resource exploration programs in a more cost-effective manner.

4.3.2 Where to go next?

The RPM approach, thought to enhance geological mapping of the arctic and make mapping programs more effective, raises further questions and presents further research opportunities as it continues to evolve. It would be useful to explore spectral signatures and related statistics of individual surficial material classes as to identify how spectrally different on a statistical level groups of sediments or classes of sediments are on a numerical level. Incorporating additional data alongside these imageries would also be useful – such as RADARSAT for provision of textural information, and digital elevation models (DEMs) for topographical data. Topographical data is available at varied scales, and can provide further insight into drainage and moisture content. As the creation of ROIs is critical to this process, it would be imperative to further develop and streamline their production and determine whether their creation is most effective by using a single method or source for their derivation (i.e. fieldwork, visual imagery interpretation, air photo interpretation), or a combination of these means. The RPM method is a relatively new approach and requires further investigation to optimize its process to satisfy the needs of the geological mapping and in turn the resource exploration industry.

References

Aldrich, J., 1997. R. A. Fisher and the Making of Maximum Likelihood 1912-1922. Vol. 12, No 3, pp 162-176

Aplin, P., Atkinson, P.M. and Curran, P.J., 1999. Per-field classification of land use using the forthcoming very fine spatial resolution satellite sensors: problems and potential solutions. In P.M. Atkinson and N.J. Tate (Eds), Advances in Remote Sensing and GIS Analysis, pp. 219–239 (New York: John Wiley and Sons).

Aylsworth, J. M. and Shilts, W. W. 1989. Glacial features around the Keewatin Ice divide: Districts of MacKenzie and Keewatin; Geological Survey of Canada, Paper 88-24, 21 p. Canadian Journal of Remote Sensing, Vol. 38, No. 1, pp. 69-90.

Batterson, M., Taylor, D., 2007. Till Geochemistry surveys and preliminary Quaternary mapping of the Burin Peninsula and adjacent areas. IN current Research. Newfoundland Department of Mines and Energy, Geological Survey Branch, Report 07-1 pp 197-214.

Baatz, M. and Schäpe, A. 2000. "Multiresolution segmentation – an optimization approach for high quality multi-scale image segmentation". In *Angewandte Geographische Informationsverarbeitung XII*, Edited by: Stroble, J., Blaschke, T. and Griesebner, G. 12–23. Karlsruhe: Herbert Wichmann Verlag.

Behnia, P., Harris J. R., Rainbird, R. H., Williamson, M. C. and Sheshpari, M. 2012. Remote predictive mapping of bedrock geology using image classification of Landsat and SPOT data, western Minto Inlier, Victoria Island, Northwest Territories, Canada. International Journal of Remote Sensing. Vol. 33, No. 21, pp 6876–6903.

Benediktsson, J., Swain, P., Ersoy, O., 1990. Neural Network Approaches versus Statistical Methods in Classification of Multisource Remote Sensing Data. IEEE Transactions on Geoscience and Remote Sensing, Vol 28, No. 4, pp 540-552

Boulton G., and Clark, C., 1990 A highly mobile Laurentide ice sheet revealed by satellite images of glacial lineations. Nature. Vol. 346, pp. 813-817

Briggs, W.L., 1987. A Multigrid Tutorial; Society for Industrial and Applied Mathematics, (SIAM) *SIAM Journal on Scientific Computing*, 14(2), 506–510.

Brown, O; Harris, J R; Utting, D, 2008. Case study 6. Surficial mapping of northern Baffin Island using LANDSAT and topographic data. Remote predictive mapping: an aid for northern mapping; by Harris, J R (ed.); Geological Survey of Canada, Open File 5643, 2008; p. 225-232; 1 DVD

Brown, O; Harris, J R; Utting, D; Little, E C., 2007. Remote predictive mapping of surficial materials on northern Baffin Island: developing and testing techniques using Landsat TM and digital elevation data. Geological Survey of Canada, Current Research (Online) 2007-B1, 2007; 12 pages, doi:10.4095/223434

Campbell, J E; Harris, J R; Huntley, D H; McMartin, I; Wityk, U; Dredge, L A; Eagles, S. 2013 Remote predictive mapping of surficial earth materials: Wager Bay North area, Nunavut - NTS 46-E (N), 46-K (SW), 46-L, 46-M (SW), 56-H (N), 56-I and 56-J (S) Geological Survey of Canada, Open File 7118, 42 pages, doi:10.4095/293158

Campbell, J E; McMartin, I, 2014. Surficial geology, Lefroy Bay (southwest), Nunavut. Geological Survey of Canada, Canadian Geoscience Map 152, 2014; 1 sheet doi:10.4095/293975

Campbell, J.E. and McMartin, I. 2010. Surficial geological mapping in the Wager Bay area, Nunavut - filling in the gaps; *in* Palmer, E. (ed.), 38th annual Yellowknife Geoscience Forum, Abstracts of talks and posters, Northwest Territories Geoscience Office, Vol. 2010, pp 6-7

Campbell, J.E. and McMartin, I. 2011. Regional glacial patterns in the Repulse Bay - Wager Bay area, Nunavut; Geohydro 2011, Proceedings of the joint meeting of the Canadian Quaternary Association and the Canadian Chapter of the International Association of Hydrogeologists, Quebec City, Quebec, August 2011, Doc. 2156

Campbell, J.E., McMartin, I., Tremblay, T., Wityk, U. and Dredge, L.A. 2011. New insights on the surficial geology of the Repulse Bay area, Nunavut: implications for mineral exploration; *in* Fischer, B.J. and Watson, D.M. (eds), 39th annual Yellowknife Geoscience Forum, Abstracts of talks and posters, Northwest Territories Geoscience Office, Vol. 2011, p. 24-25

Clark CD, Knight JK, Gray JT. 2000. Geomorphological reconstruction of the Labrador Sector of the Laurentide Ice Sheet. Quaternary Science Reviews 19: pp 1343–1366.

Clark, C. , Hughes, A., Greenwood, S., Spagnolo, M., Ng, F., 2009. Size and shape characteristics of drumlins, derived from large sample and associated scaling laws. Quaternary Science Reviews. Vol. 28, pp 677-692.

Clark, C., 1997. Reconstructing the Evolutionary Dynamics of Former Ice Sheets Using Multi-Temporal Evidence, Remote Sensing and GIS. Quaternary Science Reviews. Vol. 16, pp 1067-1092.

DeAngelis H., Kleman, J. 2005. Palaeo-ice streams in the northern Keewatin sector of the Laurentide ice sheet. Annals of Glaciology. Vol. 42, pp 135- 144.

DeAngelis, H., 2007. Glacial geomorphology of the east-Central Canadian Arctic; Journal of Maps pp 323-341

Drury, S.A., 2001, Image Interpretation in Geology, 3rd edition Cheltenham, UK: Nelson Thornes; Malden, MA: Blackwell Science, 304 p

Foody , G., Campbell, N, Trodd, N; 1992. Derivation and Applications of Probabilistic Measures of Class membership from the Maximum-liklihood Classification . Photogrammetric Engineering and Remote Sensing. Vol. 58, Issue: 9, pp. 1335-1341.

Foody, G.M., 1996, Approaches for the production and evaluation of fuzzy land cover classification from remotely-sensed data. International Journal of Remote Sensing, Vol. 17, pp. 1317–1340.

Franklin, S.E., Peddle, D.R., Dechka, J.A. and Stenhouse, G.B., 2002, Evidential reasoning with Landsat TM, DEM and GIS data for land cover classification in support of grizzly bear habitat mapping. International Journal of Remote Sensing, Vol. 23, pp 4633–4652.

Gallego, F.J., 2004, Remote sensing and land cover area estimation. International Journal of Remote Sensing, Vol. 25, pp. 3019–3047.

Gong, P. and Howarth, P.J., 1992, Frequency-based contextual classification and gray-level vector reduction for land-use identification. Photogrammetric Engineering and Remote Sensing, Vol. 58, pp. 423–437.

Gonzalez, R., and Woods, R. 1992. Digital Image Processing. Addison-Wesley Pub (Sd); 3 Revised ed of US ed edition (March 1992)

Grunsky, E., Harris, J.R., and McMartin, I. 2006. Predictive mapping of surficial materials, Shultz Lake area (NTS 66A), Nunavut, Canada; Geological Survey of Canada, Open File 5153, 49 p.

Grunsky, E., Harris, J.R., and McMartin, I. 2009. Predictive Mapping of Surficial Materials, Schultz Lake Area (NTS 66A), Nunavut, Canada; Society of Economic Geologists, Vol. 16, pp 177-198

Guo, Q., Kelly, M., Gong, P. and Liu, D. 2007. An object-based classification approach in mapping tree mortality using high spatial resolution imagery. *GIScience & Remote Sensing*, 44: 24–47.

Harris, J R; Rogge, D; Hitchcock, R; Ijewliw, O; Wright, D., 2005. Canadian Journal of Earth Sciences Vol. 42, No. 12, pp 2173-2193,

Harris, J; Schetselaar, E M; Lynds, T; de Kemp, E A, Remote predictive mapping: an aid for northern mapping, Geological Survey of Canada, Open File 5643, 2008

Harris, J.R. (ed), 2008. Remote predictive mapping: an aid for northern mapping, Geological Survey of Canada Open File 5643; 306 pages 1 DVD

Harris, J.R. He, J., Grunsky, E., Gorodetzky, D., and Brown, N., 2012, A Robust, Cross-validation classification method for improved mapping accuracy and confidence metrics, Canadian Journal of Remote Sensing, Vol. 38, No. 2, pp 1-22

Harris, J.R., Grunsky, E., and McMartin, I., 2008, Classification of remotely sensed imagery for surficial geological mapping in Canada's north, Case Study *7 in* Remote Predictive Mapping: An Aid for Northern Mapping, (ed.) J. R. Harris; Geological Survey of Canada, Open File 5643, pp 233-244.

Harris, J.R., Martel, E., Currie, M., Pierce, K., Pilkington, M., and Keating, P., 2008, Snowbird Lake, Northwest Terrirotires, Case Study 1 *in* Remote Predictive Mapping: An Aid for Northern Mapping, (ed.) J.R. Harris; Geological Survey of Canada, Open File 5643, pp 161-171

Harris, J.R., Martel, E., Currie, M., Pierce, K., Pilkington, M., and Keating, P., 2008, Snowbird Lake, Northwest Terrirotires, Case Study 1 *in* Remote Predictive Mapping: An Aid for Northern Mapping, (ed.) J.R. Harris; Geological Survey of Canada, Open File 5643, pp 161-171

Hickin A., Levson, V., 2008. Are streamlined landofms in the northern Cordillera evidence of ice streams? *In* Quebec 2008: 400 years of discoveries. Joint meeting of the Geological Association of Canada, Mineralogical Association of Canada, Society of Economic Geologists and the Society for Geology Applied to Mineral Deposits. May 26-28. Quebec City Convention Centre, Quebec.

Interpretation, 4th ed. Wiley & Sons. Liverman D., Batterson, M., Bell, T., Nolan, L., Marich, A., Putt, M., 2006. Digital elevation models from the Shuttle Radar Topography Mission – New insights into the Quaternary history of Newfoundland. *In* Current Research. Newfoundland Department of Mines and Energy, Geological Survey Branch, Report 06-1, pp 177-189.

Jakosky, B. M. 1986. Global Duricrust on Mars: Analysis of Remote Sensing Data; Journal of Geophysical Research, Vol. 91, No. B3, pp 3547-3559.

Kerr, D E; Eagles, S., 2012 40th Annual Yellowknife Geoscience Forum, abstracts of talks and posters; by Watson, D M (ed.); Northwest Territories Geoscience Office, Yellowknife Geoscience Forum Abstracts Vol. 2012; pp 21-22

Kontoes, C., Wilkinson, G.G., Burrill, A., Goffredo, S. and Megier, J., 1993, An experimental system for the integration of GIS data in knowledge-based image analysis for remote sensing of agriculture. International Journal of Geographical Information Systems, Vol. 7, pp 247–262.

Landgrebe, D.A., 2003, Signal Theory Methods in Multispectral Remote Sensing (Hoboken, NJ: John Wiley and Sons).

LaRocque, A., Leblon, B., Harris, J., Jefferson, C., Tschirhart, V., Shelat, Y., 2012. Canadian Journal of Remote Sensing. Vol. 38. No. 3, pp 281-305.

Lesemann, J E; Sharpe, D R; Giroux, D. 2013. A remote predictive surficial materials map, eastern Victoria Island, Northwest Territories and Nunavut. Geological Survey of Canada, Open File 7230, 2013; 1 sheet, doi:10.4095/292622

Lillesand T. M. & Kiefer R. W., 2000. Remote Sensing and Image Interpretation, 4th ed. Wiley and Sons.

Lowell, T.V. and Fisher, T.G. 2005: What if we had looked from space first? Using SRTM DEM data to generate alternative hypothesis for deglaciation of the Laurentide Ice Sheet. In Water, Ice, Land, and Life: The Quaternary Interface. Canadian Quaternary Association 2005 Conference, June 5-8, 2005, University of Manitoba, Winnipeg, Manitoba. Abstract Volume, page A52.

Lu, D. and Weng, Q. 2007. A survey of image classification methods and techniques for improving classification performance; International Journal of Remote Sensing, Vol. 28, No. 5, pp 823-870

Lytwyn, J 2010. Remote sensing and GIS investigation of glacial features in the region of Devil's Lake State Park, South-Central Wisconsin, USA; Volume 123, Issues 1–2, 1 November 2010, Pages 46–60

Martel, E., Harris, J R; Currie, M; Pearce, K. 2005. Snowbird Lake (NTS 65D) Remote Predictive Mapping and Geoscience Data Compilation; Northwest Territories. Geological Survey of Canada, Open File NWT 2005-08

McMartin and Campbell, in press. Surficial geology, Curtis Lake (North), Nunavut; Geological Survey of Canada, Canadian Geoscience Map, scale 1:100 000.

McMartin, I., Campbell, J.E., Dredge, L.A. and McCurdy, M.W. 2013. Till composition and ice-flow indicators West of Repulse Bay: 2010 and 2011 results from the GEM Wager Bay Surficial Geology Activity; Geological Survey of Canada, Open File 7288.

McMartin, I., Campbell, J.E., Dredge, L.A., Corrigan, D. and Huntley, D. 2012. Glacial history and dispersal patterns north of Wager Bay, Nunavut; *in* Watson, D.M. (compiler), 40th annual Yellowknife Geoscience Forum Abstracts of talks and posters, Northwest Territories Geoscience Office, Vol. 2012, pp 29.

McMartin, I. and Henderson, P. 2004: Evidence from Keewatin (Central Nunavut) for paleo-ice divide migration; Geographie Physique et Quaternaire, v. 58, p. 163–186.

Mellon, M., Jackosky, B., Kieffer, H., 2000. High-Resolution Thermal Inertia Mapping from Mars Global Surveyor Thermal Emission Spectrometer. Icarus. Vol. 148, pp 437-455.

Mie., S., Fenton, M., Paulen, R., 2005. Integrations of remote-sensing and geological data as aids to mapping surficial sediments in north-western Alberta. Alberta Energy and Utilities Board, Alberta Geological Survey, Earth Sciences Report ESR 2005-03.

Pal, M. and Mather, P.M., 2003, An assessment of the effectiveness of decision tree methods for land cover classification. Remote Sensing of Environment, Vol. 86, pp 554–565.

Paola, D., Schowengerdt, R., 1995. A review and analysis of backpropagation neural networks for classification of remotely-sensed multi-spectral imagery, International Journal of Remote Sensing, Vol. 16, No. 16, pp 3033-3058

Paola, J. D., 1994, Neural Network Classification of Multispectral Imagery, M.Sc. Thesis, University of Arizona.

Paul, D., Hanmer, S., Tella, S., Peterson, T.D., and LeCheminant, A.N. 2002. Compilation , bedrock geology of part of the western Churchill Province, Nunavut – Northwest Territories; Geological Survey of Canada, Open File 4236, scale 1:100000

Paulen, R. C. and I. McMartin, eds. 2009. Application of till and stream sediment heavy mineral and geochemical methods to mineral exploration in western and northern Canada. GAC Short Course Notes 18 ed. St. John's Nfld.: Geological Association of Canada.

Prest, V.K., Grant, D.R. and Rampton, V.N., 1968. Glacial Map of Canada, Geological Survey of Canada, Map 1253A, Scale 1:5 000 000.Sabins F., 2007, Remote Sensing: Principals and Interpretation, Waveland Pr Inc. new York, 512 p.

Prest, V.K., Grant, D.R. and Rampton, V.N., 1968. Glacial Map of Canada, Geological Survey of Canada, Map 1253A, Scale 1:5 000 000.

Rencz, A., Harris, J.R., Sangster, D., and Budkewitsch, P. 2000: Spectral characteristics of bedrock map units using LANDSAT TM and topographic data: Application to bedrock mapping in Borden Peninsula, Nunavut, *in* Current Research 2000-C4; Geological Survey of Canada.

Ross, M., Campbell, J., Parent, M., Adams, R., 2009. Palaeo-ice streams and the subglacial landscape mosaic of the North American mid-continental prairies. Boreas, Vol. 38, pp 421–439.

Sabins F., 2007, Remote Sensing: Principals and Interpretation, Waveland Pr Inc. new York, 512 p.

San Miguel-Ayanz, J. and Biging, G.S.,1997, Comparison of single-stage and multi-stage classification approaches for cover type mapping with TM and SPOT data. Remote Sensing of Environment, Vol. 59, pp 92–104.

Schau, M., Dredge, L., Rencz, A.N., Chung, C.-J.F., 1993. Geoscience and Remote Sensing Symposium, 1993. IGARSS '93. Better Understanding of Earth Environment., International

Schetselaar, E., Harris, J., Lynds, T., De Kemp, E. 2007. Remote Predictive Mapping 1. Remote Predictive Mapping (RPM): A Strategy for Geological Mapping of Canada's North. Geoscience Canada; North America, Vol. 34, No. 3 and 4, pp 93-111

Schetselaar, E., Ryan, J., 2009. Remote Predictive Mapping of the Boothia mainland area, Nunavut, Canada: an iterative approach using Landsat ETM, aeromagnetic, and geological Field Data. Canadian Journal of Remote Sensing, Vol.35. Suppl. 1., pp S72-S94

Shelat, Y., Leblon, B., Larocque, A., Harris, J., Jefferson, C., Lentz, D., Tschirhart, V., 2012. Effects of incidence angles and image combinations on mapping accuracy of surficial materials in the Umiujalik Lake area, Nunavut, using RADARSAT-2 polarmetric and Landsat-7 images, and DEM data. Part 1. Nonpolarimetric analysis. Canadian Journal of Remote Sensing, Vol 38, No. 3, pp 383-403.

Smith, M.J., Pain C.F., 2009. Applications of Remote Sensing in Geomorphology. Progress in Physical Geography. Vol. 33. No 4, pp 568-582

Smits P.C., Dellepiane S., G., Schowengerdt, R.A., 1999. Quality assessment of image classification algorithms for land-cover mapping: a review and a proposal for cost-based approach. International Joural of Remote Sensig. Vol 20., No 8, pp 1461-1486.

Spagnolo, M., Clark, C., Hughes, A., Dunlop, P., Stokes, C., 2010. The Planar Shape of Drumlins. Sedimentary Geology Vol. 232, pp 119-129.

Stevens, C W; Kerr, D E; Wolfe, S A; Eagles, S. 2013. Predictive surficial materials and surficial geology derived from LANDSAT 7, Hearne Lake, NTS 85I, Northwest Territories. Geological Survey of Canada, Open File 7233, 2013; 22 pages, doi:10.4095/292394

Stokes, C., Clark, C., Winsborrow, M., 2006. Subglacial bedform evidence for a major palaeo-ice stream and its retreat phases in Amundsen Gulf, Canadian Arctic Archipelago. Journal of Quaternary Science. Vol. 21, No. 4, pp 399-412.

Strahler, A., 1980. The use of prior probabilities in Maximum Liklihood Classification of Remotely Sensed Data. Remote Sensing of Environment. Vol. 10, pp 135-163.

Stuckens, J., Coppin, P.R., and Bauer, M.E., 2000. Integrating contextual information with per-pixel classification for improved land cover classification. Remote Sensing of Environment, Vol. 71, pp 282–296.

Sugden, D. E. 1978. Glacial erosion by the Laurentide Ice Sheet; Journal of Glaciology Vol 20, pp 367-391.

Tippett, C., 1985. Glacial dispersal train of Paleozoic erratics, central Baffin Island, N.W.T., Canada. Canadian Journal of Earth Science. Vol. 22, pp 1818-1826

Tso, B. and Mather, P.M., 2009. *Classification Methods for Remote Sensing Data. 2nd Edition;* (Cornwall, Great Britain: TJ International Ltd).

Vincent, R. K., 1997, Fundamentals of geological and environmental remote sensing, Prentice Hall series in geographic information science, 366 p.

Walsh, , S. J., D.R., Malanson, G.P. 1998. An overview of scale, pattern, process relationships in geomorphology: a remote sensing and GIS perspective Geomorphology; Vol. 21 (3-4), pp 183-205

Wityk, U; Ross, M; McMartin, I; Campbell, J; Grunsky, E; Harris, J; 2011. Developing and testing surficial materials classification using remote predictive mapping methods: preliminary results near Repulse Bay, Nunavut Geological Association of Canada-Mineralogical Association of Canada, Joint Annual Meeting, Programs with Abstracts Vol. 36, 2011; pp 235 (ESS Cont.# 20100420)

Wityk, U; Ross, M; McMartin, I; Campbell, J; Grunsky, E; Harris, J. 2012. Developing and testing surficial sediments classification methods using remote predictive mapping,

Repulse Bay area, Nunavut. 33rd Canadian Symposium on Remote Sensing, abstracts volume; 2012; 1 page

Wityk, U., Harris, J.R., McMartin, I., Campbell, J.E., Ross, M., and Grunsky, E., 2013. Remote Predictive Mapping of Surficial Materials West of Repulse Bay, Nunavut (NTS 46M-SW, 46L-W and -S, 46K-SW); Geological Survey of Canada, Open File 7357. doi:10.4095/2925

Appendix A: Description of 21 classes

	Code	Description	Visual Spectral Characteristics (LANDSAT Bands 7, 4, 2)	Vegetation	Moisture
EXPOSED ALLUVIAL SEDIMENTS	Ap	Alluvial sands and minor silts; exposed	White Grey, greyish-blue	None	Water saturated
MARINE GULLIED SEDIMENTS	Mg	Marine silts and clays; exposed sediments; gullied	White with some purple/lilac	None	Dry
MARINE SILTY SANDS	MS1	Marine fine sands, silts and clays; some surface runoff features	Bright green/yellowish-green	Grass-covered	Unsaturated
	MS2	Marine sands and silts; nearshore deposits; coarser than MS1	Mottled/brownish-green	Grass- and lichen-covered	Unsaturated
ORGANICS	O	Thin organic deposits	Emerald Green – spectrally variable – mottled greens and browns	Grasses, moss, peat and sedges	Heavily saturated; may include small ponds
SAND AND GRAVEL	SG1	Glaciofluvial and marine sands and gravels; occur as beaches,littoral deposits, deltas, eskers, outwash terraces	Red/Brown	Grasses and dried lichen	Dry
	SG2	Marine fine-grained sands, silty-sands; occur on coastal plains in NTS 46L and M	Green - brighter	Grasses	Moist/moderately dry
	SG3	Glaciofluvial and marine sands and gravels; exposed; occur as beaches, deltas, eskers, outwash terraces	Light - White/Yellow/ Rose	None	Dry
BEDROCK	R1	Exposed bedrock	Bright Red (pink)	None	Dry

	R2	Bedrock with some discontinuous till cover	Greenish –pink	Some lichen cover	Dry
BOULDER FIELDS	B	Broken Bedrock; continuous boulder cover	Bright red (linear patterns)	Can be some lichen-covered	Dry
TILL BLANKET	Tb1	Thick drift cover with little boulder cover or exposed bedrock	Brownish-Green	Grassy with moss	Moist
	Tb2	Thick drift cover; more boulders and less vegetated than Tb1	Reddish-Green	Grass and moss	Moist
MODIFIED TILL	Tm1	Modified till; eroded in places; may include sand and gravel; bouldery	Greenish-Red	Moss and grass	Moist
	Tm2	Modified till; less bouldery than Tm1	Reddish-Green	Moss and grass	Moist
TILL VENEER	Tv1	Thin drift cover, mixed with bedrock and boulders or bedrock and sand; contains more boulder/bedrock terrain than Tv2	Reddish Green - Greenish Red	Sparse grasses; moss	Moist
	Tv2	Thin drift cover; contains more moisture and vegetation than Tv1	Brownish-Green	Grasses; moss	Moist
CARBONATE TILL	Ct	Till with carbonate clasts and calcareous matrix	Bright Green (Yellowy, Neon Green), smooth and little variability between pixels	Sparse short grasses, some moss; unvegetated "stripes"	Moist
RIBBED TILL	Tr	Till mixed with sand, gravel and boulders; eroded, disorganized gravelly ridges, terraces and hummocks	Mottled pattern on imagery	Mossy, little grass, lichen	Moist
SHALLOW WATER	Sw	Heavily sediment laden water (where bottom sediments can be seen)	Aqua - greenish blue	None	Shallow water (running or standing)

ICE/SNOW	Ice/Snow	Frozen water	Bright Blue	None	Frozen

Appendix B: Confusion Matrices for 4 Classifications: GK1, GK2, Stat1, Stat2

These tables were created using the class combination and associated ROIs with the classification. These, and output classification (using the corresponding classes) were inputted into the post-classification algorithm to produce a confusion matrix. This matrix measures how accurately the ROIs were in predicting surficial units on the LANDSAT, producing an overall percentage accuracy as well as accuracy per individual class.

These tables were created using the class combination and associated ROIs with the classification. These, and output classification (using the corresponding classes) were inputted into the post-classification algorithm to produce a confusion matrix. This matrix measures how accurately the ROIs were in predicting surficial units on the LANDSAT, producing an overall percentage accuracy as well as accuracy per individual class.

GK1	60.54%	Geological-Knowledge class combination #1, on LANDSAT imagery. Confusion Matrix.														
Class	Ap	Sw	Ms_1	Ms_2 SG2	O	SG_1	SG_3	B	Ct	Mg	Ice/ Snow	R1 and2	Tb_1 and2	Tm_1 and2	Tv_1 and2	Total
Ap	**77.06**	5.17	0	0	0	0.22	27.69	0	0	7.93	55.79	0.06	0	0	0	3.3
Sw	0	**94.4**	0	0	0	0	0.15	0	0	0	1.05	0	0	0	0	0.62
Ms_1	0.2	0	**91.88**	12.37	0	2.01	0	0	0	1.75	0	0	0.24	0	0	5.97
Ms_2_ SG2	0.2	0	6.18	**59.18**	2.43	19.89	1.51	0	4.99	0.1	0	0	7.31	0.02	0.37	8.41
O	0	0	0	1.19	**78.54**	2.62	0.15	0	0.03	0	0	0.06	1.43	1.37	0.41	1.48
SG_1	0	0	0.16	7.09	1.21	**25.52**	1.66	0	1.03	0	0	1.47	5.2	0.93	7.13	4.32
SG_3	9.04	0.43	0.05	0.71	1.21	0.84	**61.88**	0	0	1.99	13.68	0.32	0.09	0.07	0	1.71
B	0	0	0	0	0	0.61	0	**89.19**	0	0	0	10.91	5.45	17.52	6.27	7.42
Ct	0	0	1.45	10.07	0	5.57	0.61	0	**90.59**	0	0	0.26	14.4	0.17	2.17	13.61
Mg	10.86	0	0	0	0	0	3.78	0	0	**88.23**	21.05	0	0	0	0	5.53
Ice/Snow	0	0	0	0	0	0	0	0	0	0	**7.37**	0	0	0	0	0.02
R1and2	2.64	0	0	0	0	5.4	1.66	3.65	0	0	1.05	**48.6**	0.77	4.01	10.46	4.22
Tb_1 and2	0	0	0.27	9.27	13.36	16.32	0.45	0.27	2.86	0	0	1.28	**48.01**	8.9	2.05	19.1
Tm_1 and2	0	0	0	0.08	2.02	5.52	0	6.22	0	0	0	22.7	15	**61.66**	22.02	17.85
Tv_1 and2	0	0	0	0.04	1.21	15.49	0.45	0.68	0.5	0	0	14.35	2.11	5.36	**49.12**	6.42
Total	100	100	100	100	100	100	100	100	100	100	100	100	100	100	100	100

GK2	**60.42%**	Geological-Knowledge class combination #2, on LANDSAT imagery. Confusion Matrix.												
Class	Ap	Sw	Mg	Ms_1	Ms_2_SG	Ice/Snow	O	SG_1	R	T	SG_3	B	Ct	Total
Unclassified	0	0	0	0	0	0	0	0	0	0	0	0	0	0
Ap	**77.06**	5.17	7.93	0	0	55.79	0	0.22	0.06	0	27.69	0	0	3.3
Sw	0	**94.4**	0	0	0	1.05	0	0	0	0	0.15	0	0	0.62
Mg	10.86	0	**88.23**	0	0	21.05	0	0	0	0	3.78	0	0	5.53
Ms_1	0.2	0	1.75	**91.88**	12.37	0	0	0	2.01	0	0.14	0	0	5.97
Ms_2_SG2	0.2	0	0.1	6.34	**61.63**	0	2.43	20.78	0	0	5.43	1.51	0	9.27
Ice/Snow	0	0	0	0	0	**7.37**	0	0	0	0	0	0	0	0.02
O	0	0	0	0	1.23	0	**81.78**	2.67	0.13	1.85	0.15	0	0.03	1.83
SG_1	0	0	0	0.11	7.69	0	1.21	**31.09**	3.89	7.23	1.82	0	1.43	6.48
R1	2.64	0	0	0	0	1.05	0	12.37	**64.09**	11.53	1.97	5.68	0	10.1
T	0	0	0	0.16	6.22	0	13.36	23.01	15.69	**49.65**	0.45	2.16	2.16	30.26
SG_3	9.04	0.43	1.99	0.05	0.71	13.68	1.21	0.84	0.32	0.08	**61.88**	0	0	1.72
B	0	0	0	0	0	0	0	1.28	15.56	14.83	0	**92.16**	0	10.92
Ct	0	0	0	1.45	10.15	0	0	5.74	0.26	9.27	0.61	0	**91.15**	13.98
Total	100	100	100	100	100	100	100	100	100	100	100	100	100	100

STAT1	**62.17**	Statistically erived class combination #1, on LANDSAT imagery. Confusion Matrix														
Class	Ap	Mg	Ms_1	Ms_2	O	R1	Tb_1	Tb_2	Tm_2	SG_3	B	Ct	R2_Tm1	Tv_1and2	Total
Unclassifi	`	0	0	0	0	0	0	0	0	0	0	0	0	0	0
Ap	**76.14**	7.93	0	0	0	0	0	0	0	27.69	0	0	0.02	0	3.38
Mg	10.86	**88.23**	0	0	0	0	0.03	0	0	3.78	0	0	0	0	6
Ms_1	0.3	1.85	**91.94**	15.27	0	0	0.52	0	0	0	0	0	0	0	6.24
Ms_2	0.2	0	6.08	**62.99**	2.43	0	9.73	0.11	0	1.66	0	4.79	0	0.45	6.02
O	0	0	0.05	1.77	**76.92**	0	0.93	0.17	2.04	0	0	0.1	0	0.33	1.08
R1	3.55	0	0	0	0	**70.75**	0	0.6	0.65	0.91	2.43	0	6.24	3.57	2.58
Tb_1	0	0	0.75	8.43	6.88	0	**56.35**	4.82	4.81	0.45	0	8.31	0.07	2.09	14.46
Tb_2	0	0	0	0.19	6.88	0.38	6.86	**48.8**	20.07	0.3	1.08	0	6.29	5.66	11.35
Tm_2	0	0	0	0.06	4.05	1.32	5.73	14.14	**53.51**	0.61	0.54	0	11.73	13.74	9.98
SG_3	8.93	1.99	0.05	0.63	1.21	0.38	0.13	0.02	0.12	**63.39**	0	0	0.39	0.12	1.84
B	0	0	0	0	0	12.45	0	10.54	2.16	0	**86.22**	0	20.9	4.8	7.02
Ct	0	0	1.13	10.01	0	0	18.64	0.02	0.2	0.45	0	**86.07**	0.09	2.3	12.68
R2_Tm1	0	0	0	0	0	10.94	0	18.23	11.79	0	9.19	0	**45.62**	15.7	11.22
Tv_1and2	0	0	0	0.63	1.62	3.77	1.07	2.55	4.65	0.76	0.54	0.73	8.64	**51.25**	6.16
Total	100	100	100	100	100	100	100	100	100	100	100	100	100	100	100

STAT2	**60.64**	Statistically erived class combination #2, on LANDSAT imagery. Confusion Matrix.														
Class	Ap	Mg	Ms_1	O	R1	R2	Tb_1	Tb_2	Tm_1	Tm_2	SG_3	B	Ct	SG1_ SG2_ MS2	Tv_1 and2	Total
Unclassifi	0	0	0	0	0	0	0	0	0	0	0	0	0	0	0	0
Ap	**76.14**	7.93	0	0	0	0	0	0	0	0	27.69	0	0	0.09	0	3.12
Mg	10.86	**88.23**	0	0	0	0	0	0	0	0	3.78	0	0	0	0	5.53
Ms_1	0.1	1.75	**92.2**	0	0	0	0.87	0	0	0	0.15	0	0	11.02	0	6.49
O	0	0	0	**77.33**	0	0	0.9	0.17	0	1.84	0	0	0	1.67	0.25	1.09
R1	3.55	0	0	0	**66.23**	10.02	0	0.54	2.43	0.45	0.61	2.57	0	0.6	1.97	2
R2	0	0	0	0	10	**31.98**	0	2.51	4.32	1.39	0.76	1.89	0	2.93	14.39	3.34
Tb_1	0	0	1.18	6.88	0	0.29	**56.99**	4.82	0	4.57	0.3	0	9.08	13.51	1.39	14.76
Tb_2	0	0	0	6.88	0.38	2.6	7.11	**48.03**	3.15	19.09	0.15	0.95	0	6.21	4.55	10.61
Tm_1	0	0	0	0	9.43	25.63	0	21.96	**64.77**	15.62	0	12.16	0	1.09	13.33	12.34
Tm_2	0	0	0	4.05	0.75	9.15	5.73	12.87	7.77	**50.69**	0.61	0.41	0	2.09	11.6	8.48
SG_3	9.04	1.99	0.05	1.21	0.38	0.48	0.12	0.02	0.03	0.12	**62.03**	0	0	0.81	0	1.7
B	0	0	0	0	10.94	4.24	0	6.23	14.78	1.02	0	**81.62**	0	0.05	3.81	4.57
Ct	0	0	1.24	0	0	0.39	19.25	0	0	0.2	0.45	0	**87**	8.3	2.13	12.46
SG1_ SG2_ MS2	0.3	0.1	5.32	2.02	0.19	0.67	8.25	0.32	0	0.69	2.72	0	3.26	**45.21**	3.49	8.13
Tv_1 and2	0	0	0	1.62	1.7	14.55	0.78	2.53	2.76	4.32	0.76	0.41	0.67	6.42	**43.09**	5.36
Total	100	100	100	100	100	100	100	100	100	100	100	100	100	100	100	100

Appendix C : Confusion Matrices for 4 Classifications : LS1, LS2, S1, S2

These tables were created using the class combination and associated ROIs with the classification. These, and output classification (using the corresponding classes) were inputted into the post-classification algorithm to produce a confusion matrix. This matrix measures how accurately the ROIs were in predicting surficial units on the LANDSAT, producing an overall percentage accuracy as well as accuracy per individual class.

LANDSAT 1	**60.54%**	LANDSAT imagery + Class combination (geological knowledge) #1														
Class	Ap	Sw	Ms_1	Ms_2_SG2	O	SG_1	SG_3	B	Ct	Mg	Ice/ Snow	R1and2	Tb_1and2	Tm_1 and2	Tv_1 and2	Total
Unclassified	0	0	0	0	0	0	0	0	0	0	0	0	0	0	0	0
Ap	**77.06**	5.17	0	0	0	0.22	27.69	0	0	7.93	55.79	0.06	0	0	0	3.3
Sw	0	**94.4**	0	0	0	0	0.15	0	0	0	1.05	0	0	0	0	0.62
Ms_1	0.2	0	**91.88**	12.37	0	2.01	0	0	0	1.75	0	0	0.24	0	0	5.97
Ms_2_ SG2	0.2	0	6.18	**59.18**	2.43	19.89	1.51	0	4.99	0.1	0	0	7.31	0.02	0.37	8.41
O	0	0	0	1.19	**78.54**	2.62	0.15	0	0.03	0	0	0.06	1.43	1.37	0.41	1.48
SG_1	0	0	0.16	7.09	1.21	**25.52**	1.66	0	1.03	0	0	1.47	5.2	0.93	7.13	4.32
SG_3	9.04	0.43	0.05	0.71	1.21	0.84	**61.88**	0	0	1.99	13.68	0.32	0.09	0.07	0	1.71
B	0	0	0	0	0	0.61	0	**89.19**	0	0	0	10.91	5.45	17.52	6.27	7.42
Ct	0	0	1.45	10.07	0	5.57	0.61	0	**90.59**	0	0	0.26	14.4	0.17	2.17	13.61
Mg	10.86	0	0	0	0	0	3.78	0	0	**88.23**	21.05	0	0	0	0	5.53
Ice/Snow	0	0	0	0	0	0	0	0	0	0	**7.37**	0	0	0	0	0.02
R1and2	2.64	0	0	0	0	5.4	1.66	3.65	0	0	1.05	**48.6**	0.77	4.01	10.46	4.22
Tb_1and2	0	0	0.27	9.27	13.36	16.32	0.45	0.27	2.86	0	0	1.28	**48.01**	8.9	2.05	19.1
Tm_1and2	0	0	0	0.08	2.02	5.52	0	6.22	0	0	0	22.7	15	**61.66**	22.02	17.85
Tv_1and2	0	0	0	0.04	1.21	15.49	0.45	0.68	0.5	0	0	14.35	2.11	5.36	**49.12**	6.42
Total	100	100	100	100	100	100	100	100	100	100	100	100	100	100	100	100

LANDSAT2	**60.42%**	LANDSAT imagery + Class combination (geological knowledge) #2													
Class	Ap	Sw	Mg	Ms_1	Ms_2_SG2	Ice/Snow	O	SG_1	R	T	SG_3	B	Ct	Total
Unclassified	0	0	0	0	0	0	0	0	0	0	0	0	0	0
Ap	**77.06**	5.17	7.93	0	0	55.79	0	0.22	0.06	0	27.69	0	0	3.3
Sw	0	**94.4**	0	0	0	1.05	0	0	0	0	0.15	0	0	0.62
Mg	10.86	0	**88.23**	0	0	21.05	0	0	0	0	3.78	0	0	5.53
Ms_1	0.2	0	1.75	**91.88**	12.37	0	0	2.01	0	0.14	0	0	0	5.97
Ms_2_SG2	0.2	0	0.1	6.34	**61.63**	0	2.43	20.78	0	5.43	1.51	0	5.22	9.27
Ice/Snow	0	0	0	0	0	**7.37**	0	0	0	0	0	0	0	0.02
O	0	0	0	0	1.23	0	**81.78**	2.67	0.13	1.85	0.15	0	0.03	1.83
SG_1	0	0	0	0.11	7.69	0	1.21	**31.09**	3.89	7.23	1.82	0	1.43	6.48
R1	2.64	0	0	0	0	1.05	0	12.37	**64.09**	11.53	1.97	5.68	0	10.1
T	0	0	0	0.16	6.22	0	13.36	23.01	15.69	**49.65**	0.45	2.16	2.16	30.26
SG_3	9.04	0.43	1.99	0.05	0.71	13.68	1.21	0.84	0.32	0.08	**61.88**	0	0	1.72
B	0	0	0	0	0	0	0	1.28	15.56	14.83	0	**92.16**	0	10.92
Ct	0	0	0	1.45	10.15	0	0	5.74	0.26	9.27	0.61	0	**91.15**	13.98
Total	100	100	100	100	100	100	100	100	100	100	100	100	100	100

SPOT 1	**54.29%**	SPOT imagery + Class combination (geological knowledge) #1												
Class	Ap	R	Ms_1	Ms_2_SG2	O	SG_1	SG_3	B	Ct	R1and2	Tb_1and2	Tm_1 and2	Tv_1and2	Total
Unclassifi	0	0	0	0	0	0	0	0	0	0	0	0	0	0
Ap	**77.22**	3.74	0	0.04	0.11	0.15	17.58	0	0	0.06	0	0	0	2.69
Mg	11.78	**89.96**	0	0.2	0.11	1.13	7.52	0	0.03	0.32	0.04	0.2	0.17	5.78
Ms_1	0.09	1.68	**91.49**	14.77	0.22	6.9	0.2	0	0.02	0	0.67	0	0.2	6.53
Ms_2_SG	0.28	0.33	5.2	**44.89**	4.15	14.74	1.68	0	1.46	0.78	13.66	1.04	1.16	9.18
O	0	0	0.1	3.57	**81.5**	1.41	0.2	0	2.75	0.09	9.26	1.18	0.09	4.74
SG_1	0	0.09	0.17	6.91	**0.22**	**26.3**	2.82	0.25	0.41	4.24	1.2	3.36	10.1	3.75
SG_3	10.49	3.27	0.02	0.2	0.22	1.08	**67.45**	0	0.71	1.44	0	0.05	0.09	1.96
B	0	0.09	0	0.02	0	0.78	0.2	**87.07**	0.02	21.11	4.83	23.71	8.95	8.85
Ct	0	0	2.81	20.6	4.26	7.03	0.07	0	**89.27**	1.85	7.84	4.43	2.48	13.11
R1and2	0.14	0.46	0	0.05	0	9.32	1.21	4.5	0.11	**38.91**	0.51	4.54	13.92	4.22
Tb_1and2	0	0	0.02	5.1	8.52	3.22	0.13	0.06	1.76	1.07	**47.3**	7.04	6.01	17.95
Tm_1and2	0	0.22	0.19	1.82	0.56	11.69	0.27	6.56	3.05	18.89	11.33	**42.94**	29.96	14.83
Tv_1and2	0	0.15	0	1.84	0.11	16.25	0.67	1.56	0.45	11.25	3.38	11.51	**26.88**	6.4
Total	100	100	100	100	100	100	100	100	100	100	100	100	100	100

SPOT 2	**53.18%**	SPOT imagery + Class combination (geological knowledge) #2										
Class	Ap	Mg	Ms_1	Ms_2_SG2	O	SG_1	R	T	SG_3	B	Ct	Total
Unclassified	0	0	0	0	0	0	0	0	0	0	0	0
Ap	**77.22**	3.74	0	0.04	0.11	0.15	0.06	0	17.58	0	0	2.69
Mg	11.78	**90.01**	0	0.2	0.11	1.18	0.43	0.14	7.52	0	0.03	5.82
Ms_1	0.09	1.68	**91.49**	14.77	0.22	6.9	0	0.42	0.2	0	0.02	6.53
Ms_2_SG2	0.28	0.33	5.22	**47.18**	4.6	15.26	0.87	11.93	1.68	0	1.73	11.37
O	0	0	0.1	3.93	**83.18**	1.51	0.06	7.74	0.2	0	2.79	5.89
SG_1	0	0.15	0.19	9.07	0.34	**41.26**	8.74	6.96	3.02	1	0.87	7.19
R1	0.14	0.64	0.05	0.2	0	15.62	**52.18**	13.49	1.68	7.56	0.21	10.93
T	0	0.07	0.07	3.39	6.84	8.84	11.8	**38.64**	0.34	1.56	3.77	23.38
SG_3	10.49	3.27	0.02	0.2	0.22	1.08	1.44	0.03	**67.45**	0	0.71	1.96
B	0	0.11	0	0.05	0	0.96	22.67	14.04	0.27	**89.82**	0.02	10.79
Ct	0	0	2.85	20.97	4.37	7.23	1.76	6.62	0.07	0.06	**89.87**	13.44
Total	100	100	100	100	100	100	100	100	100	100	100	100

Appendix D: User Accuracies for LS1, LS2, S1 and S2 classifications

LANDSAT 1

Class	Prod. Acc.	User Acc.
	(Percent)	(Percent)
Ap	77.06	64.6
Sw	94.4	99.1
Ms_1	91.88	80.5
Ms_2_SG2	59.18	49.93
O	78.54	36.74
SG_1	25.52	29.8
SG_3	61.88	67.16
B	89.19	25.01
Ct	90.59	56.27
Mg	88.23	92.27
Ice/Snow	7.37	100
R1and2	48.6	50.8
Tb_1and2	48.01	81.73
Tm_1and2	61.66	56.22
Tv_1and2	49.12	52.5

LANDSAT 2

Class	Prod. Acc.	User Acc.
	(Percent)	(Percent)
Ap	77.06	64.6
Sw	94.4	99.1
Mg	88.23	92.27
Ms_1	91.88	80.5
Ms_2_SG2	61.63	47.16
Ice/Snow	7.37	100
O	81.78	30.98
SG_1	31.09	24.23
R1	64.09	27.99
T	49.65	91.3
SG_3	61.88	67.05
B	92.16	17.56
Ct	91.15	55.15

SPOT 1

Class	Prod. Acc.	User Acc.
	(Percent)	(Percent)
Ap	77.22	79.15
Mg	89.96	89.37
Ms_1	91.49	73.54
Ms_2_SG2	44.89	34.43
O	81.5	19.5
SG_1	26.3	35.32
SG_3	67.45	64.96
B	87.07	20
Ct	89.27	57.6
R1and2	38.91	40.6
Tb_1and2	47.3	86.67
Tm_1and2	42.94	47.57
Tv_1and2	26.88	29.09

SPOT 2

Class	Prod. Acc.	User Acc.
	(Percent)	(Percent)
Ap	77.22	79.15
Mg	90.01	88.91
Ms_1	91.49	73.54
Ms_2_SG2	47.18	29.22
O	83.18	15.99
SG_1	41.26	28.91
R1	52.18	21.02
T	38.64	92.96
SG_3	67.45	64.96
B	89.82	16.93
Ct	89.87	56.55

Appendix E: Correspondence Results: pixel-to-pixel correspondence of 4 classifications (LS1, LS2, S1, S2) to modified surficial materials map

Class	Classification	Intersect	Geology	Match% (Intersect/Geology)
AP	466	227	761	**29.83**
Mg	922	522	1777	**29.38**
Ms1	2363	340	1011	**33.63**
MS2_SG2	3710	1692	4792	**35.31**
O	105	6	32	**18.75**
SG1_SG3*	2742	213	3047	**6.99**
R	1705	404	2111	**19.14**
Tb	1281	498	2559	**19.46**
Tv	3068	266	786	**33.84**
Tb_CT	1821	781	2559	**30.52**

*SG1_SG3 combined bc no "SG3" on surficial sediments map
**Tb_Ct combined bc no "Ct" on surficial sediments map

Appendix F: Transform Divergence Statistic: LANDSAT, 21 classes

Input File: land_in_mos_sub_utm.dat
ROI Name: (Jeffries-Matusita, Transformed Divergence)

Ap [Purple] 994 points:
Sw [Aquamarine] 2668 points: (1.99157907 2.00000000)
Mg [Blue3] 2150 points: (1.39697431 1.81804679)
Ms_1 [Red] 1859 points: (1.99995916 2.00000000)
Ms_2 [Blue3] 1578 points: (1.99865887 1.99999991)
Ice/Snow [Blue] 4804 points: (1.99977493 2.00000000)
O [Green] 545 points: (1.99869615 2.00000000)
SG_1 [Blue] 1799 points: (1.99181495 1.99999644)
SG_2 [Red] 949 points: (1.99944200 2.00000000)
R1 [White] 530 points: (1.98331714 2.00000000)
R2 [Black] 1037 points: (1.98537145 1.99999998)
Tb_1 [Green] 6890 points: (1.99874860 2.00000000)
Tb_2 [Cyan] 4667 points: (1.99657999 2.00000000)
Tm_1 [Green] 3336 points: (1.99548974 2.00000000)
Tm_2 [Red] 2452 points: (1.99725334 2.00000000)
Tv_1 [Aquamarine] 1437 points: (1.99262147 2.00000000)
Tv_2 [Sienna] 1002 points: (1.99526716 2.00000000)
SG_3 [Sea Green] 854 points: (0.77480216 0.91477605)
B [White] 745 points: (1.99533675 2.00000000)
Ct [White] 3007 points: (1.99894550 2.00000000)
Tr [Maroon] 3425 points: (1.99589289 2.00000000)

Sw [Aquamarine] 2668 points:
Ap [Purple] 994 points: (1.99157907 2.00000000)
Mg [Blue3] 2150 points: (1.98976057 2.00000000)
Ms_1 [Red] 1859 points: (2.00000000 2.00000000)
Ms_2 [Blue3] 1578 points: (1.99999999 2.00000000)
Ice/Snow [Blue] 4804 points: (1.99998914 2.00000000)
O [Green] 545 points: (2.00000000 2.00000000)
SG_1 [Blue] 1799 points: (1.99999997 2.00000000)
SG_2 [Red] 949 points: (2.00000000 2.00000000)
R1 [White] 530 points: (2.00000000 2.00000000)
R2 [Black] 1037 points: (2.00000000 2.00000000)
Tb_1 [Green] 6890 points: (1.99999999 2.00000000)
Tb_2 [Cyan] 4667 points: (2.00000000 2.00000000)
Tm_1 [Green] 3336 points: (2.00000000 2.00000000)
Tm_2 [Red] 2452 points: (2.00000000 2.00000000)
Tv_1 [Aquamarine] 1437 points: (2.00000000 2.00000000)
Tv_2 [Sienna] 1002 points: (2.00000000 2.00000000)
SG_3 [Sea Green] 854 points: (1.99561690 2.00000000)
B [White] 745 points: (2.00000000 2.00000000)
Ct [White] 3007 points: (2.00000000 2.00000000)
Tr [Maroon] 3425 points: (2.00000000 2.00000000)

Mg [Blue3] 2150 points:
Ap [Purple] 994 points: (1.39697431 1.81804679)
Sw [Aquamarine] 2668 points: (1.98976057 2.00000000)
Ms_1 [Red] 1859 points: (1.99994244 2.00000000)
Ms_2 [Blue3] 1578 points: (1.99706392 1.99999983)
Ice/Snow [Blue] 4804 points: (1.99973402 2.00000000)
O [Green] 545 points: (1.99883879 2.00000000)
SG_1 [Blue] 1799 points: (1.99792036 1.99999979)
SG_2 [Red] 949 points: (1.99882114 2.00000000)
R1 [White] 530 points: (1.99996256 2.00000000)
R2 [Black] 1037 points: (1.99987195 2.00000000)
Tb_1 [Green] 6890 points: (1.99962241 2.00000000)
Tb_2 [Cyan] 4667 points: (1.99999373 2.00000000)
Tm_1 [Green] 3336 points: (1.99999702 2.00000000)
Tm_2 [Red] 2452 points: (1.99997998 2.00000000)
Tv_1 [Aquamarine] 1437 points: (1.99993004 2.00000000)
Tv_2 [Sienna] 1002 points: (1.99973571 2.00000000)
SG_3 [Sea Green] 854 points: (1.76791681 1.88781183)
B [White] 745 points: (1.99999961 2.00000000)
Ct [White] 3007 points: (1.99991952 2.00000000)
Tr [Maroon] 3425 points: (1.99993485 2.00000000)

Ms_1 [Red] 1859 points:
Ap [Purple] 994 points: (1.99995916 2.00000000)
Sw [Aquamarine] 2668 points: (2.00000000 2.00000000)
Mg [Blue3] 2150 points: (1.99994244 2.00000000)
Ms_2 [Blue3] 1578 points: (1.39357624 1.50697672)
Ice/Snow [Blue] 4804 points: (2.00000000 2.00000000)
O [Green] 545 points: (1.99541352 1.99985519)
SG_1 [Blue] 1799 points: (1.81080257 1.89259973)
SG_2 [Red] 949 points: (1.55429915 1.60293191)
R1 [White] 530 points: (1.99999184 2.00000000)
R2 [Black] 1037 points: (1.99901319 1.99990247)
Tb_1 [Green] 6890 points: (1.88350589 1.93510313)
Tb_2 [Cyan] 4667 points: (1.99665824 1.99998941)
Tm_1 [Green] 3336 points: (1.99991642 2.00000000)
Tm_2 [Red] 2452 points: (1.99641261 1.99998914)
Tv_1 [Aquamarine] 1437 points: (1.99740956 1.99998645)
Tv_2 [Sienna] 1002 points: (1.99296160 1.99797269)
SG_3 [Sea Green] 854 points: (1.98199568 2.00000000)
B [White] 745 points: (1.99999842 2.00000000)
Ct [White] 3007 points: (1.92848884 1.99897306)
Tr [Maroon] 3425 points: (1.99540160 1.99998353)

Ms_2 [Blue3] 1578 points:
Ap [Purple] 994 points: (1.99865887 1.99999991)
Sw [Aquamarine] 2668 points: (1.99999999 2.00000000)
Mg [Blue3] 2150 points: (1.99706392 1.99999983)
Ms_1 [Red] 1859 points: (1.39357624 1.50697672)
Ice/Snow [Blue] 4804 points: (1.99999777 2.00000000)
O [Green] 545 points: (1.88029199 1.97099966)
SG_1 [Blue] 1799 points: (0.95147084 1.26426934)
SG_2 [Red] 949 points: (0.55130744 0.70144454)
R1 [White] 530 points: (1.99800694 1.99999114)
R2 [Black] 1037 points: (1.96332238 1.98637527)
Tb_1 [Green] 6890 points: (1.01508221 1.18519071)
Tb_2 [Cyan] 4667 points: (1.88774694 1.98807635)
Tm_1 [Green] 3336 points: (1.99788403 1.99988502)
Tm_2 [Red] 2452 points: (1.92180090 1.98685951)
Tv_1 [Aquamarine] 1437 points: (1.93891542 1.98565343)
Tv_2 [Sienna] 1002 points: (1.80590131 1.88049362)
SG_3 [Sea Green] 854 points: (1.94389246 1.99999965)
B [White] 745 points: (1.99990056 1.99999108)
Ct [White] 3007 points: (1.27360842 1.67259211)
Tr [Maroon] 3425 points: (1.86200251 1.96924419)

Ice/Snow [Blue] 4804 points:
Ap [Purple] 994 points: (1.99977493 2.00000000)
Sw [Aquamarine] 2668 points: (1.99998914 2.00000000)
Mg [Blue3] 2150 points: (1.99973402 2.00000000)
Ms_1 [Red] 1859 points: (2.00000000 2.00000000)
Ms_2 [Blue3] 1578 points: (1.99999777 2.00000000)
O [Green] 545 points: (1.99999745 2.00000000)
SG_1 [Blue] 1799 points: (1.99999254 2.00000000)
SG_2 [Red] 949 points: (1.99999917 2.00000000)
R1 [White] 530 points: (1.99999936 2.00000000)
R2 [Black] 1037 points: (1.99999878 2.00000000)
Tb_1 [Green] 6890 points: (1.99999993 2.00000000)
Tb_2 [Cyan] 4667 points: (1.99999955 2.00000000)
Tm_1 [Green] 3336 points: (1.99999928 2.00000000)
Tm_2 [Red] 2452 points: (1.99999888 2.00000000)
Tv_1 [Aquamarine] 1437 points: (1.99999809 2.00000000)
Tv_2 [Sienna] 1002 points: (1.99999864 2.00000000)
SG_3 [Sea Green] 854 points: (1.99998234 2.00000000)

B [White] 745 points: (1.99999936 2.00000000)
Ct [White] 3007 points: (2.00000000 2.00000000)
Tr [Maroon] 3425 points: (1.99999912 2.00000000)

O [Green] 545 points:
Ap [Purple] 994 points: (1.99869615 2.00000000)
Sw [Aquamarine] 2668 points: (2.00000000 2.00000000)
Mg [Blue3] 2150 points: (1.99883879 2.00000000)
Ms_1 [Red] 1859 points: (1.99541352 1.99985519)
Ms_2 [Blue3] 1578 points: (1.88029199 1.97099966)
Ice/Snow [Blue] 4804 points: (1.99999745 2.00000000)
SG_1 [Blue] 1799 points: (1.75321911 1.94141062)
SG_2 [Red] 949 points: (1.87913002 1.96340765)
R1 [White] 530 points: (1.99803896 1.99989943)
R2 [Black] 1037 points: (1.96122182 1.99690203)
Tb_1 [Green] 6890 points: (1.71826471 1.99670496)
Tb_2 [Cyan] 4667 points: (1.83519650 1.99999464)
Tm_1 [Green] 3336 points: (1.99034424 1.99997816)
Tm_2 [Red] 2452 points: (1.79770606 1.99528609)
Tv_1 [Aquamarine] 1437 points: (1.96291065 1.99892389)
Tv_2 [Sienna] 1002 points: (1.95029668 1.98997025)
SG_3 [Sea Green] 854 points: (1.96641674 2.00000000)
B [White] 745 points: (1.99975270 1.99999999)
Ct [White] 3007 points: (1.98049556 1.99997660)
Tr [Maroon] 3425 points: (1.78095526 1.95007765)

SG_1 [Blue] 1799 points:
Ap [Purple] 994 points: (1.99181495 1.99999644)
Sw [Aquamarine] 2668 points: (1.99999997 2.00000000)
Mg [Blue3] 2150 points: (1.99792036 1.99999979)
Ms_1 [Red] 1859 points: (1.81080257 1.89259973)
Ms_2 [Blue3] 1578 points: (0.95147084 1.26426934)
Ice/Snow [Blue] 4804 points: (1.99999254 2.00000000)
O [Green] 545 points: (1.75321911 1.94141062)
SG_2 [Red] 949 points: (0.80008964 1.05231912)
R1 [White] 530 points: (1.63804201 1.92066733)
R2 [Black] 1037 points: (1.10782464 1.28333723)
Tb_1 [Green] 6890 points: (0.73493769 0.90636207)
Tb_2 [Cyan] 4667 points: (1.27486648 1.74759777)
Tm_1 [Green] 3336 points: (1.59047599 1.92740191)
Tm_2 [Red] 2452 points: (1.17579251 1.69123675)
Tv_1 [Aquamarine] 1437 points: (0.98119453 1.31600258)
Tv_2 [Sienna] 1002 points: (0.67608360 0.81312881)
SG_3 [Sea Green] 854 points: (1.91296380 1.99999358)
B [White] 745 points: (1.85329251 1.97749505)
Ct [White] 3007 points: (1.33267012 1.78278028)
Tr [Maroon] 3425 points: (0.91973996 1.45503426)

SG_2 [Red] 949 points:
Ap [Purple] 994 points: (1.99944200 2.00000000)
Sw [Aquamarine] 2668 points: (2.00000000 2.00000000)
Mg [Blue3] 2150 points: (1.99882114 2.00000000)
Ms_1 [Red] 1859 points: (1.55429915 1.60293191)
Ms_2 [Blue3] 1578 points: (0.55130744 0.70144454)
Ice/Snow [Blue] 4804 points: (1.99999917 2.00000000)
O [Green] 545 points: (1.87913002 1.96340765)
SG_1 [Blue] 1799 points: (0.80008964 1.05231912)
R1 [White] 530 points: (1.99663825 1.99997161)
R2 [Black] 1037 points: (1.94650922 1.98059931)
Tb_1 [Green] 6890 points: (1.00678582 1.17183893)
Tb_2 [Cyan] 4667 points: (1.91705046 1.99523775)
Tm_1 [Green] 3336 points: (1.99326639 1.99992046)
Tm_2 [Red] 2452 points: (1.89986821 1.99077938)
Tv_1 [Aquamarine] 1437 points: (1.89680702 1.98467615)
Tv_2 [Sienna] 1002 points: (1.73429204 1.79642567)
SG_3 [Sea Green] 854 points: (1.94583892 2.00000000)
B [White] 745 points: (1.99974150 1.99999128)
Ct [White] 3007 points: (1.29106431 1.69131240)
Tr [Maroon] 3425 points: (1.81450733 1.97557935)

R1 [White] 530 points:
Ap [Purple] 994 points: (1.98331714 2.00000000)
Sw [Aquamarine] 2668 points: (2.00000000 2.00000000)
Mg [Blue3] 2150 points: (1.99996256 2.00000000)
Ms_1 [Red] 1859 points: (1.99999184 2.00000000)
Ms_2 [Blue3] 1578 points: (1.99800694 1.99999114)
Ice/Snow [Blue] 4804 points: (1.99999936 2.00000000)
O [Green] 545 points: (1.99803896 1.99989943)
SG_1 [Blue] 1799 points: (1.63804201 1.92066733)
SG_2 [Red] 949 points: (1.99663825 1.99997161)
R2 [Black] 1037 points: (0.93743011 1.11204065)
Tb_1 [Green] 6890 points: (1.98299266 1.99867690)
Tb_2 [Cyan] 4667 points: (1.60197468 1.96761555)
Tm_1 [Green] 3336 points: (1.21001041 1.74288524)
Tm_2 [Red] 2452 points: (1.66399364 1.93501509)
Tv_1 [Aquamarine] 1437 points: (1.24179993 1.50443651)
Tv_2 [Sienna] 1002 points: (1.62503736 1.79258093)
SG_3 [Sea Green] 854 points: (1.98123252 2.00000000)
B [White] 745 points: (1.43726902 1.84056486)
Ct [White] 3007 points: (1.99923004 1.99997654)
Tr [Maroon] 3425 points: (1.58782765 1.77959866)

R2 [Black] 1037 points:
Ap [Purple] 994 points: (1.98537145 1.99999998)
Sw [Aquamarine] 2668 points: (2.00000000 2.00000000)
Mg [Blue3] 2150 points: (1.99987195 2.00000000)
Ms_1 [Red] 1859 points: (1.99901319 1.99990247)
Ms_2 [Blue3] 1578 points: (1.96332238 1.98637527)
Ice/Snow [Blue] 4804 points: (1.99999878 2.00000000)
O [Green] 545 points: (1.96122182 1.99690203)
SG_1 [Blue] 1799 points: (1.10782464 1.28333723)
SG_2 [Red] 949 points: (1.94650922 1.98059931)
R1 [White] 530 points: (0.93743011 1.11204065)
Tb_1 [Green] 6890 points: (1.78332638 1.84544054)
Tb_2 [Cyan] 4667 points: (1.08722984 1.45643144)
Tm_1 [Green] 3336 points: (0.80228592 1.17568598)
Tm_2 [Red] 2452 points: (1.06353171 1.38501004)
Tv_1 [Aquamarine] 1437 points: (0.34310960 0.38192127)
Tv_2 [Sienna] 1002 points: (0.71835299 0.75527867)
SG_3 [Sea Green] 854 points: (1.96036021 1.99999995)
B [White] 745 points: (1.34424480 1.53681187)
Ct [White] 3007 points: (1.93951445 1.98674430)
Tr [Maroon] 3425 points: (1.02527311 1.18384500)

Tb_1 [Green] 6890 points:
Ap [Purple] 994 points: (1.99874860 2.00000000)
Sw [Aquamarine] 2668 points: (1.99999999 2.00000000)
Mg [Blue3] 2150 points: (1.99962241 2.00000000)
Ms_1 [Red] 1859 points: (1.88350589 1.93510313)
Ms_2 [Blue3] 1578 points: (1.01508221 1.18519071)
Ice/Snow [Blue] 4804 points: (1.99999993 2.00000000)
O [Green] 545 points: (1.71826471 1.99670496)
SG_1 [Blue] 1799 points: (0.73493769 0.90636207)
SG_2 [Red] 949 points: (1.00678582 1.17183893)
R1 [White] 530 points: (1.98299266 1.99867690)
R2 [Black] 1037 points: (1.78332638 1.84544054)
Tb_2 [Cyan] 4667 points: (1.49803302 1.71744876)
Tm_1 [Green] 3336 points: (1.92547431 1.97095643)
Tm_2 [Red] 2452 points: (1.32927221 1.59907772)
Tv_1 [Aquamarine] 1437 points: (1.69788934 1.75394316)
Tv_2 [Sienna] 1002 points: (1.34716607 1.40827273)
SG_3 [Sea Green] 854 points: (1.94696181 2.00000000)
B [White] 745 points: (1.99246614 1.99469959)
Ct [White] 3007 points: (0.93069426 1.31014616)
Tr [Maroon] 3425 points: (1.37989949 1.56376622)

Tb_2 [Cyan] 4667 points:
Ap [Purple] 994 points: (1.99657999 2.00000000)
Sw [Aquamarine] 2668 points: (2.00000000 2.00000000)
Mg [Blue3] 2150 points: (1.99999373 2.00000000)

Ms_1 [Red] 1859 points: (1.99665824 1.99998941)
Ms_2 [Blue3] 1578 points: (1.88774694 1.98807635)
Ice/Snow [Blue] 4804 points: (1.99999955 2.00000000)
O [Green] 545 points: (1.83519650 1.99999464)
SG_1 [Blue] 1799 points: (1.27486648 1.74759777)
SG_2 [Red] 949 points: (1.91705046 1.99523775)
R1 [White] 530 points: (1.60197468 1.96761555)
R2 [Black] 1037 points: (1.08722984 1.45643144)
Tb_1 [Green] 6890 points: (1.49803302 1.71744876)
Tm_1 [Green] 3336 points: (0.80486226 1.06955321)
Tm_2 [Red] 2452 points: (0.41268991 0.47674847)
Tv_1 [Aquamarine] 1437 points: (0.78371185 0.96015653)
Tv_2 [Sienna] 1002 points: (1.28951178 1.52554060)
SG_3 [Sea Green] 854 points: (1.98204362 2.00000000)
B [White] 745 points: (1.45844680 1.89652658)
Ct [White] 3007 points: (1.98399014 1.99368329)
Tr [Maroon] 3425 points: (0.59573140 0.68955780)

Tm_1 [Green] 3336 points:
Ap [Purple] 994 points: (1.99548974 2.00000000)
Sw [Aquamarine] 2668 points: (2.00000000 2.00000000)
Mg [Blue3] 2150 points: (1.99999702 2.00000000)
Ms_1 [Red] 1859 points: (1.99991642 2.00000000)
Ms_2 [Blue3] 1578 points: (1.99788403 1.99988502)
Ice/Snow [Blue] 4804 points: (1.99999928 2.00000000)
O [Green] 545 points: (1.99034424 1.99997816)
SG_1 [Blue] 1799 points: (1.59047599 1.92740191)
SG_2 [Red] 949 points: (1.99326639 1.99992046)
R1 [White] 530 points: (1.21001041 1.74288524)
R2 [Black] 1037 points: (0.80228592 1.17568598)
Tb_1 [Green] 6890 points: (1.92547431 1.97095643)
Tb_2 [Cyan] 4667 points: (0.80486226 1.06955321)
Tm_2 [Red] 2452 points: (0.89305578 0.95475340)
Tv_1 [Aquamarine] 1437 points: (0.67845608 0.84408539)
Tv_2 [Sienna] 1002 points: (1.40832081 1.59888748)
SG_3 [Sea Green] 854 points: (1.98964731 2.00000000)
B [White] 745 points: (0.84978735 0.93708650)
Ct [White] 3007 points: (1.99920808 1.99952893)
Tr [Maroon] 3425 points: (1.16648376 1.20605826)

Tm_2 [Red] 2452 points:
Ap [Purple] 994 points: (1.99725334 2.00000000)
Sw [Aquamarine] 2668 points: (2.00000000 2.00000000)
Mg [Blue3] 2150 points: (1.99997998 2.00000000)
Ms_1 [Red] 1859 points: (1.99641261 1.99998914)
Ms_2 [Blue3] 1578 points: (1.92180090 1.98685951)
Ice/Snow [Blue] 4804 points: (1.99999888 2.00000000)
O [Green] 545 points: (1.79770606 1.99528609)
SG_1 [Blue] 1799 points: (1.17579251 1.69123675)
SG_2 [Red] 949 points: (1.89986821 1.99077938)
R1 [White] 530 points: (1.66399364 1.93501509)
R2 [Black] 1037 points: (1.06353171 1.38501004)
Tb_1 [Green] 6890 points: (1.32927221 1.59907772)
Tb_2 [Cyan] 4667 points: (0.41268991 0.47674847)
Tm_1 [Green] 3336 points: (0.89305578 0.95475340)
Tv_1 [Aquamarine] 1437 points: (0.77053682 0.89743624)
Tv_2 [Sienna] 1002 points: (1.08231966 1.28640432)
SG_3 [Sea Green] 854 points: (1.97527472 2.00000000)
B [White] 745 points: (1.64584766 1.78247060)
Ct [White] 3007 points: (1.97216023 1.98267668)
Tr [Maroon] 3425 points: (0.39958184 0.43004242)

Tv_1 [Aquamarine] 1437 points:
Ap [Purple] 994 points: (1.99262147 2.00000000)
Sw [Aquamarine] 2668 points: (2.00000000 2.00000000)
Mg [Blue3] 2150 points: (1.99993004 2.00000000)
Ms_1 [Red] 1859 points: (1.99740956 1.99998645)
Ms_2 [Blue3] 1578 points: (1.93891542 1.98565343)
Ice/Snow [Blue] 4804 points: (1.99999809 2.00000000)
O [Green] 545 points: (1.96291065 1.99892389)
SG_1 [Blue] 1799 points: (0.98119453 1.31600258)
SG_2 [Red] 949 points: (1.89680702 1.98467615)
R1 [White] 530 points: (1.24179993 1.50443651)
R2 [Black] 1037 points: (0.34310960 0.38192127)
Tb_1 [Green] 6890 points: (1.69788934 1.75394316)
Tb_2 [Cyan] 4667 points: (0.78371185 0.96015653)
Tm_1 [Green] 3336 points: (0.67845608 0.84408539)
Tm_2 [Red] 2452 points: (0.77053682 0.89743624)
Tv_2 [Sienna] 1002 points: (0.52567561 0.57823596)
SG_3 [Sea Green] 854 points: (1.97226400 2.00000000)
B [White] 745 points: (1.38706076 1.51623848)
Ct [White] 3007 points: (1.94307807 1.97879904)
Tr [Maroon] 3425 points: (0.66063403 0.69501911)

Tv_2 [Sienna] 1002 points:
Ap [Purple] 994 points: (1.99526716 2.00000000)
Sw [Aquamarine] 2668 points: (2.00000000 2.00000000)
Mg [Blue3] 2150 points: (1.99973571 2.00000000)
Ms_1 [Red] 1859 points: (1.99296160 1.99797269)
Ms_2 [Blue3] 1578 points: (1.80590131 1.88049362)
Ice/Snow [Blue] 4804 points: (1.99999864 2.00000000)
O [Green] 545 points: (1.95029668 1.98997025)
SG_1 [Blue] 1799 points: (0.67608360 0.81312881)
SG_2 [Red] 949 points: (1.73429204 1.79642567)
R1 [White] 530 points: (1.62503736 1.79258093)
R2 [Black] 1037 points: (0.71835299 0.75527867)
Tb_1 [Green] 6890 points: (1.34716607 1.40827273)
Tb_2 [Cyan] 4667 points: (1.28951178 1.52554060)
Tm_1 [Green] 3336 points: (1.40832081 1.59888748)
Tm_2 [Red] 2452 points: (1.08231966 1.28640432)
Tv_1 [Aquamarine] 1437 points: (0.52567561 0.57823596)
SG_3 [Sea Green] 854 points: (1.96057790 2.00000000)
B [White] 745 points: (1.82722463 1.86964376)
Ct [White] 3007 points: (1.65877976 1.78970939)
Tr [Maroon] 3425 points: (0.95327861 1.08979023)

SG_3 [Sea Green] 854 points:
Ap [Purple] 994 points: (0.77480216 0.91477605)
Sw [Aquamarine] 2668 points: (1.99561690 2.00000000)
Mg [Blue3] 2150 points: (1.76791681 1.88781183)
Ms_1 [Red] 1859 points: (1.98199568 2.00000000)
Ms_2 [Blue3] 1578 points: (1.94389246 1.99999965)
Ice/Snow [Blue] 4804 points: (1.99998234 2.00000000)
O [Green] 545 points: (1.96641674 2.00000000)
SG_1 [Blue] 1799 points: (1.91296380 1.99999358)
SG_2 [Red] 949 points: (1.94583892 2.00000000)
R1 [White] 530 points: (1.98123252 2.00000000)
R2 [Black] 1037 points: (1.96036021 1.99999995)
Tb_1 [Green] 6890 points: (1.94696181 2.00000000)
Tb_2 [Cyan] 4667 points: (1.98204362 2.00000000)
Tm_1 [Green] 3336 points: (1.98964731 2.00000000)
Tm_2 [Red] 2452 points: (1.97527472 2.00000000)
Tv_1 [Aquamarine] 1437 points: (1.97226400 2.00000000)
Tv_2 [Sienna] 1002 points: (1.96057790 2.00000000)
B [White] 745 points: (1.99564881 2.00000000)
Ct [White] 3007 points: (1.97045353 2.00000000)
Tr [Maroon] 3425 points: (1.97035690 2.00000000)

B [White] 745 points:
Ap [Purple] 994 points: (1.99533675 2.00000000)
Sw [Aquamarine] 2668 points: (2.00000000 2.00000000)
Mg [Blue3] 2150 points: (1.99999961 2.00000000)
Ms_1 [Red] 1859 points: (1.99999842 2.00000000)
Ms_2 [Blue3] 1578 points: (1.99990056 1.99999108)
Ice/Snow [Blue] 4804 points: (1.99999936 2.00000000)
O [Green] 545 points: (1.99975270 1.99999999)
SG_1 [Blue] 1799 points: (1.85329251 1.97749505)
SG_2 [Red] 949 points: (1.99974150 1.99999128)
R1 [White] 530 points: (1.43726902 1.84056486)
R2 [Black] 1037 points: (1.34424480 1.53681187)

Tb_1 [Green] 6890 points: (1.99246614 1.99469959)
Tb_2 [Cyan] 4667 points: (1.45844680 1.89652658)
Tm_1 [Green] 3336 points: (0.84978735 0.93708650)
Tm_2 [Red] 2452 points: (1.64584766 1.78247060)
Tv_1 [Aquamarine] 1437 points: (1.38706076 1.51623848)
Tv_2 [Sienna] 1002 points: (1.82722463 1.86964376)
SG_3 [Sea Green] 854 points: (1.99564881 2.00000000)
Ct [White] 3007 points: (1.99982753 1.99997642)
Tr [Maroon] 3425 points: (1.78004432 1.88610822)

Ct [White] 3007 points:
Ap [Purple] 994 points: (1.99894550 2.00000000)
Sw [Aquamarine] 2668 points: (2.00000000 2.00000000)
Mg [Blue3] 2150 points: (1.99991952 2.00000000)
Ms_1 [Red] 1859 points: (1.92848884 1.99897306)
Ms_2 [Blue3] 1578 points: (1.27360842 1.67259211)
Ice/Snow [Blue] 4804 points: (2.00000000 2.00000000)
O [Green] 545 points: (1.98049556 1.99997660)
SG_1 [Blue] 1799 points: (1.33267012 1.78278028)
SG_2 [Red] 949 points: (1.29106431 1.69131240)
R1 [White] 530 points: (1.99923004 1.99997654)
R2 [Black] 1037 points: (1.93951445 1.98674430)
Tb_1 [Green] 6890 points: (0.93069426 1.31014616)
Tb_2 [Cyan] 4667 points: (1.98399014 1.99368329)
Tm_1 [Green] 3336 points: (1.99920808 1.99952893)
Tm_2 [Red] 2452 points: (1.97216023 1.98267668)
Tv_1 [Aquamarine] 1437 points: (1.94307807 1.97879904)
Tv_2 [Sienna] 1002 points: (1.65877976 1.78970939)
SG_3 [Sea Green] 854 points: (1.97045353 2.00000000)
B [White] 745 points: (1.99982753 1.99997642)
Tr [Maroon] 3425 points: (1.95623796 1.97248269)

Tr [Maroon] 3425 points:
Ap [Purple] 994 points: (1.99589289 2.00000000)
Sw [Aquamarine] 2668 points: (2.00000000 2.00000000)
Mg [Blue3] 2150 points: (1.99993485 2.00000000)
Ms_1 [Red] 1859 points: (1.99540160 1.99998353)
Ms_2 [Blue3] 1578 points: (1.86200251 1.96924419)
Ice/Snow [Blue] 4804 points: (1.99999912 2.00000000)
O [Green] 545 points: (1.78095526 1.95007765)
SG_1 [Blue] 1799 points: (0.91973996 1.45503426)
SG_2 [Red] 949 points: (1.81450733 1.97557935)
R1 [White] 530 points: (1.58782765 1.77959866)
R2 [Black] 1037 points: (1.02527311 1.18384500)
Tb_1 [Green] 6890 points: (1.37989949 1.56376622)
Tb_2 [Cyan] 4667 points: (0.59573140 0.68955780)
Tm_1 [Green] 3336 points: (1.16648376 1.20605826)
Tm_2 [Red] 2452 points: (0.39958184 0.43004242)
Tv_1 [Aquamarine] 1437 points: (0.66063403 0.69501911)
Tv_2 [Sienna] 1002 points: (0.95327861 1.08979023)
SG_3 [Sea Green] 854 points: (1.97035690 2.00000000)
B [White] 745 points: (1.78004432 1.88610822)
Ct [White] 3007 points: (1.95623796 1.97248269)

Pair Separation (least to most);

R2 [Black] 1037 points and Tv_1 [Aquamarine] 1437 points - 0.34310960
Tm_2 [Red] 2452 points and Tr [Maroon] 3425 points - 0.39958184
Tb_2 [Cyan] 4667 points and Tm_2 [Red] 2452 points - 0.41268991
Tv_1 [Aquamarine] 1437 points and Tv_2 [Sienna] 1002 points - 0.52567561
Ms_2 [Blue3] 1578 points and SG_2 [Red] 949 points - 0.55130744
Tb_2 [Cyan] 4667 points and Tr [Maroon] 3425 points - 0.59573140
Tv_1 [Aquamarine] 1437 points and Tr [Maroon] 3425 points - 0.66063403
SG_1 [Blue] 1799 points and Tv_2 [Sienna] 1002 points - 0.67608360
Tm_1 [Green] 3336 points and Tv_1 [Aquamarine] 1437 points - 0.67845608
R2 [Black] 1037 points and Tv_2 [Sienna] 1002 points - 0.71835299
SG_1 [Blue] 1799 points and Tb_1 [Green] 6890 points - 0.73493769
Tm_2 [Red] 2452 points and Tv_1 [Aquamarine] 1437 points - 0.77053682
Ap [Purple] 994 points and SG_3 [Sea Green] 854 points - 0.77480216
Tb_2 [Cyan] 4667 points and Tv_1 [Aquamarine] 1437 points - 0.78371185
SG_1 [Blue] 1799 points and SG_2 [Red] 949 points - 0.80008964
R2 [Black] 1037 points and Tm_1 [Green] 3336 points - 0.80228592
Tb_2 [Cyan] 4667 points and Tm_1 [Green] 3336 points - 0.80486226
Tm_1 [Green] 3336 points and B [White] 745 points - 0.84978735
Tm_1 [Green] 3336 points and Tm_2 [Red] 2452 points - 0.89305578
SG_1 [Blue] 1799 points and Tr [Maroon] 3425 points - 0.91973996
Tb_1 [Green] 6890 points and Ct [White] 3007 points - 0.93069426
R1 [White] 530 points and R2 [Black] 1037 points - 0.93743011
Ms_2 [Blue3] 1578 points and SG_1 [Blue] 1799 points - 0.95147084
Tv_2 [Sienna] 1002 points and Tr [Maroon] 3425 points - 0.95327861
SG_1 [Blue] 1799 points and Tv_1 [Aquamarine] 1437 points - 0.98119453
SG_2 [Red] 949 points and Tb_1 [Green] 6890 points - 1.00678582
Ms_2 [Blue3] 1578 points and Tb_1 [Green] 6890 points - 1.01508221
R2 [Black] 1037 points and Tr [Maroon] 3425 points - 1.02527311
R2 [Black] 1037 points and Tm_2 [Red] 2452 points - 1.06353171
Tm_2 [Red] 2452 points and Tv_2 [Sienna] 1002 points - 1.08231966
R2 [Black] 1037 points and Tb_2 [Cyan] 4667 points - 1.08722984
SG_1 [Blue] 1799 points and R2 [Black] 1037 points - 1.10782464
Tm_1 [Green] 3336 points and Tr [Maroon] 3425 points - 1.16648376
SG_1 [Blue] 1799 points and Tm_2 [Red] 2452 points - 1.17579251
R1 [White] 530 points and Tm_1 [Green] 3336 points - 1.21001041
R1 [White] 530 points and Tv_1 [Aquamarine] 1437 points - 1.24179993
Ms_2 [Blue3] 1578 points and Ct [White] 3007 points - 1.27360842
SG_1 [Blue] 1799 points and Tb_2 [Cyan] 4667 points - 1.27486648
Tb_2 [Cyan] 4667 points and Tv_2 [Sienna] 1002 points - 1.28951178
SG_2 [Red] 949 points and Ct [White] 3007 points - 1.29106431

Tb_1 [Green] 6890 points and Tm_2 [Red] 2452 points - 1.32927221
SG_1 [Blue] 1799 points and Ct [White] 3007 points - 1.33267012
R2 [Black] 1037 points and B [White] 745 points - 1.34424480
Tb_1 [Green] 6890 points and Tv_2 [Sienna] 1002 points - 1.34716607
Tb_1 [Green] 6890 points and Tr [Maroon] 3425 points - 1.37989949
Tv_1 [Aquamarine] 1437 points and B [White] 745 points - 1.38706076
Ms_1 [Red] 1859 points and Ms_2 [Blue3] 1578 points - 1.39357624
Ap [Purple] 994 points and Mg [Blue3] 2150 points - 1.39697431
Tm_1 [Green] 3336 points and Tv_2 [Sienna] 1002 points - 1.40832081
R1 [White] 530 points and B [White] 745 points - 1.43726902
Tb_2 [Cyan] 4667 points and B [White] 745 points - 1.45844680
Tb_1 [Green] 6890 points and Tb_2 [Cyan] 4667 points - 1.49803302
Ms_1 [Red] 1859 points and SG_2 [Red] 949 points - 1.55429915
R1 [White] 530 points and Tr [Maroon] 3425 points - 1.58782765
SG_1 [Blue] 1799 points and Tm_1 [Green] 3336 points - 1.59047599
R1 [White] 530 points and Tb_2 [Cyan] 4667 points - 1.60197468
R1 [White] 530 points and Tv_2 [Sienna] 1002 points - 1.62503736
SG_1 [Blue] 1799 points and R1 [White] 530 points - 1.63804201
Tm_2 [Red] 2452 points and B [White] 745 points - 1.64584766
Tv_2 [Sienna] 1002 points and Ct [White] 3007 points - 1.65877976
R1 [White] 530 points and Tm_2 [Red] 2452 points - 1.66399364
Tb_1 [Green] 6890 points and Tv_1 [Aquamarine] 1437 points - 1.69788934
O [Green] 545 points and Tb_1 [Green] 6890 points - 1.71826471
SG_2 [Red] 949 points and Tv_2 [Sienna] 1002 points - 1.73429204
O [Green] 545 points and SG_1 [Blue] 1799 points - 1.75321911
Mg [Blue3] 2150 points and SG_3 [Sea Green] 854 points - 1.76791681
B [White] 745 points and Tr [Maroon] 3425 points - 1.78004432
O [Green] 545 points and Tr [Maroon] 3425 points - 1.78095526
R2 [Black] 1037 points and Tb_1 [Green] 6890 points - 1.78332638
O [Green] 545 points and Tm_2 [Red] 2452 points - 1.79770606
Ms_2 [Blue3] 1578 points and Tv_2 [Sienna] 1002 points - 1.80590131
Ms_1 [Red] 1859 points and SG_1 [Blue] 1799 points - 1.81080257
SG_2 [Red] 949 points and Tr [Maroon] 3425 points - 1.81450733
Tv_2 [Sienna] 1002 points and B [White] 745 points - 1.82722463
O [Green] 545 points and Tb_2 [Cyan] 4667 points - 1.83519650
SG_1 [Blue] 1799 points and B [White] 745 points - 1.85329251
Ms_2 [Blue3] 1578 points and Tr [Maroon] 3425 points - 1.86200251
O [Green] 545 points and SG_2 [Red] 949 points - 1.87913002
Ms_2 [Blue3] 1578 points and O [Green] 545 points - 1.88029199
Ms_1 [Red] 1859 points and Tb_1 [Green] 6890 points - 1.88350589
Ms_2 [Blue3] 1578 points and Tb_2 [Cyan] 4667 points - 1.88774694
SG_2 [Red] 949 points and Tv_1 [Aquamarine] 1437 points - 1.89680702
SG_2 [Red] 949 points and Tm_2 [Red] 2452 points - 1.89986821
SG_1 [Blue] 1799 points and SG_3 [Sea Green] 854 points - 1.91296380
SG_2 [Red] 949 points and Tb_2 [Cyan] 4667 points - 1.91705046
Ms_2 [Blue3] 1578 points and Tm_2 [Red] 2452 points - 1.92180090
Tb_1 [Green] 6890 points and Tm_1 [Green] 3336 points - 1.92547431
Ms_1 [Red] 1859 points and Ct [White] 3007 points - 1.92848884
Ms_2 [Blue3] 1578 points and Tv_1 [Aquamarine] 1437 points - 1.93891542
R2 [Black] 1037 points and Ct [White] 3007 points - 1.93951445
Tv_1 [Aquamarine] 1437 points and Ct [White] 3007 points - 1.94307807
Ms_2 [Blue3] 1578 points and SG_3 [Sea Green] 854 points - 1.94389246
SG_2 [Red] 949 points and SG_3 [Sea Green] 854 points - 1.94583892
SG_2 [Red] 949 points and R2 [Black] 1037 points - 1.94650922
Tb_1 [Green] 6890 points and SG_3 [Sea Green] 854 points - 1.94696181
O [Green] 545 points and Tv_2 [Sienna] 1002 points - 1.95029668
Ct [White] 3007 points and Tr [Maroon] 3425 points - 1.95623796
R2 [Black] 1037 points and SG_3 [Sea Green] 854 points - 1.96036021
Tv_2 [Sienna] 1002 points and SG_3 [Sea Green] 854 points - 1.96057790
O [Green] 545 points and R2 [Black] 1037 points - 1.96122182
O [Green] 545 points and Tv_1 [Aquamarine] 1437 points - 1.96291065
Ms_2 [Blue3] 1578 points and R2 [Black] 1037 points - 1.96332238
O [Green] 545 points and SG_3 [Sea Green] 854 points - 1.96641674
SG_3 [Sea Green] 854 points and Tr [Maroon] 3425 points - 1.97035690
SG_3 [Sea Green] 854 points and Ct [White] 3007 points - 1.97045353
Tm_2 [Red] 2452 points and Ct [White] 3007 points - 1.97216023
Tv_1 [Aquamarine] 1437 points and SG_3 [Sea Green] 854 points - 1.97226400
Tm_2 [Red] 2452 points and SG_3 [Sea Green] 854 points - 1.97527472
O [Green] 545 points and Ct [White] 3007 points - 1.98049556
R1 [White] 530 points and SG_3 [Sea Green] 854 points - 1.98123252

Ms_1 [Red] 1859 points and SG_3 [Sea Green] 854 points - 1.98199568
Tb_2 [Cyan] 4667 points and SG_3 [Sea Green] 854 points - 1.98204362
R1 [White] 530 points and Tb_1 [Green] 6890 points - 1.98299266
Ap [Purple] 994 points and R1 [White] 530 points - 1.98331714
Tb_2 [Cyan] 4667 points and Ct [White] 3007 points - 1.98399014
Ap [Purple] 994 points and R2 [Black] 1037 points - 1.98537145
Tm_1 [Green] 3336 points and SG_3 [Sea Green] 854 points - 1.98964731
Sw [Aquamarine] 2668 points and Mg [Blue3] 2150 points - 1.98976057
O [Green] 545 points and Tm_1 [Green] 3336 points - 1.99034424
Ap [Purple] 994 points and Sw [Aquamarine] 2668 points - 1.99157907
Ap [Purple] 994 points and SG_1 [Blue] 1799 points - 1.99181495
Tb_1 [Green] 6890 points and B [White] 745 points - 1.99246614
Ap [Purple] 994 points and Tv_1 [Aquamarine] 1437 points - 1.99262147
Ms_1 [Red] 1859 points and Tv_2 [Sienna] 1002 points - 1.99296160
SG_2 [Red] 949 points and Tm_1 [Green] 3336 points - 1.99326639
Ap [Purple] 994 points and Tv_2 [Sienna] 1002 points - 1.99526716
Ap [Purple] 994 points and B [White] 745 points - 1.99533675
Ms_1 [Red] 1859 points and Tr [Maroon] 3425 points - 1.99540160
Ms_1 [Red] 1859 points and O [Green] 545 points - 1.99541352
Ap [Purple] 994 points and Tm_1 [Green] 3336 points - 1.99548974
Sw [Aquamarine] 2668 points and SG_3 [Sea Green] 854 points - 1.99561690
SG_3 [Sea Green] 854 points and B [White] 745 points - 1.99564881
Ap [Purple] 994 points and Tr [Maroon] 3425 points - 1.99589289
Ms_1 [Red] 1859 points and Tm_2 [Red] 2452 points - 1.99641261
Ap [Purple] 994 points and Tb_2 [Cyan] 4667 points - 1.99657999
SG_2 [Red] 949 points and R1 [White] 530 points - 1.99663825
Ms_1 [Red] 1859 points and Tb_2 [Cyan] 4667 points - 1.99665824
Mg [Blue3] 2150 points and Ms_2 [Blue3] 1578 points - 1.99706392
Ap [Purple] 994 points and Tm_2 [Red] 2452 points - 1.99725334
Ms_1 [Red] 1859 points and Tv_1 [Aquamarine] 1437 points - 1.99740956
Ms_2 [Blue3] 1578 points and Tm_1 [Green] 3336 points - 1.99788403
Mg [Blue3] 2150 points and SG_1 [Blue] 1799 points - 1.99792036
Ms_2 [Blue3] 1578 points and R1 [White] 530 points - 1.99800694
O [Green] 545 points and R1 [White] 530 points - 1.99803896
Ap [Purple] 994 points and Ms_2 [Blue3] 1578 points - 1.99865887
Ap [Purple] 994 points and O [Green] 545 points - 1.99869615
Ap [Purple] 994 points and Tb_1 [Green] 6890 points - 1.99874860
Mg [Blue3] 2150 points and SG_2 [Red] 949 points - 1.99882114
Mg [Blue3] 2150 points and O [Green] 545 points - 1.99883879
Ap [Purple] 994 points and Ct [White] 3007 points - 1.99894550
Ms_1 [Red] 1859 points and R2 [Black] 1037 points - 1.99901319
Tm_1 [Green] 3336 points and Ct [White] 3007 points - 1.99920808
R1 [White] 530 points and Ct [White] 3007 points - 1.99923004
Ap [Purple] 994 points and SG_2 [Red] 949 points - 1.99944200
Mg [Blue3] 2150 points and Tb_1 [Green] 6890 points - 1.99962241
Mg [Blue3] 2150 points and Ice/Snow [Blue] 4804 points - 1.99973402
Mg [Blue3] 2150 points and Tv_2 [Sienna] 1002 points - 1.99973571
SG_2 [Red] 949 points and B [White] 745 points - 1.99974150
O [Green] 545 points and B [White] 745 points - 1.99975270
Ap [Purple] 994 points and Ice/Snow [Blue] 4804 points - 1.99977493
B [White] 745 points and Ct [White] 3007 points - 1.99982753
Mg [Blue3] 2150 points and R2 [Black] 1037 points - 1.99987195
Ms_2 [Blue3] 1578 points and B [White] 745 points - 1.99990056
Ms_1 [Red] 1859 points and Tm_1 [Green] 3336 points - 1.99991642
Mg [Blue3] 2150 points and Ct [White] 3007 points - 1.99991952
Mg [Blue3] 2150 points and Tv_1 [Aquamarine] 1437 points - 1.99993004
Mg [Blue3] 2150 points and Tr [Maroon] 3425 points - 1.99993485
Mg [Blue3] 2150 points and Ms_1 [Red] 1859 points - 1.99994244
Ap [Purple] 994 points and Ms_1 [Red] 1859 points - 1.99995916
Mg [Blue3] 2150 points and R1 [White] 530 points - 1.99996256
Mg [Blue3] 2150 points and Tm_2 [Red] 2452 points - 1.99997998
Ice/Snow [Blue] 4804 points and SG_3 [Sea Green] 854 points - 1.99998234
Sw [Aquamarine] 2668 points and Ice/Snow [Blue] 4804 points - 1.99998914
Ms_1 [Red] 1859 points and R1 [White] 530 points - 1.99999184
Ice/Snow [Blue] 4804 points and SG_1 [Blue] 1799 points - 1.99999254
Mg [Blue3] 2150 points and Tb_2 [Cyan] 4667 points - 1.99999373
Mg [Blue3] 2150 points and Tm_1 [Green] 3336 points - 1.99999702
Ice/Snow [Blue] 4804 points and O [Green] 545 points - 1.99999745
Ms_2 [Blue3] 1578 points and Ice/Snow [Blue] 4804 points - 1.99999777
Ice/Snow [Blue] 4804 points and Tv_1 [Aquamarine] 1437 points - 1.99999809

Ms_1 [Red] 1859 points and B [White] 745 points - 1.99999842
Ice/Snow [Blue] 4804 points and Tv_2 [Sienna] 1002 points - 1.99999864
Ice/Snow [Blue] 4804 points and R2 [Black] 1037 points - 1.99999878
Ice/Snow [Blue] 4804 points and Tm_2 [Red] 2452 points - 1.99999888
Ice/Snow [Blue] 4804 points and Tr [Maroon] 3425 points - 1.99999912
Ice/Snow [Blue] 4804 points and SG_2 [Red] 949 points - 1.99999917
Ice/Snow [Blue] 4804 points and Tm_1 [Green] 3336 points - 1.99999928
Ice/Snow [Blue] 4804 points and R1 [White] 530 points - 1.99999936
Ice/Snow [Blue] 4804 points and B [White] 745 points - 1.99999936
Ice/Snow [Blue] 4804 points and Tb_2 [Cyan] 4667 points - 1.99999955
Mg [Blue3] 2150 points and B [White] 745 points - 1.99999961
Ice/Snow [Blue] 4804 points and Tb_1 [Green] 6890 points - 1.99999993
Sw [Aquamarine] 2668 points and SG_1 [Blue] 1799 points - 1.99999997
Sw [Aquamarine] 2668 points and Tb_1 [Green] 6890 points - 1.99999999
Sw [Aquamarine] 2668 points and Ms_2 [Blue3] 1578 points - 1.99999999
Sw [Aquamarine] 2668 points and SG_2 [Red] 949 points - 2.00000000
Ice/Snow [Blue] 4804 points and Ct [White] 3007 points - 2.00000000
Ms_1 [Red] 1859 points and Ice/Snow [Blue] 4804 points - 2.00000000
Sw [Aquamarine] 2668 points and Tv_1 [Aquamarine] 1437 points - 2.00000000
Sw [Aquamarine] 2668 points and Tr [Maroon] 3425 points - 2.00000000
Sw [Aquamarine] 2668 points and O [Green] 545 points - 2.00000000
Sw [Aquamarine] 2668 points and Ct [White] 3007 points - 2.00000000
Sw [Aquamarine] 2668 points and R1 [White] 530 points - 2.00000000
Sw [Aquamarine] 2668 points and R2 [Black] 1037 points - 2.00000000
Sw [Aquamarine] 2668 points and Tv_2 [Sienna] 1002 points - 2.00000000
Sw [Aquamarine] 2668 points and Ms_1 [Red] 1859 points - 2.00000000
Sw [Aquamarine] 2668 points and Tb_2 [Cyan] 4667 points - 2.00000000
Sw [Aquamarine] 2668 points and B [White] 745 points - 2.00000000
Sw [Aquamarine] 2668 points and Tm_1 [Green] 3336 points - 2.00000000
Sw [Aquamarine] 2668 points and Tm_2 [Red] 2452 points - 2.00000000

Appendix G: Transform Divergence Statistic: SPOT, 21 classes

Input File: spot_ms.dat
ROI Name: (Jeffries-Matusita, Transformed Divergence)

Ap [Purple] 2209 points:
Sw [Aquamarine] 5935 points: (1.99969489 2.00000000)
Mg [Blue3] 4794 points: (1.15940690 1.59911040)
Ms_1 [Red] 4135 points: (1.99969004 2.00000000)
Ms_2 [Blue3] 3490 points: (1.98839490 1.99860862)
Ice/Snow [Blue] 10750 points: (1.97150221 1.99966928)
O [Green] 1214 points: (1.99590839 1.99986261)
SG_1 [Blue] 3991 points: (1.98231179 1.99745987)
SG_2 [Red] 2066 points: (1.99576035 2.00000000)
R1 [White] 1169 points: (1.97783111 1.99998505)
R2 [Black] 2306 points: (1.99141103 1.99992336)
Tb_1 [Green] 15499 points: (1.99337200 1.99996906)
Tb_2 [Cyan] 10409 points: (1.98921418 1.99998203)
Tm_1 [Green] 7485 points: (1.99259512 1.99999756)
Tm_2 [Red] 5461 points: (1.99265641 1.99998894)
Tv_1 [Aquamarine] 3227 points: (1.98999800 1.99998814)
Tv_2 [Sienna] 2231 points: (1.99104248 1.99999769)
SG_3 [Sea Green] 1500 points: (0.85453263 1.03501394)
B [White] 1601 points: (1.99752336 1.99999970)
Ct [White] 6662 points: (1.99522795 2.00000000)
Tr [Maroon] 7685 points: (1.97754662 1.99908765)

Sw [Aquamarine] 5935 points:
Ap [Purple] 2209 points: (1.99969489 2.00000000)
Mg [Blue3] 4794 points: (1.94608945 2.00000000)
Ms_1 [Red] 4135 points: (2.00000000 2.00000000)
Ms_2 [Blue3] 3490 points: (1.99993919 2.00000000)
Ice/Snow [Blue] 10750 points: (1.61654697 1.99979132)
O [Green] 1214 points: (1.99703790 1.99999161)
SG_1 [Blue] 3991 points: (1.99989771 2.00000000)
SG_2 [Red] 2066 points: (1.99963388 2.00000000)
R1 [White] 1169 points: (1.99999994 2.00000000)
R2 [Black] 2306 points: (1.99996435 2.00000000)
Tb_1 [Green] 15499 points: (1.99999860 2.00000000)
Tb_2 [Cyan] 10409 points: (2.00000000 2.00000000)
Tm_1 [Green] 7485 points: (2.00000000 2.00000000)
Tm_2 [Red] 5461 points: (2.00000000 2.00000000)
Tv_1 [Aquamarine] 3227 points: (1.99999998 2.00000000)
Tv_2 [Sienna] 2231 points: (1.99992916 2.00000000)
SG_3 [Sea Green] 1500 points: (1.99860870 2.00000000)
B [White] 1601 points: (2.00000000 2.00000000)
Ct [White] 6662 points: (1.99999998 2.00000000)
Tr [Maroon] 7685 points: (1.99999997 2.00000000)

Mg [Blue3] 4794 points:
Ap [Purple] 2209 points: (1.15940690 1.59911040)
Sw [Aquamarine] 5935 points: (1.94608945 2.00000000)
Ms_1 [Red] 4135 points: (1.99550703 2.00000000)
Ms_2 [Blue3] 3490 points: (1.90560995 1.99347666)
Ice/Snow [Blue] 10750 points: (1.75406491 1.98875064)
O [Green] 1214 points: (1.82595458 1.99857369)
SG_1 [Blue] 3991 points: (1.85910376 1.99151490)
SG_2 [Red] 2066 points: (1.95963236 1.99999999)
R1 [White] 1169 points: (1.97632948 1.99979746)
R2 [Black] 2306 points: (1.87697671 1.99866747)
Tb_1 [Green] 15499 points: (1.91708066 1.99981192)
Tb_2 [Cyan] 10409 points: (1.91227569 1.99982746)
Tm_1 [Green] 7485 points: (1.93248244 1.99988797)
Tm_2 [Red] 5461 points: (1.90111657 1.99988793)
Tv_1 [Aquamarine] 3227 points: (1.92484945 1.99990838)
Tv_2 [Sienna] 2231 points: (1.86713869 1.99997126)
SG_3 [Sea Green] 1500 points: (1.44542292 1.73244970)
B [White] 1601 points: (1.98395581 1.99999495)
Ct [White] 6662 points: (1.96738384 2.00000000)
Tr [Maroon] 7685 points: (1.87627945 1.99759750)

Ms_1 [Red] 4135 points:
Ap [Purple] 2209 points: (1.99969004 2.00000000)
Sw [Aquamarine] 5935 points: (2.00000000 2.00000000)
Mg [Blue3] 4794 points: (1.99550703 2.00000000)
Ms_2 [Blue3] 3490 points: (1.31177143 1.53090504)
Ice/Snow [Blue] 10750 points: (1.99996914 2.00000000)
O [Green] 1214 points: (1.97098088 1.99997889)
SG_1 [Blue] 3991 points: (1.66916227 1.80549026)
SG_2 [Red] 2066 points: (1.39392955 1.48835978)
R1 [White] 1169 points: (1.99833973 1.99999274)
R2 [Black] 2306 points: (1.96437259 1.97676100)
Tb_1 [Green] 15499 points: (1.78445251 1.90235262)
Tb_2 [Cyan] 10409 points: (1.90377404 1.98487914)
Tm_1 [Green] 7485 points: (1.98485098 1.99711058)
Tm_2 [Red] 5461 points: (1.86909330 1.93024221)
Tv_1 [Aquamarine] 3227 points: (1.94464325 1.95729213)
Tv_2 [Sienna] 2231 points: (1.89601677 1.93257355)
SG_3 [Sea Green] 1500 points: (1.97244456 2.00000000)
B [White] 1601 points: (1.99916783 1.99998915)
Ct [White] 6662 points: (1.93375059 1.99998242)
Tr [Maroon] 7685 points: (1.87014883 1.95338975)

Ms_2 [Blue3] 3490 points:
Ap [Purple] 2209 points: (1.98839490 1.99860862)
Sw [Aquamarine] 5935 points: (1.99993919 2.00000000)
Mg [Blue3] 4794 points: (1.90560995 1.99347666)
Ms_1 [Red] 4135 points: (1.31177143 1.53090504)
Ice/Snow [Blue] 10750 points: (1.99407275 1.99999181)
O [Green] 1214 points: (1.48647927 1.55293607)
SG_1 [Blue] 3991 points: (0.67128998 0.73196443)
SG_2 [Red] 2066 points: (0.73940811 0.97997007)
R1 [White] 1169 points: (1.91529206 1.98928763)
R2 [Black] 2306 points: (1.51132366 1.57570970)
Tb_1 [Green] 15499 points: (0.47988370 0.55595781)
Tb_2 [Cyan] 10409 points: (0.99894179 1.19886945)
Tm_1 [Green] 7485 points: (1.72315101 1.85031857)
Tm_2 [Red] 5461 points: (1.01406635 1.10696156)
Tv_1 [Aquamarine] 3227 points: (1.48070083 1.56045135)
Tv_2 [Sienna] 2231 points: (1.22988577 1.31299786)
SG_3 [Sea Green] 1500 points: (1.80724355 1.99876507)
B [White] 1601 points: (1.94073624 1.99400378)
Ct [White] 6662 points: (1.30333014 1.96831839)
Tr [Maroon] 7685 points: (0.94205006 0.99654189)

Ice/Snow [Blue] 10750 points:
Ap [Purple] 2209 points: (1.97150221 1.99966928)
Sw [Aquamarine] 5935 points: (1.61654697 1.99979132)
Mg [Blue3] 4794 points: (1.75406491 1.98875064)
Ms_1 [Red] 4135 points: (1.99996914 2.00000000)
Ms_2 [Blue3] 3490 points: (1.99407275 1.99999181)
O [Green] 1214 points: (1.91114994 1.99982222)
SG_1 [Blue] 3991 points: (1.99411398 1.99997092)
SG_2 [Red] 2066 points: (1.99562647 2.00000000)
R1 [White] 1169 points: (1.99932966 1.99999889)
R2 [Black] 2306 points: (1.99497644 1.99999983)
Tb_1 [Green] 15499 points: (1.99614964 1.99999989)
Tb_2 [Cyan] 10409 points: (1.99766088 2.00000000)
Tm_1 [Green] 7485 points: (1.99961110 2.00000000)
Tm_2 [Red] 5461 points: (1.99790574 2.00000000)
Tv_1 [Aquamarine] 3227 points: (1.99919906 2.00000000)
Tv_2 [Sienna] 2231 points: (1.99521799 2.00000000)
SG_3 [Sea Green] 1500 points: (1.97753429 1.99482494)
B [White] 1601 points: (1.99993624 2.00000000)
Ct [White] 6662 points: (1.99783718 2.00000000)
Tr [Maroon] 7685 points: (1.99644466 1.99999639)

O [Green] 1214 points:
Ap [Purple] 2209 points: (1.99590839 1.99986261)
Sw [Aquamarine] 5935 points: (1.99703790 1.99999161)
Mg [Blue3] 4794 points: (1.82595458 1.99857369)
Ms_1 [Red] 4135 points: (1.97098088 1.99997889)
Ms_2 [Blue3] 3490 points: (1.48647927 1.55293607)
Ice/Snow [Blue] 10750 points: (1.91114994 1.99982222)
SG_1 [Blue] 3991 points: (1.69702734 1.76376273)
SG_2 [Red] 2066 points: (1.87252361 1.99659252)
R1 [White] 1169 points: (1.99234057 1.99983158)
R2 [Black] 2306 points: (1.86256869 1.92652321)
Tb_1 [Green] 15499 points: (1.26660536 1.40840879)
Tb_2 [Cyan] 10409 points: (1.38000875 1.68721434)
Tm_1 [Green] 7485 points: (1.96261670 1.99034773)
Tm_2 [Red] 5461 points: (1.68111743 1.75928413)
Tv_1 [Aquamarine] 3227 points: (1.94702105 1.97848541)
Tv_2 [Sienna] 2231 points: (1.81508089 1.88097468)
SG_3 [Sea Green] 1500 points: (1.90066434 1.99995436)
B [White] 1601 points: (1.99685348 1.99997527)
Ct [White] 6662 points: (1.79183790 1.99886600)
Tr [Maroon] 7685 points: (1.65259756 1.70220428)

SG_1 [Blue] 3991 points:
Ap [Purple] 2209 points: (1.98231179 1.99745987)
Sw [Aquamarine] 5935 points: (1.99989771 2.00000000)
Mg [Blue3] 4794 points: (1.85910376 1.99151490)
Ms_1 [Red] 4135 points: (1.66916227 1.80549026)
Ms_2 [Blue3] 3490 points: (0.67128998 0.73196443)
Ice/Snow [Blue] 10750 points: (1.99411398 1.99997092)
O [Green] 1214 points: (1.69702734 1.76376273)
SG_2 [Red] 2066 points: (0.74849758 0.94950671)
R1 [White] 1169 points: (1.27812709 1.67739171)
R2 [Black] 2306 points: (0.57309470 0.64745264)
Tb_1 [Green] 15499 points: (0.88600814 0.98966620)
Tb_2 [Cyan] 10409 points: (0.92067465 1.28386752)
Tm_1 [Green] 7485 points: (1.14342755 1.50162908)
Tm_2 [Red] 5461 points: (0.62773373 0.85872383)
Tv_1 [Aquamarine] 3227 points: (0.55420663 0.62672845)
Tv_2 [Sienna] 2231 points: (0.41766646 0.47682918)
SG_3 [Sea Green] 1500 points: (1.71944914 1.99743161)
B [White] 1601 points: (1.56187922 1.85670788)
Ct [White] 6662 points: (1.37308881 1.92947331)
Tr [Maroon] 7685 points: (0.47883136 0.60148080)

SG_2 [Red] 2066 points:
Ap [Purple] 2209 points: (1.99576035 2.00000000)
Sw [Aquamarine] 5935 points: (1.99963388 2.00000000)
Mg [Blue3] 4794 points: (1.95963236 1.99999999)
Ms_1 [Red] 4135 points: (1.39392955 1.48835978)
Ms_2 [Blue3] 3490 points: (0.73940811 0.97997007)
Ice/Snow [Blue] 10750 points: (1.99562647 2.00000000)
O [Green] 1214 points: (1.87252361 1.99659252)
SG_1 [Blue] 3991 points: (0.74849758 0.94950671)
R1 [White] 1169 points: (1.90175516 1.97707779)
R2 [Black] 2306 points: (1.46682254 1.52533156)
Tb_1 [Green] 15499 points: (1.07927046 1.40395004)
Tb_2 [Cyan] 10409 points: (1.37800573 1.82875110)
Tm_1 [Green] 7485 points: (1.68722732 1.85262112)
Tm_2 [Red] 5461 points: (1.19000204 1.48095891)
Tv_1 [Aquamarine] 3227 points: (1.31680243 1.37015244)
Tv_2 [Sienna] 2231 points: (1.09687432 1.15377751)
SG_3 [Sea Green] 1500 points: (1.87144384 2.00000000)
B [White] 1601 points: (1.92534438 1.98076680)
Ct [White] 6662 points: (1.37562594 1.88280369)
Tr [Maroon] 7685 points: (1.15339715 1.48794228)

R1 [White] 1169 points:
Ap [Purple] 2209 points: (1.97783111 1.99998505)
Sw [Aquamarine] 5935 points: (1.99999994 2.00000000)
Mg [Blue3] 4794 points: (1.97632948 1.99979746)
Ms_1 [Red] 4135 points: (1.99833973 1.99999274)
Ms_2 [Blue3] 3490 points: (1.91529206 1.98928763)
Ice/Snow [Blue] 10750 points: (1.99932966 1.99999889)
O [Green] 1214 points: (1.99234057 1.99983158)
SG_1 [Blue] 3991 points: (1.27812709 1.67739171)
SG_2 [Red] 2066 points: (1.90175516 1.97707779)
R2 [Black] 2306 points: (0.78070844 0.97680240)
Tb_1 [Green] 15499 points: (1.93740685 1.98212219)
Tb_2 [Cyan] 10409 points: (1.43377652 1.91662445)
Tm_1 [Green] 7485 points: (0.96618964 1.27091670)
Tm_2 [Red] 5461 points: (1.48526076 1.73246116)
Tv_1 [Aquamarine] 3227 points: (0.88849406 1.11449195)
Tv_2 [Sienna] 2231 points: (1.40411473 1.59727385)
SG_3 [Sea Green] 1500 points: (1.87905047 1.99998947)
B [White] 1601 points: (0.74908922 0.97181667)
Ct [White] 6662 points: (1.97851499 1.99830418)
Tr [Maroon] 7685 points: (1.39265253 1.65509533)

R2 [Black] 2306 points:
Ap [Purple] 2209 points: (1.99141103 1.99992336)
Sw [Aquamarine] 5935 points: (1.99996435 2.00000000)
Mg [Blue3] 4794 points: (1.87697671 1.99866747)
Ms_1 [Red] 4135 points: (1.96437259 1.97676100)
Ms_2 [Blue3] 3490 points: (1.51132366 1.57570970)
Ice/Snow [Blue] 10750 points: (1.99497644 1.99999983)
O [Green] 1214 points: (1.86256869 1.92652321)
SG_1 [Blue] 3991 points: (0.57309470 0.64745264)
SG_2 [Red] 2066 points: (1.46682254 1.52533156)
R1 [White] 1169 points: (0.78070844 0.97680240)
Tb_1 [Green] 15499 points: (1.46310222 1.50701645)
Tb_2 [Cyan] 10409 points: (1.09127455 1.38232752)
Tm_1 [Green] 7485 points: (0.72621063 1.03544337)
Tm_2 [Red] 5461 points: (0.74851424 0.87276370)
Tv_1 [Aquamarine] 3227 points: (0.23422158 0.24579024)
Tv_2 [Sienna] 2231 points: (0.36953467 0.38057006)
SG_3 [Sea Green] 1500 points: (1.85246963 1.99993931)
B [White] 1601 points: (1.18874297 1.34646029)
Ct [White] 6662 points: (1.68446157 1.96948261)
Tr [Maroon] 7685 points: (0.72059606 0.77780080)

Tb_1 [Green] 15499 points:
Ap [Purple] 2209 points: (1.99337200 1.99996906)
Sw [Aquamarine] 5935 points: (1.99999860 2.00000000)
Mg [Blue3] 4794 points: (1.91708066 1.99981192)
Ms_1 [Red] 4135 points: (1.78445251 1.90235262)
Ms_2 [Blue3] 3490 points: (0.47988370 0.55595781)
Ice/Snow [Blue] 10750 points: (1.99614964 1.99999989)
O [Green] 1214 points: (1.26660536 1.40840879)
SG_1 [Blue] 3991 points: (0.88600814 0.98966620)
SG_2 [Red] 2066 points: (1.07927046 1.40395004)
R1 [White] 1169 points: (1.93740685 1.98212219)
R2 [Black] 2306 points: (1.46310222 1.50701645)
Tb_2 [Cyan] 10409 points: (0.56077588 0.69247953)
Tm_1 [Green] 7485 points: (1.68381470 1.81779467)
Tm_2 [Red] 5461 points: (0.77864403 0.87088532)
Tv_1 [Aquamarine] 3227 points: (1.42058253 1.52946021)
Tv_2 [Sienna] 2231 points: (1.07264121 1.12809716)
SG_3 [Sea Green] 1500 points: (1.86583032 1.99999119)
B [White] 1601 points: (1.95612600 1.99260218)
Ct [White] 6662 points: (1.31682034 1.82975166)
Tr [Maroon] 7685 points: (0.76931884 0.81331143)

Tb_2 [Cyan] 10409 points:
Ap [Purple] 2209 points: (1.98921418 1.99998203)
Sw [Aquamarine] 5935 points: (2.00000000 2.00000000)
Mg [Blue3] 4794 points: (1.91227569 1.99982746)
Ms_1 [Red] 4135 points: (1.90377404 1.98487914)
Ms_2 [Blue3] 3490 points: (0.99894179 1.19886945)
Ice/Snow [Blue] 10750 points: (1.99766088 2.00000000)
O [Green] 1214 points: (1.38000875 1.68721434)

SG_1 [Blue] 3991 points: (0.92067465 1.28386752)
SG_2 [Red] 2066 points: (1.37800573 1.82875110)
R1 [White] 1169 points: (1.43377652 1.91662445)
R2 [Black] 2306 points: (1.09127455 1.38232752)
Tb_1 [Green] 15499 points: (0.56077588 0.69247953)
Tm_1 [Green] 7485 points: (0.86555033 1.27567465)
Tm_2 [Red] 5461 points: (0.34538232 0.39414718)
Tv_1 [Aquamarine] 3227 points: (0.93584474 1.35288794)
Tv_2 [Sienna] 2231 points: (0.88769324 1.25811964)
SG_3 [Sea Green] 1500 points: (1.85359951 1.99999128)
B [White] 1601 points: (1.46701742 1.93138473)
Ct [White] 6662 points: (1.33690549 1.86460795)
Tr [Maroon] 7685 points: (0.40057162 0.45904141)

Tm_1 [Green] 7485 points:
Ap [Purple] 2209 points: (1.99259512 1.99999756)
Sw [Aquamarine] 5935 points: (2.00000000 2.00000000)
Mg [Blue3] 4794 points: (1.93248244 1.99988797)
Ms_1 [Red] 4135 points: (1.98485098 1.99711058)
Ms_2 [Blue3] 3490 points: (1.72315101 1.85031857)
Ice/Snow [Blue] 10750 points: (1.99961110 2.00000000)
O [Green] 1214 points: (1.96261670 1.99034773)
SG_1 [Blue] 3991 points: (1.14342755 1.50162908)
SG_2 [Red] 2066 points: (1.68722732 1.85262112)
R1 [White] 1169 points: (0.96618964 1.27091670)
R2 [Black] 2306 points: (0.72621063 1.03544337)
Tb_1 [Green] 15499 points: (1.68381470 1.81779467)
Tb_2 [Cyan] 10409 points: (0.86555033 1.27567465)
Tm_2 [Red] 5461 points: (0.71007257 0.76154813)
Tv_1 [Aquamarine] 3227 points: (0.60101015 0.74000058)
Tv_2 [Sienna] 2231 points: (0.94991237 1.17225484)
SG_3 [Sea Green] 1500 points: (1.90176100 1.99999900)
B [White] 1601 points: (0.64284046 0.70325779)
Ct [White] 6662 points: (1.84381924 1.93620889)
Tr [Maroon] 7685 points: (0.80085542 0.89052981)

Tm_2 [Red] 5461 points:
Ap [Purple] 2209 points: (1.99265641 1.99998894)
Sw [Aquamarine] 5935 points: (2.00000000 2.00000000)
Mg [Blue3] 4794 points: (1.90111657 1.99988793)
Ms_1 [Red] 4135 points: (1.86909330 1.93024221)
Ms_2 [Blue3] 3490 points: (1.01406635 1.10696156)
Ice/Snow [Blue] 10750 points: (1.99790574 2.00000000)
O [Green] 1214 points: (1.68111743 1.75928413)
SG_1 [Blue] 3991 points: (0.62773373 0.85872383)
SG_2 [Red] 2066 points: (1.19000204 1.48095891)
R1 [White] 1169 points: (1.48526076 1.73246116)
R2 [Black] 2306 points: (0.74851424 0.87276370)
Tb_1 [Green] 15499 points: (0.77864403 0.87088532)
Tb_2 [Cyan] 10409 points: (0.34538232 0.39414718)
Tm_1 [Green] 7485 points: (0.71007257 0.76154813)
Tv_1 [Aquamarine] 3227 points: (0.61610099 0.73813032)
Tv_2 [Sienna] 2231 points: (0.53322797 0.66482672)
SG_3 [Sea Green] 1500 points: (1.85223334 1.99999096)
B [White] 1601 points: (1.49470606 1.73348588)
Ct [White] 6662 points: (1.30536941 1.64073196)
Tr [Maroon] 7685 points: (0.12961442 0.14041880)

Tv_1 [Aquamarine] 3227 points:
Ap [Purple] 2209 points: (1.98999800 1.99998814)
Sw [Aquamarine] 5935 points: (1.99999998 2.00000000)
Mg [Blue3] 4794 points: (1.92484945 1.99990838)
Ms_1 [Red] 4135 points: (1.94464325 1.95729213)
Ms_2 [Blue3] 3490 points: (1.48070083 1.56045135)
Ice/Snow [Blue] 10750 points: (1.99919906 2.00000000)
O [Green] 1214 points: (1.94702105 1.97848541)
SG_1 [Blue] 3991 points: (0.55420663 0.62672845)
SG_2 [Red] 2066 points: (1.31680243 1.37015244)
R1 [White] 1169 points: (0.88849406 1.11449195)
R2 [Black] 2306 points: (0.23422158 0.24579024)
Tb_1 [Green] 15499 points: (1.42058253 1.52946021)
Tb_2 [Cyan] 10409 points: (0.93584474 1.35288794)
Tm_1 [Green] 7485 points: (0.60101015 0.74000058)
Tm_2 [Red] 5461 points: (0.61610099 0.73813032)
Tv_2 [Sienna] 2231 points: (0.35061180 0.36146949)
SG_3 [Sea Green] 1500 points: (1.84340406 1.99999584)
B [White] 1601 points: (1.09530360 1.25119373)
Ct [White] 6662 points: (1.62266163 1.93345540)
Tr [Maroon] 7685 points: (0.53947641 0.63433295)

Tv_2 [Sienna] 2231 points:
Ap [Purple] 2209 points: (1.99104248 1.99999769)
Sw [Aquamarine] 5935 points: (1.99992916 2.00000000)
Mg [Blue3] 4794 points: (1.86713869 1.99997126)
Ms_1 [Red] 4135 points: (1.89601677 1.93257355)
Ms_2 [Blue3] 3490 points: (1.22988577 1.31299786)
Ice/Snow [Blue] 10750 points: (1.99521799 2.00000000)
O [Green] 1214 points: (1.81508089 1.88097468)
SG_1 [Blue] 3991 points: (0.41766646 0.47682918)
SG_2 [Red] 2066 points: (1.09687432 1.15377751)
R1 [White] 1169 points: (1.40411473 1.59727385)
R2 [Black] 2306 points: (0.36953467 0.38057006)
Tb_1 [Green] 15499 points: (1.07264121 1.12809716)
Tb_2 [Cyan] 10409 points: (0.88769324 1.25811964)
Tm_1 [Green] 7485 points: (0.94991237 1.17225484)
Tm_2 [Red] 5461 points: (0.53322797 0.66482672)
Tv_1 [Aquamarine] 3227 points: (0.35061180 0.36146949)
SG_3 [Sea Green] 1500 points: (1.82969739 1.99999965)
B [White] 1601 points: (1.59878908 1.72790335)
Ct [White] 6662 points: (1.56646037 1.89261266)
Tr [Maroon] 7685 points: (0.54171934 0.63144640)

SG_3 [Sea Green] 1500 points:
Ap [Purple] 2209 points: (0.85453263 1.03501394)
Sw [Aquamarine] 5935 points: (1.99860870 2.00000000)
Mg [Blue3] 4794 points: (1.44542292 1.73244970)
Ms_1 [Red] 4135 points: (1.97244456 2.00000000)
Ms_2 [Blue3] 3490 points: (1.80724355 1.99876507)
Ice/Snow [Blue] 10750 points: (1.97753429 1.99482494)
O [Green] 1214 points: (1.90066434 1.99995436)
SG_1 [Blue] 3991 points: (1.71944914 1.99743161)
SG_2 [Red] 2066 points: (1.87144384 2.00000000)
R1 [White] 1169 points: (1.87905047 1.99998947)
R2 [Black] 2306 points: (1.85246963 1.99993931)
Tb_1 [Green] 15499 points: (1.86583032 1.99999119)
Tb_2 [Cyan] 10409 points: (1.85359951 1.99999128)
Tm_1 [Green] 7485 points: (1.90176100 1.99999900)
Tm_2 [Red] 5461 points: (1.85223334 1.99999096)
Tv_1 [Aquamarine] 3227 points: (1.84340406 1.99999584)
Tv_2 [Sienna] 2231 points: (1.82969739 1.99999965)
B [White] 1601 points: (1.95361828 1.99999998)
Ct [White] 6662 points: (1.93202644 2.00000000)
Tr [Maroon] 7685 points: (1.77089660 1.99804191)

B [White] 1601 points:
Ap [Purple] 2209 points: (1.99752336 1.99999970)
Sw [Aquamarine] 5935 points: (2.00000000 2.00000000)
Mg [Blue3] 4794 points: (1.98395581 1.99999495)
Ms_1 [Red] 4135 points: (1.99916783 1.99998915)
Ms_2 [Blue3] 3490 points: (1.94073624 1.99400378)
Ice/Snow [Blue] 10750 points: (1.99993624 2.00000000)
O [Green] 1214 points: (1.99685348 1.99997527)
SG_1 [Blue] 3991 points: (1.56187922 1.85670788)
SG_2 [Red] 2066 points: (1.92534438 1.98076680)
R1 [White] 1169 points: (0.74908922 0.97181667)
R2 [Black] 2306 points: (1.18874297 1.34646029)
Tb_1 [Green] 15499 points: (1.95612600 1.99260218)
Tb_2 [Cyan] 10409 points: (1.46701742 1.93138473)
Tm_1 [Green] 7485 points: (0.64284046 0.70325779)
Tm_2 [Red] 5461 points: (1.49470606 1.73348588)

Tv_1 [Aquamarine] 3227 points: (1.09530360 1.25119373)
Tv_2 [Sienna] 2231 points: (1.59878908 1.72790335)
SG_3 [Sea Green] 1500 points: (1.95361828 1.99999998)
Ct [White] 6662 points: (1.99326168 1.99901156)
Tr [Maroon] 7685 points: (1.51721080 1.73834988)

Ct [White] 6662 points:
Ap [Purple] 2209 points: (1.99522795 2.00000000)
Sw [Aquamarine] 5935 points: (1.99999998 2.00000000)
Mg [Blue3] 4794 points: (1.96738384 2.00000000)
Ms_1 [Red] 4135 points: (1.93375059 1.99998242)
Ms_2 [Blue3] 3490 points: (1.30333014 1.96831839)
Ice/Snow [Blue] 10750 points: (1.99783718 2.00000000)
O [Green] 1214 points: (1.79183790 1.99886600)
SG_1 [Blue] 3991 points: (1.37308881 1.92947331)
SG_2 [Red] 2066 points: (1.37562594 1.88280369)
R1 [White] 1169 points: (1.97851499 1.99830418)
R2 [Black] 2306 points: (1.68446157 1.96948261)
Tb_1 [Green] 15499 points: (1.31682034 1.82975166)
Tb_2 [Cyan] 10409 points: (1.33690549 1.86460795)
Tm_1 [Green] 7485 points: (1.84381924 1.93620889)
Tm_2 [Red] 5461 points: (1.30536941 1.64073196)
Tv_1 [Aquamarine] 3227 points: (1.62266163 1.93345540)
Tv_2 [Sienna] 2231 points: (1.56646037 1.89261266)
SG_3 [Sea Green] 1500 points: (1.93202644 2.00000000)
B [White] 1601 points: (1.99326168 1.99901156)
Tr [Maroon] 7685 points: (1.26902730 1.69578611)

Tr [Maroon] 7685 points:
Ap [Purple] 2209 points: (1.97754662 1.99908765)
Sw [Aquamarine] 5935 points: (1.99999997 2.00000000)
Mg [Blue3] 4794 points: (1.87627945 1.99759750)
Ms_1 [Red] 4135 points: (1.87014883 1.95338975)
Ms_2 [Blue3] 3490 points: (0.94205006 0.99654189)
Ice/Snow [Blue] 10750 points: (1.99644466 1.99999639)
O [Green] 1214 points: (1.65259756 1.70220428)
SG_1 [Blue] 3991 points: (0.47883136 0.60148080)
SG_2 [Red] 2066 points: (1.15339715 1.48794228)
R1 [White] 1169 points: (1.39265253 1.65509533)
R2 [Black] 2306 points: (0.72059606 0.77780080)
Tb_1 [Green] 15499 points: (0.76931884 0.81331143)
Tb_2 [Cyan] 10409 points: (0.40057162 0.45904141)
Tm_1 [Green] 7485 points: (0.80085542 0.89052981)
Tm_2 [Red] 5461 points: (0.12961442 0.14041880)
Tv_1 [Aquamarine] 3227 points: (0.53947641 0.63433295)
Tv_2 [Sienna] 2231 points: (0.54171934 0.63144640)
SG_3 [Sea Green] 1500 points: (1.77089660 1.99804191)
B [White] 1601 points: (1.51721080 1.73834988)
Ct [White] 6662 points: (1.26902730 1.69578611)

Pair Separation (least to most);

Tm_2 [Red] 5461 points and Tr [Maroon] 7685 points - 0.12961442
R2 [Black] 2306 points and Tv_1 [Aquamarine] 3227 points - 0.23422158
Tb_2 [Cyan] 10409 points and Tm_2 [Red] 5461 points - 0.34538232
Tv_1 [Aquamarine] 3227 points and Tv_2 [Sienna] 2231 points - 0.35061180
R2 [Black] 2306 points and Tv_2 [Sienna] 2231 points - 0.36953467
Tb_2 [Cyan] 10409 points and Tr [Maroon] 7685 points - 0.40057162
SG_1 [Blue] 3991 points and Tv_2 [Sienna] 2231 points - 0.41766646
SG_1 [Blue] 3991 points and Tr [Maroon] 7685 points - 0.47883136
Ms_2 [Blue3] 3490 points and Tb_1 [Green] 15499 points - 0.47988370
Tm_2 [Red] 5461 points and Tv_2 [Sienna] 2231 points - 0.53322797
Tv_1 [Aquamarine] 3227 points and Tr [Maroon] 7685 points - 0.53947641
Tv_2 [Sienna] 2231 points and Tr [Maroon] 7685 points - 0.54171934
SG_1 [Blue] 3991 points and Tv_1 [Aquamarine] 3227 points - 0.55420663
Tb_1 [Green] 15499 points and Tb_2 [Cyan] 10409 points - 0.56077588
SG_1 [Blue] 3991 points and R2 [Black] 2306 points - 0.57309470
Tm_1 [Green] 7485 points and Tv_1 [Aquamarine] 3227 points - 0.60101015
Tm_2 [Red] 5461 points and Tv_1 [Aquamarine] 3227 points - 0.61610099
SG_1 [Blue] 3991 points and Tm_2 [Red] 5461 points - 0.62773373
Tm_1 [Green] 7485 points and B [White] 1601 points - 0.64284046
Ms_2 [Blue3] 3490 points and SG_1 [Blue] 3991 points - 0.67128998
Tm_1 [Green] 7485 points and Tm_2 [Red] 5461 points - 0.71007257
R2 [Black] 2306 points and Tr [Maroon] 7685 points - 0.72059606
R2 [Black] 2306 points and Tm_1 [Green] 7485 points - 0.72621063
Ms_2 [Blue3] 3490 points and SG_2 [Red] 2066 points - 0.73940811
SG_1 [Blue] 3991 points and SG_2 [Red] 2066 points - 0.74849758
R2 [Black] 2306 points and Tm_2 [Red] 5461 points - 0.74851424
R1 [White] 1169 points and B [White] 1601 points - 0.74908922
Tb_1 [Green] 15499 points and Tr [Maroon] 7685 points - 0.76931884
Tb_1 [Green] 15499 points and Tm_2 [Red] 5461 points - 0.77864403
R1 [White] 1169 points and R2 [Black] 2306 points - 0.78070844
Tm_1 [Green] 7485 points and Tr [Maroon] 7685 points - 0.80085542
Ap [Purple] 2209 points and SG_3 [Sea Green] 1500 points - 0.85453263
Tb_2 [Cyan] 10409 points and Tm_1 [Green] 7485 points - 0.86555033
SG_1 [Blue] 3991 points and Tb_1 [Green] 15499 points - 0.88600814
Tb_2 [Cyan] 10409 points and Tv_2 [Sienna] 2231 points - 0.88769324
R1 [White] 1169 points and Tv_1 [Aquamarine] 3227 points - 0.88849406
SG_1 [Blue] 3991 points and Tb_2 [Cyan] 10409 points - 0.92067465
Tb_2 [Cyan] 10409 points and Tv_1 [Aquamarine] 3227 points - 0.93584474
Ms_2 [Blue3] 3490 points and Tr [Maroon] 7685 points - 0.94205006
Tm_1 [Green] 7485 points and Tv_2 [Sienna] 2231 points - 0.94991237
R1 [White] 1169 points and Tm_1 [Green] 7485 points - 0.96618964
Ms_2 [Blue3] 3490 points and Tb_2 [Cyan] 10409 points - 0.99894179

Ms_2 [Blue3] 3490 points and Tm_2 [Red] 5461 points - 1.01406635
Tb_1 [Green] 15499 points and Tv_2 [Sienna] 2231 points - 1.07264121
SG_2 [Red] 2066 points and Tb_1 [Green] 15499 points - 1.07927046
R2 [Black] 2306 points and Tb_2 [Cyan] 10409 points - 1.09127455
Tv_1 [Aquamarine] 3227 points and B [White] 1601 points - 1.09530360
SG_2 [Red] 2066 points and Tv_2 [Sienna] 2231 points - 1.09687432
SG_1 [Blue] 3991 points and Tm_1 [Green] 7485 points - 1.14342755
SG_2 [Red] 2066 points and Tr [Maroon] 7685 points - 1.15339715
Ap [Purple] 2209 points and Mg [Blue3] 4794 points - 1.15940690
R2 [Black] 2306 points and B [White] 1601 points - 1.18874297
SG_2 [Red] 2066 points and Tm_2 [Red] 5461 points - 1.19000204
Ms_2 [Blue3] 3490 points and Tv_2 [Sienna] 2231 points - 1.22988577
O [Green] 1214 points and Tb_1 [Green] 15499 points - 1.26660536
Ct [White] 6662 points and Tr [Maroon] 7685 points - 1.26902730
SG_1 [Blue] 3991 points and R1 [White] 1169 points - 1.27812709
Ms_2 [Blue3] 3490 points and Ct [White] 6662 points - 1.30333014
Tm_2 [Red] 5461 points and Ct [White] 6662 points - 1.30536941
Ms_1 [Red] 4135 points and Ms_2 [Blue3] 3490 points - 1.31177143
SG_2 [Red] 2066 points and Tv_1 [Aquamarine] 3227 points - 1.31680243
Tb_1 [Green] 15499 points and Ct [White] 6662 points - 1.31682034
Tb_2 [Cyan] 10409 points and Ct [White] 6662 points - 1.33690549
SG_1 [Blue] 3991 points and Ct [White] 6662 points - 1.37308881
SG_2 [Red] 2066 points and Ct [White] 6662 points - 1.37562594
SG_2 [Red] 2066 points and Tb_2 [Cyan] 10409 points - 1.37800573
O [Green] 1214 points and Tb_2 [Cyan] 10409 points - 1.38000875
R1 [White] 1169 points and Tr [Maroon] 7685 points - 1.39265253
Ms_1 [Red] 4135 points and SG_2 [Red] 2066 points - 1.39392955
R1 [White] 1169 points and Tv_2 [Sienna] 2231 points - 1.40411473
Tb_1 [Green] 15499 points and Tv_1 [Aquamarine] 3227 points - 1.42058253
R1 [White] 1169 points and Tb_2 [Cyan] 10409 points - 1.43377652
Mg [Blue3] 4794 points and SG_3 [Sea Green] 1500 points - 1.44542292
R2 [Black] 2306 points and Tb_1 [Green] 15499 points - 1.46310222
SG_2 [Red] 2066 points and R2 [Black] 2306 points - 1.46682254
Tb_2 [Cyan] 10409 points and B [White] 1601 points - 1.46701742
Ms_2 [Blue3] 3490 points and Tv_1 [Aquamarine] 3227 points - 1.48070083
R1 [White] 1169 points and Tm_2 [Red] 5461 points - 1.48526076
Ms_2 [Blue3] 3490 points and O [Green] 1214 points - 1.48647927
Tm_2 [Red] 5461 points and B [White] 1601 points - 1.49470606
Ms_2 [Blue3] 3490 points and R2 [Black] 2306 points - 1.51132366
B [White] 1601 points and Tr [Maroon] 7685 points - 1.51721080
SG_1 [Blue] 3991 points and B [White] 1601 points - 1.56187922
Tv_2 [Sienna] 2231 points and Ct [White] 6662 points - 1.56646037
Tv_2 [Sienna] 2231 points and B [White] 1601 points - 1.59878908
Sw [Aquamarine] 5935 points and Ice/Snow [Blue] 10750 points - 1.61654697
Tv_1 [Aquamarine] 3227 points and Ct [White] 6662 points - 1.62266163
O [Green] 1214 points and Tr [Maroon] 7685 points - 1.65259756
Ms_1 [Red] 4135 points and SG_1 [Blue] 3991 points - 1.66916227
O [Green] 1214 points and Tm_2 [Red] 5461 points - 1.68111743
Tb_1 [Green] 15499 points and Tm_1 [Green] 7485 points - 1.68381470
R2 [Black] 2306 points and Ct [White] 6662 points - 1.68446157
SG_2 [Red] 2066 points and Tm_1 [Green] 7485 points - 1.68722732
O [Green] 1214 points and SG_1 [Blue] 3991 points - 1.69702734
SG_1 [Blue] 3991 points and SG_3 [Sea Green] 1500 points - 1.71944914
Ms_2 [Blue3] 3490 points and Tm_1 [Green] 7485 points - 1.72315101
Mg [Blue3] 4794 points and Ice/Snow [Blue] 10750 points - 1.75406491
SG_3 [Sea Green] 1500 points and Tr [Maroon] 7685 points - 1.77089660
Ms_1 [Red] 4135 points and Tb_1 [Green] 15499 points - 1.78445251
O [Green] 1214 points and Ct [White] 6662 points - 1.79183790
Ms_2 [Blue3] 3490 points and SG_3 [Sea Green] 1500 points - 1.80724355
O [Green] 1214 points and Tv_2 [Sienna] 2231 points - 1.81508089
Mg [Blue3] 4794 points and O [Green] 1214 points - 1.82595458
Tv_2 [Sienna] 2231 points and SG_3 [Sea Green] 1500 points - 1.82969739
Tv_1 [Aquamarine] 3227 points and SG_3 [Sea Green] 1500 points - 1.84340406
Tm_1 [Green] 7485 points and Ct [White] 6662 points - 1.84381924
Tm_2 [Red] 5461 points and SG_3 [Sea Green] 1500 points - 1.85223334
R2 [Black] 2306 points and SG_3 [Sea Green] 1500 points - 1.85246963
Tb_2 [Cyan] 10409 points and SG_3 [Sea Green] 1500 points - 1.85359951
Mg [Blue3] 4794 points and SG_1 [Blue] 3991 points - 1.85910376
O [Green] 1214 points and R2 [Black] 2306 points - 1.86256869
Tb_1 [Green] 15499 points and SG_3 [Sea Green] 1500 points - 1.86583032

Mg [Blue3] 4794 points and Tv_2 [Sienna] 2231 points - 1.86713869
Ms_1 [Red] 4135 points and Tm_2 [Red] 5461 points - 1.86909330
Ms_1 [Red] 4135 points and Tr [Maroon] 7685 points - 1.87014883
SG_2 [Red] 2066 points and SG_3 [Sea Green] 1500 points - 1.87144384
O [Green] 1214 points and SG_2 [Red] 2066 points - 1.87252361
Mg [Blue3] 4794 points and Tr [Maroon] 7685 points - 1.87627945
Mg [Blue3] 4794 points and R2 [Black] 2306 points - 1.87697671
R1 [White] 1169 points and SG_3 [Sea Green] 1500 points - 1.87905047
Ms_1 [Red] 4135 points and Tv_2 [Sienna] 2231 points - 1.89601677
O [Green] 1214 points and SG_3 [Sea Green] 1500 points - 1.90066434
Mg [Blue3] 4794 points and Tm_2 [Red] 5461 points - 1.90111657
SG_2 [Red] 2066 points and R1 [White] 1169 points - 1.90175516
Tm_1 [Green] 7485 points and SG_3 [Sea Green] 1500 points - 1.90176100
Ms_1 [Red] 4135 points and Tb_2 [Cyan] 10409 points - 1.90377404
Mg [Blue3] 4794 points and Ms_2 [Blue3] 3490 points - 1.90560995
Ice/Snow [Blue] 10750 points and O [Green] 1214 points - 1.91114994
Mg [Blue3] 4794 points and Tb_2 [Cyan] 10409 points - 1.91227569
Ms_2 [Blue3] 3490 points and R1 [White] 1169 points - 1.91529206
Mg [Blue3] 4794 points and Tb_1 [Green] 15499 points - 1.91708066
Mg [Blue3] 4794 points and Tv_1 [Aquamarine] 3227 points - 1.92484945
SG_2 [Red] 2066 points and B [White] 1601 points - 1.92534438
SG_3 [Sea Green] 1500 points and Ct [White] 6662 points - 1.93202644
Mg [Blue3] 4794 points and Tm_1 [Green] 7485 points - 1.93248244
Ms_1 [Red] 4135 points and Ct [White] 6662 points - 1.93375059
R1 [White] 1169 points and Tb_1 [Green] 15499 points - 1.93740685
Ms_2 [Blue3] 3490 points and B [White] 1601 points - 1.94073624
Ms_1 [Red] 4135 points and Tv_1 [Aquamarine] 3227 points - 1.94464325
Sw [Aquamarine] 5935 points and Mg [Blue3] 4794 points - 1.94608945
O [Green] 1214 points and Tv_1 [Aquamarine] 3227 points - 1.94702105
SG_3 [Sea Green] 1500 points and B [White] 1601 points - 1.95361828
Tb_1 [Green] 15499 points and B [White] 1601 points - 1.95612600
Mg [Blue3] 4794 points and SG_2 [Red] 2066 points - 1.95963236
O [Green] 1214 points and Tm_1 [Green] 7485 points - 1.96261670
Ms_1 [Red] 4135 points and R2 [Black] 2306 points - 1.96437259
Mg [Blue3] 4794 points and Ct [White] 6662 points - 1.96738384
Ms_1 [Red] 4135 points and O [Green] 1214 points - 1.97098088
Ap [Purple] 2209 points and Ice/Snow [Blue] 10750 points - 1.97150221
Ms_1 [Red] 4135 points and SG_3 [Sea Green] 1500 points - 1.97244456
Mg [Blue3] 4794 points and R1 [White] 1169 points - 1.97632948
Ice/Snow [Blue] 10750 points and SG_3 [Sea Green] 1500 points - 1.97753429
Ap [Purple] 2209 points and Tr [Maroon] 7685 points - 1.97754662
Ap [Purple] 2209 points and R1 [White] 1169 points - 1.97783111
R1 [White] 1169 points and Ct [White] 6662 points - 1.97851499
Ap [Purple] 2209 points and SG_1 [Blue] 3991 points - 1.98231179
Mg [Blue3] 4794 points and B [White] 1601 points - 1.98395581
Ms_1 [Red] 4135 points and Tm_1 [Green] 7485 points - 1.98485098
Ap [Purple] 2209 points and Ms_2 [Blue3] 3490 points - 1.98839490
Ap [Purple] 2209 points and Tb_2 [Cyan] 10409 points - 1.98921418
Ap [Purple] 2209 points and Tv_1 [Aquamarine] 3227 points - 1.98999800
Ap [Purple] 2209 points and Tv_2 [Sienna] 2231 points - 1.99104248
Ap [Purple] 2209 points and R2 [Black] 2306 points - 1.99141103
O [Green] 1214 points and R1 [White] 1169 points - 1.99234057
Ap [Purple] 2209 points and Tm_1 [Green] 7485 points - 1.99259512
Ap [Purple] 2209 points and Tm_2 [Red] 5461 points - 1.99265641
B [White] 1601 points and Ct [White] 6662 points - 1.99326168
Ap [Purple] 2209 points and Tb_1 [Green] 15499 points - 1.99337200
Ms_2 [Blue3] 3490 points and Ice/Snow [Blue] 10750 points - 1.99407275
Ice/Snow [Blue] 10750 points and SG_1 [Blue] 3991 points - 1.99411398
Ice/Snow [Blue] 10750 points and R2 [Black] 2306 points - 1.99497644
Ice/Snow [Blue] 10750 points and Tv_2 [Sienna] 2231 points - 1.99521799
Ap [Purple] 2209 points and Ct [White] 6662 points - 1.99522795
Mg [Blue3] 4794 points and Ms_1 [Red] 4135 points - 1.99550703
Ice/Snow [Blue] 10750 points and SG_2 [Red] 2066 points - 1.99562647
Ap [Purple] 2209 points and SG_2 [Red] 2066 points - 1.99576035
Ap [Purple] 2209 points and O [Green] 1214 points - 1.99590839
Ice/Snow [Blue] 10750 points and Tb_1 [Green] 15499 points - 1.99614964
Ice/Snow [Blue] 10750 points and Tr [Maroon] 7685 points - 1.99644466
O [Green] 1214 points and B [White] 1601 points - 1.99685348
Sw [Aquamarine] 5935 points and O [Green] 1214 points - 1.99703790
Ap [Purple] 2209 points and B [White] 1601 points - 1.99752336

Ice/Snow [Blue] 10750 points and Tb_2 [Cyan] 10409 points - 1.99766088
Ice/Snow [Blue] 10750 points and Ct [White] 6662 points - 1.99783718
Ice/Snow [Blue] 10750 points and Tm_2 [Red] 5461 points - 1.99790574
Ms_1 [Red] 4135 points and R1 [White] 1169 points - 1.99833973
Sw [Aquamarine] 5935 points and SG_3 [Sea Green] 1500 points - 1.99860870
Ms_1 [Red] 4135 points and B [White] 1601 points - 1.99916783
Ice/Snow [Blue] 10750 points and Tv_1 [Aquamarine] 3227 points - 1.99919906
Ice/Snow [Blue] 10750 points and R1 [White] 1169 points - 1.99932966
Ice/Snow [Blue] 10750 points and Tm_1 [Green] 7485 points - 1.99961110
Sw [Aquamarine] 5935 points and SG_2 [Red] 2066 points - 1.99963388
Ap [Purple] 2209 points and Ms_1 [Red] 4135 points - 1.99969004
Ap [Purple] 2209 points and Sw [Aquamarine] 5935 points - 1.99969489
Sw [Aquamarine] 5935 points and SG_1 [Blue] 3991 points - 1.99989771
Sw [Aquamarine] 5935 points and Tv_2 [Sienna] 2231 points - 1.99992916
Ice/Snow [Blue] 10750 points and B [White] 1601 points - 1.99993624
Sw [Aquamarine] 5935 points and Ms_2 [Blue3] 3490 points - 1.99993919
Sw [Aquamarine] 5935 points and R2 [Black] 2306 points - 1.99996435
Ms_1 [Red] 4135 points and Ice/Snow [Blue] 10750 points - 1.99996914
Sw [Aquamarine] 5935 points and Tb_1 [Green] 15499 points - 1.99999860
Sw [Aquamarine] 5935 points and R1 [White] 1169 points - 1.99999994
Sw [Aquamarine] 5935 points and Tr [Maroon] 7685 points - 1.99999997
Sw [Aquamarine] 5935 points and Tv_1 [Aquamarine] 3227 points - 1.99999998
Sw [Aquamarine] 5935 points and Ct [White] 6662 points - 1.99999998
Sw [Aquamarine] 5935 points and Tb_2 [Cyan] 10409 points - 2.00000000
Sw [Aquamarine] 5935 points and Tm_2 [Red] 5461 points - 2.00000000
Sw [Aquamarine] 5935 points and Ms_1 [Red] 4135 points - 2.00000000
Sw [Aquamarine] 5935 points and Tm_1 [Green] 7485 points - 2.00000000
Sw [Aquamarine] 5935 points and B [White] 1601 points - 2.00000000

Appendix H: Transform Divergence Statistic Summary Combination 1 , LANDSAT

This table presents a summary of the average spectral separability on LANDSAT imagery using transform divergence analysis between each of the classes in combination #1. Values of 1.9 and greater indicate good separation, values between 1.5 and 1.9, moderate separation and values <1.5 with poor separation.

	B	Ct	Ice/ Snow	Mg	Ms1	Ms2+SG2	O	R	SG1	SG3	Sw	Tb 1&2	Tm 1&2	Tv 1&2
Ap	2.00	2.00	2.00	1.86		2.00	2.00	2.00	2.00	0.91	2.00	2.00	2.00	2.00
B		2.00	2.00	2.00	2.00	2.00	2.00	1.65	1.98	2.00	2.00	1.94	1.33	1.63
Ct			2.00	2.00	2.00	1.67	2.00	2.00	1.78	2.00	2.00	1.79	2.00	1.92
Ice/ Snow				2.00	2.00	2.00	2.00	2.00	2.00	2.00	2.00	2.00	2.00	2.00
Mg					2.00	2.00	2.00	2.00	2.00	1.92	2.00	2.00	2.00	2.00
Ms1						1.48	2.00	2.00	1.89	2.00	2.00	1.96	2.00	2.00
Ms2							1.96	1.99	1.06	2.00	2.00	1.43	2.00	1.90
O								2.00	1.94	2.00	2.00	2.00	2.00	1.99
R									1.31	2.00	2.00	1.65	1.40	0.73
SG1										2.00	2.00	0.67	1.75	0.85
SG3											2.00	2.00	2.00	2.00
Sw												2.00	2.00	2.00
Tb 1&2													1.21	0.93
Tm 1&2														0.93

Appendix I: Transform Divergence Statistic Summary Combination 2 , LANDSAT

This table presents a summary of the average spectral separability on LANDSAT imagery using transform divergence analysis between each of the classes in combination #2. Values of 1.9 and greater indicate good separation, values between 1.5 and 1.9, moderate separation and values <1.5 with poor separation.

	B	Ct	Ice/Snow	Mg	Ms1	Ms2+SG2	O	R	SG1	SG3	Sw	T
Ap	2.00	2.00	2.00	1.86	2.00	2.00	2.00	2.00	2.00	0.91	2.00	2.00
B		2.00	2.00	2.00	2.00	2.00	2.00	1.65	1.98	2.00	2.00	1.81
Ct			2.00	2.00	2.00	1.67	2.00	2.00	1.78	2.00	2.00	1.89
Ice/Snow				2.00	2.00	2.00	2.00	2.00	2.00	2.00	2.00	2.00
Mg					2.00	2.00	2.00	2.00	2.00	1.92	2.00	2.00
Ms1						1.48	2.00	2.00	1.89	2.00	2.00	1.99
Ms2							1.96	1.99	1.06	2.00	2.00	1.70
O								2.00	1.94	2.00	2.00	2.00
R									1.31	2.00	2.00	1.35
SG1										2.00	2.00	0.67
SG3											2.00	2.00
Sw												2.00

Appendix J: Transform Divergence Statistic Summary
Combination 1 , SPOT

This table presents a summary of the average spectral separability on SPOT imagery using transform divergence analysis between each of the classes in combination #2. Values of 1.9 and greater indicate good separation, values between 1.5 and 1.9, moderate separation and values <1.5 with poor separation.

	B	Ct	Mg	Ms1	Ms2+SG2	O	R	SG1	SG3	Tb1&2	Tm1&2	Tv1&2
Ap	2.00	2.00	1.60	2.00	2.00	2.00	2.00	2.00	1.04	2.00	2.00	2.00
B		2.00	2.00	2.00	1.99	2.00	1.14	1.86	2.00	1.97	1.24	1.46
Ct			2.00	2.00	1.93	2.00	1.98	1.93	2.00	1.83	1.83	1.91
Mg				2.00	2.00	2.00	1.99	1.99	1.73	2.00	2.00	2.00
Ms1					1.47	2.00	1.99	1.81	2.00	1.94	1.96	1.93
Ms2_SG2						1.66	1.59	0.56	2.00	0.78	1.41	1.22
O							1.93	1.76	2.00	1.44	1.91	1.93
R								0.77	2.00	1.30	0.82	0.37
SG1									2.00	0.87	1.10	0.44
SG3										2.00	2.00	2.00
Tb1&2											0.90	1.06
Tm1&2												0.61

Appendix K: Transform Divergence Statistic Summary
Combination 2 , SPOT

This table presents a summary of the average spectral separability on SPOT imagery using transform divergence analysis between each of the classes in combination #2. Values of 1.9 and greater indicate good separation, values between 1.5 and 1.9, moderate separation and values <1.5 with poor separation.

	B	Ct	Mg	Ms1	Ms2+SG2	O	R	SG1	SG3	T
Ap	2.00	2.00	1.60	2.00	2.00	2.00	2.00	2.00	1.04	2.00
B		2.00	2.00	2.00	1.99	2.00	1.14	1.86	2.00	1.88
Ct			2.00	2.00	1.93	2.00	1.98	1.93	2.00	1.82
Mg				2.00	2.00	2.00	1.99	1.99	1.73	2.00
Ms1					1.47	2.00	1.99	1.81	2.00	1.92
Ms2						1.66	1.59	0.56	2.00	0.80
O							1.93	1.76	2.00	1.55
R								0.77	2.00	0.86
SG1									2.00	0.62
SG3										2.00

Appendix L: Publications from this Thesis Work

Campbell, J E; Harris, J R; Huntley, D H; McMartin, I; Wityk, U; Dredge, L A; Eagles, S. 2013 Remote predictive mapping of surficial earth materials: Wager Bay North area, Nunavut - NTS 46-E (N), 46-K (SW), 46-L, 46-M (SW), 56-H (N), 56-I and 56-J (S) Geological Survey of Canada, Open File 7118, 42 pages, doi:10.4095/293158

Wityk, U; Harris, J R; McMartin, I; Campbell, J E; Ross, M; Grunsky, E. 2013. Remote predictive mapping of surficial materials west of Repulse Bay, Nunavut (NTS 46M-SW, 46L-W and -S, 46K-SW). Geological Survey of Canada, Open File 7357, 2013; 24 pages, doi:10.4095/292578. Natural Resources Canada / Resources naturelles Canada

Wityk, U L; Ross, M; McMartin, I; Campbell, J; Harris, J; Grunsky, E. (Abstract) Surficial materials mapping using remote sensing and classification methods, Repulse Bay area, Nunavut - geological knowledge vs. statistical approach. CANQUA-CGRG Binannual Meeting, abstracts; 2013; p. 258. CANQUA-CGRG Binannual Meeting; Edmonton; CA; August 18-21, 2013

Wityk, U; Ross, M; McMartin, I; Campbell, J; Grunsky, E; Harris, J. (Abstract) Developing and testing surficial sediments classification methods using remote predictive mapping, Repulse Bay area, Nunavut. 33rd Canadian Symposium on Remote Sensing, abstracts; by Canadian Symposium on Remote Sensing; 2012; p. 57. Earth Sciences Sector, Contribution Series 20120002. 33rd Canadian Symposium on Remote Sensing; Ottawa; CA; June 11-14, 2012

Wityk, U; Ross, M; McMartin, I; Campbell, J; Grunsky, E; Harris, J. (Abstract) Developing and testing surficial materials classification using remote predictive mapping methods: preliminary results near Repulse Bay, Nunavut Geological Association of Canada-Mineralogical Association of Canada, Joint Annual Meeting, Programs with Abstracts vol. 36, 2011; p. 235. Earth Sciences Sector, Contribution Series 20100420 2011 GAC-MAC-SEG-SGA Joint Annual Meeting; Ottawa; CA; May 25-27, 2011